universität wien

DISSERTATION / DOCTORAL THESIS

Titel der Dissertation /Title of the Doctoral Thesis

„The short life of the Hoyle organ in cephalopods: Formation, differentiation and degradation by programmed cell death“

verfasst von / submitted by

Mag. rer.nat. Norbert Cyran

angestrebter akademischer Grad / in partial fulfilment of the requirements for the degree of

Doktor der Naturwissenschaften (Dr. rer.nat.)

Wien, 02. August 2017

Studienkennzahl lt. Studienblatt:	A 091 439
Dissertationsgebiet lt. Studienblatt: :	Zoologie
Betreut von / Supervisor:	Univ.-Prof. i.R. Dr. Waltraud Klepal

Table of contents

I. Introduction

The hatching process is a critical step in embryonic development, where the animal has to overcome the protective egg integument and promptly has to achieve abilities essential for survival such as swimming, prey capturing or camouflage techniques, sometimes supported by parental care. Therefore, several different and frequently convergent mechanisms for supporting hatching are evolved within the animal kingdom: Mechanical devices have been recorded in insects, such as sharp chitinized spines (egg-burster) laterally on the sternit edges (Weismann, 1863) or on their head (Sikes, 1930; Nuttall, 1917; Arndt & Hurka, 1992). The grain moth *Sitotroga cerealella* (Lepidoptera) simply gnaws its way out of its egg (Sikes & Wigglesworth, 1931), while the mealworm *Tenebrio molitor* lacks completely any perforation tools (Wheeler, 1899). It swallows amniotic fluid before hatching to fill the shell completely and thus breaks it by body expansion. Reptiles and birds use an egg tooth (Chang & Chen, 2016; Garcia, 2007; Wetherbee, 1959) to perforate the egg enclosure. Within cephalopoda, octopods frequently bear stiff bundles of rodlets (Kölliker's tufts) (Brocco et al., 1974; von Querner, 1927; Fioroni, 1962b) along their mantle surface and several sepiolid species have a terminal spine on their posterior mantle pole (von Byern et al., 2016; Boletzky, 1991).

Hatching can likewise be supported chemically by choriolytic (chorion dissolving) enzymes, synthetized in a temporary hatching gland. Respective structures have been observed in invertebrates such as sea urchins (Ishida, 1936), insects (Kafatos & Williams, 1964), ascidians (Hoshi & Numakunai, 1981) as well as in numerous cephalopods (Boletzky, 2012; Hoyle, 1889; Naef, 1928). In vertebrates, hatching glands were described for teleosts (Willemse & Denuce, 1973; Yamagami, 1972), amphibians (Fan & Katagiri, 2001; Kitamura & Katagiri, 1998), reptiles (Yasumasu et al., 2010) and mammals (Perona & Wassarman, 1986; Sawada et al., 1990).

The cephalopod hatching gland, referred to as Hoyle organ (**HO**) (Boletzky, 2012; Hoyle, 1889; Hibbard, 1937), is an epithelial organ restricted to the posterior part of the dorsal mantle surface. Its development is initiated during late embryonic stages, some days before hatching (Orelli, 1959; Hibbard, 1937; Fioroni, 1962a). The gland synthetizes the choriolytic enzymes, which steadily weaken the egg integument and make it permeable to water. This results in an increase of osmotic pressure within the perivitelline space and a collapse of the egg at hatching (Boletzky, 2003). Enzyme effectiveness is supposed to be increased by metal ions as observed in the hatching enzymes of the teleost *Oryzias latipes*. (Yasumasu et al., 1989a) and also presumed for the cephalopod *Loligo vulgaris* (Paulij et al., 1992).

The dimension of the HO varies considerably in the different cephalopod groups (Octopoda, Teuthida, Sepiidae), which largely corresponds to the egg encapsulation design and the hatching expense: The line–shaped HO of Octopodiforms exhibits only a few scattered inconspicuous choriolytic gland cells that may be related to the embryo tightly surrounded by the chorion and with limited perivitelline space (Boletzky, 1986). Accordingly, a lower amount of enzyme is expected due to a lower dilution effect and the ability to stretch the egg capsule by body tension. Moreover, the octopod embryos primarily rely on their Kölliker tufts as hatching tool. Decapodiforms in contrast have a high number of choriolytic gland cells, forming a distinctly recognizable anchor-shaped gland structure on the dorsal posteriour mantle surface (Orelli, 1959). In comparison to the Octopodiforms, the perivitelline space is larger than the embryo size, allowing free swimming inside the egg. But this also leads to a strong dilution effect. By this, together with the thick and tough egg capsules in Sepiids (Jecklin, 1934) or the egg-enveloping gelatinous substance that aggregates between 20 and 100 eggs within an egg cluster in Theutids (Boletzky, 1998; Arkhipkin et al., 2000), would lead one to expect a considerable higher enzyme requirement in Decapodiforms.

Within one or a few days after hatching, the Hoyle organ is eliminated like all above mentioned hatching devices (Orelli, 1959). As the cellular degradation occurs immediately

after leaving the egg (Matsuno & Ouji, 1988; Arnold & Singley, 1989), it is suspected that genetically triggered mediator molecules may be involved. Usually, cellular decay during developmental reorganization occurs via programmed cell death, known as apoptosis, necrosis and autophagy with various intermediate and overlapping types (Clarke, 1990; Kerr et al., 1972; Wyllie et al., 1980). Bulk degradation of whole organs is commonly observed to be performed by autophagic cell death (Berry & Baehrecke, 2007; Arbeitman et al., 2002; Mcphee et al., 2010) or necrosis-like programmed cell death (Guimaraes & Linden, 2004; Leist & Jaattela, 2001). Morphological features of the observed degradation process of the HO indicate that a necrotic cell death mechanism is most probable in *Loligo* and *Sepiella* (Matsuno & Ouji, 1988; Arnold & Singley, 1989). There is no further information available about such cellular degradation processes in other cephalopods, therefore the dynamic alterations and chronological sequences have to be studied in detail to understand the complex procedures during cell degradation.

In *Sepia officinalis* the contribution of the development triggering molecule nitric oxide (**NO**) was investigated and found in high concentrations in the HO until shortly before hatching (Mattiello et al., 2012). NO has likewise been observed as cell death inhibitor in the gastropod *Ilyanassa obsoleta* (Leise et al., 2004) making the high amounts before gland decay plausible. It is not clear yet, whether the NO-concentration in *Sepia* remains unchanged after hatching or, as implicated, decreases and thus allows upcoming cell death signals to take effect.

For *Idiosepius pygmaeus*, a possible relationship to another epithelial mantle-structure, that engrosses the same area on the dorsal mantle epithelium, has to be evaluated: Adult Idiosepiidae possess a genus-specific adhesive organ (**AO**) (Sasaki, 1921; von Byern et al., 2008; Cyran et al., 2011), an epithelial gland system that produces glue. The AO is an adaption to their pelagic lifestyle in shallow estuaries. It allows temporary attachment to driftwood or any other flotsam (Suwanmala et al., 2006; von Byern & Klepal, 2007). First

attachment behavior was observed 14 days post-hatching (von Byern et al., 2008; Nabhitabhata, 1994), the development and maturation of the AO however is unknown so far. Earlier studies on *Idiosepius* embryos (embryonic stage 25) (von Byern et al., 2006) revealed an appropriate gland structure on the posterior dorsal mantle surface, supposed to be an early ontogenic state of the AO, on the assumption that a HO is lacking in this genus. To resolve this ambiguity, investigations on the alteration of the mantle epithelium within a period between late embryonic development and first use of the AO is required.

Objectives of this PhD project are:

•) To get an overview of the HO phenotype in different cephalopod groups and correlate the data with structural changes of the egg encapsulation during embryonic development. Shape, proportion and secretory activity of the gland may be linked to the size of the perivitelline space and thickness of the egg encapsulation. The fully developed HO of nine representative species belonging to Octopoda (*Octopus vulgaris*, *Tremoctopus gracilis*, *Argonauta hians*), Sepiida (*Idiosepius pygmaeus*, *Sepia officinalis*, *Euprymna scolopes*) and Teuthida (*Loligo gahi*, *Sepioteuthis lessoniana*, *Architeuthis* sp) are described, compared and illustrated. Besides studying the secretory cells of the HO, all other cells, associated with the gland system, are recorded and described.

•) To define for *Sepia officinalis* developmental stages of key stone events for the HO, such as first appearance of hatching gland cells and evidences for synthesis activity and release of the choriolytic content. Accompanying alterations in the egg size and eggshell-layer organization are investigated.

•) To determine morphologically the chronology of the organ decay and accompanying ciliary cells in *Sepia officinalis*. Further focus is laid on the presence of specific signalling molecules as NO in this organ degradation processes and their possible role in inhibiting cell death signals.

•) To verify the existence of a HO in *Idiosepius pygmaeus* and examine whether there is a seamless transition from the HO to the AO or if both organs develop separately at the same locality.

The **first manuscript** (Cyran et al., 2013) comprises a comparative study focusing on the phenotypic plasticity of the mature Hoyle organ among nine species belonging to the orders Octopoda, Sepiida and Teuthida. Beside a morphological characterization of the mature gland, the time of gland formation during embryonic development and the duration of the organ degradation have been examined. Parallel, structural changes of the eggs (such as thickness of the egg integument, dimension of perivitelline space) were recorded and put into context. While Sepiida and Teuthida generally develop a distinct anchor-shaped gland, it is significantly reduced to a line-shaped structure in most octopod species or even lacking. For this study I focused my evaluation on light- and electron microscopy, X-ray micro-computer tomography, drafted illustrations and video recordings.

With the **second manuscript** (Cyran et al., 2015) emphasis is laid on the presence and potential interaction of two distinct gland systems (HO and AO) in the same location for the species *Idiosepius pygmaeus*. Within this study, animals staged between the assumed first developmental stages of the AO (at embryonic stage 25) until first signs of bonding ability in paralarvae (12 days after hatching) were investigated. Finally, a clear differentiation between HO and AO could be determined, as the HO cells disappear two days after hatching, while the first AO cells appear three days later between the mantle epithelial cells. Electron microscopical techniques and X-ray micro-computer tomography were used to demonstrate morphological changes in the mantle epithelium from HO degradation to the arising adhesive gland, appearing later in the same region.

A **third manuscript** (re-submitted at the journal Hydrobiologia) aims to characterize the entire duration of the Hoyle organ of *Sepia officinalis* in detail. The intent was to

determine the first indications for cell proliferation related with the hatching gland, its differentiation throughout embryonic development and finally its degradation. Beside the morphological determination of the involved cell death mechanism, also the contribution of the developmental mediator molecule NO in activating the cell death cascade was verified. I moreover investigated collateral morphological changes along the mantle surface, such as the arrangement of the numerous ciliary tufts, associated to the perivitelline flow and the hatching process. Contribution of metal ions in enhancement of the choriolytic enzymes was evaluated. Technical applications comprised light- and electron microscopy, elemental analysis on microanatomic level (EELS and EDX) as well as immunofluorescence.

References are combined with the discussion section (see there)!

Zoologischer Anzeiger 253 (2013) 66–82

Contents lists available at ScienceDirect

Zoologischer Anzeiger

journal homepage: www.elsevier.de/jcz

Zoologischer Anzeiger

Hatching glands in cephalopods – A comparative study

Norbert Cyran[a,*], Yannick Staedler[b], Jürg Schönenberger[b], Waltraud Klepal[a], Janek von Byern[c]

[a] Core Facility Cell Imaging and Ultrastructural Research, Faculty of Life Sciences, University of Vienna, Vienna, Austria
[b] Department of Structural and Functional Botany, Faculty Centre of Biodiversity, University of Vienna, Vienna, Austria
[c] Center for Integrative Bioinformatics Vienna, Max F Perutz Laboratories, University of Vienna, Medical University of Vienna, University of Veterinary Medicine, Vienna, Austria

ARTICLE INFO

Article history:
Received 9 May 2012
Received in revised form 20 February 2013
Accepted 5 April 2013
Available online 4 July 2013
Corresponding Editor: Carsten Lüter.

Keywords:
Hoyle organ
Hatching gland
Digestive gland
Cephalopoda
Embryonic development

ABSTRACT

Hatching of embryos from their eggs involves either mechanical and/or chemical support. In particular enzymes are widely used in the animal kingdom to weaken the egg layers and facilitate the embryo's escape. Although numerous morphological and biochemical studies exist on the hatching glands of invertebrates (such as sea urchins, ascidians, insects) and vertebrates (teleosts, amphibians, and mammals), little is known about the morphology of the hatching glands (Hoyle organs) in cephalopod hatchlings.

In this study, the internal gland structure and the external appearance of the Hoyle organ are compared among several cephalopod species (*Idiosepius pygmaeus*; *Euprymna scolopes*; *Sepia officinalis*; *Loligo gahi*; *Sepioteuthis lessoniana*; *Architeuthis* sp.; *Octopus vulgaris*; *Tremoctopus gracilis*; *Argonauta hians*). In almost all cases the glandular system is restricted to the posterior part of the dorsal mantle surface. Only *Octopus* and *Argonauta* lack a specific glandular structure in this body region and the animals apparently use other mechanisms to penetrate the egg layers.

In all decapod species (*Idiosepius*; *Euprymna*; *Sepia*; *Loligo*; *Sepioteuthis*; *Architeuthis*) as well as in *Tremoctopus* only one specific cell type is present in the Hoyle organ, which synthesizes granular material. The secretory droplets are more or less uniform in electron density in *Idiosepius*, *Euprymna* and *Tremoctopus* but exhibit translucent inclusions in the other decapods. The time of gland development, first synthesis of secretory products and later degeneration after hatching vary between the species.

The present study contributes to our knowledge of glandular systems in cephalopods and allows comparison with hatching structures in other invertebrates and vertebrates.

1. Introduction

Embryos that develop within a protective egg shell need a strategy to hatch from the enclosure. Physical and/or chemical mechanisms are required to penetrate and hatch through the rough protective coats if maternal help is absent. In vertebrates as well as invertebrates the most common actions include muscular movement, a blow of the tail, and increased osmotic pressure of the perivitelline fluid, usually combined with the secretion of enzymes, which attack the chorion membrane.

In cephalopods, mechanisms effective in the process of hatching are muscular contractions (von Orelli, 1959), action of stiff bunches of rodlets (Kölliker's tufts) (von Querner, 1927; Fioroni, 1962b; von Boletzky, 1966; Brocco et al., 1974) and enzymes released from the hatching gland (termed the Hoyle organ) (von Orelli, 1959).

The Hoyle organ (HO) has been demonstrated in several cephalopod species (*e.g. Loligo* sp., *Sepia* sp., *Todarodes* sp., *Sepiella* sp.) (Hibbard, 1937; Arnold, 1965; Matsuno and Ouji, 1988; Shigeno et al., 2001a) during embryonic development. It is present exclusively on the posterior part of the dorsal mantle surface and solely in the late embryonic phase (*e.g. Sepia* sp. from stage 22 to 23, *Loligo* sp. from stage 28, *Octopus* sp. from stage 13 (von Orelli, 1959; Fioroni, 1962a; Arnold and Singley, 1989). In *Sepia* and *Loligo* the HO has an anchor-like shape; in Octopods it forms a slender and small band on the posterior mantle pole.

In cross-section the hatching gland of *Sepia* appears drop-shaped, and its individual secretory cells are filled with granular material (named "ferment" by von Orelli (1959)). Two further cell types are present in the HO; they were drawn but not discussed by von Orelli (1959).

The cells of the HO in *Loligo* are similar to those in *Sepia*, but more compressed. Based on studies by Arnold and Singley (1989) three cell types can be distinguished and are named alpha, delta and mucous cells. The alpha cells, filled with fine filamentous material and many small vesicles, have a dome-shaped apex covered with densely packed microvilli. The delta cells are filled with granules.

* Corresponding author at: Core Facility Cell Imaging and Ultrastructural Research, Faculty of Life Sciences, University of Vienna, Althanstrasse 14, 1090 Vienna, Austria. Tel.: +43 1 4277 54428; fax: +43 1 4277 9544.
E-mail address: nbc555@gmx.com (N. Cyran).

0044-5231/$ – see front matter © 2013 Elsevier GmbH. All rights reserved.
http://dx.doi.org/10.1016/j.jcz.2013.04.001

The mucous cells are not restricted to the HO but distributed over the entire surface of the embryo. The authors indicate that the alpha cells are adhesive and attach the HO to the inside of the chorion to localize the effect of the digestive enzymes secreted by the delta cells.

The digestive cells (Fz) in the HO of *Octopus* are elongate and interconnected with glandular (Dz) and epidermal cells. No information is available on the morphology and secretory composition of the glandular cells (von Orelli, 1959).

Following hatching, the production of secretory material ceases and the HO degrades within hours or a few days in all species (von Orelli, 1959).

Although the origin and function of the hatching gland in cephalopods have been known for more than 70 years, knowledge about its morphology is fragmentary. In the present study ultrastructural analyses and X-ray microtomography imaging is used to characterize and compare the HO of nine cephalopod species. For a better comparison and correlation of the morphological data, we provide some additional details about the "egg morphology" during development and at the time of hatching and behavioral observations during the hatching process.

The results help to understand the morphology of glandular cells and allow a more detailed comparison among cephalopods as well as with other invertebrates and vertebrates which develop such structures.

2. Materials and methods

Hatchlings and late embryonic stages of six Decapodiformes (*Idiosepius pygmaeus*; *Euprymna scolopes*; *Sepia officinalis*; *Loligo gahi*; *Sepioteuthis lessoniana*; *Architeuthis* sp.) and three Octopodiformes (*Octopus vulgaris*; *Tremoctopus gracilis*; *Argonauta hians*) were collected with the help of our colleagues worldwide (see acknowledgements). For the morphological comparison always the latest developmental stage of the Hoyle organ (determined by the first sign of secretory activity) was used, except for *Sepioteuthis lessoniana*, *Architeuthis* sp. and *Tremoctopus gracilis*. Specimens of these three species were given as a gift (see acknowledgement) and the specific developmental stages were not verified.

2.1. Ultrastructure

For ultrastructural analyses the samples were fixed in 2.5% glutaraldehyde with a sodium-cacodylate buffer (pH 7.4, plus 10% sucrose) for 6 h at 25 °C. The three museum samples (*Sepioteuthis*, *Architeuthis* and *Tremoctopus*) were stored earlier in 50% isopropanol and also post-fixed for the present study in 2.5% glutaraldehyde with sodium-cacodylate buffer. Subsequently all samples were immersed for 1.5 h in 1% osmium tetroxide with 0.1 M buffer solution and dehydrated in a graded series of ethanol.

For transmission electron microscopy (TEM) the samples were embedded in epon; ultrathin sections (50–70 nm) were mounted on formvar coated copper slot grids, stained with uranyle acetate and lead citrate (Reynolds, 1963), and examined in a Zeiss EM 902 and Zeiss Libra 120.

For scanning electron microscopy (SEM) the samples were washed several times in 100% acetone, dried in a critical point dryer Leica CPD 300, mounted on stubs, coated with gold in a Polaron 5800 sputter coater, and viewed in the SEM Philips XL 20.

2.2. X-ray microtomography (μCT)

For μCT the glutaraldehyde-fixed samples were washed in aqua dest. and dehydrated in a graded series of ethanol. Subsequently, the samples were contrasted for 36 h in 1% (w/v) phosphotungstic acid (PTA) in EtOH and transferred to water for scanning. The

Table 1
Overview of the relevant morphological features relating to the hatching gland of the observed species. In *Octopus vulgaris* and *Argonauta hians* we could not detect any specific glandular structures. Symbols: n.o., not observed; #, not existent; *, The quoted data correlate with the earliest stages available. An earlier occurrence of hatching gland cells is to be assumed. **, Since the cultivated animals were not observed 24 h per day, the hatching time is not detected exactly and therefore the stated degradation time may differ slightly.

	Decapodiformes						Octopodiformes		
	Idiosepius pygmaeus	*Euprymna scolopes*	*Sepia officinalis*	*Loligo gahi*	*Sepioteuthis lessoniana*	*Architeuthis* spec.	*Octopus vulgaris*	*Tremoctopus gracilis*	*Argonauta hians*
Entire shape	Anchor shaped	Anchor shaped	Anchor shaped	Anchor shaped	Anchor shaped	Anchor shaped	#	Single band posteriorly	#
Shape (cross section)	Triangular	Undetermined	Oval to circular	Triangular	Semicircular to lenticular	Triangular	#	Scattered solitary cells	#
Surface appearance	Slightly elevated	Elevated	Distinctly elevated	Slightly elevated	Distinctly elevated	Slightly elevated	#	No elevation indicated	#
Lateral boundary of the gland	Cells with long microvilli	No specific boundary cells	Ciliated cells	Ciliated epithelial cells	Ciliated epithelial cells	Ciliated epithelial cells	#	#	#
Number of secretory cell types	1	1	1	1	1	1	#	1	#
Surface contact of the gland cells	Covered by epithelial cells	Covered by epithelial cells	Direct contact; microvilli border	Direct contact; microvilli border	Covered by epithelial cells	Covered by epithelial cells	#	Covered by epithelial cells	#
Granules appearance	2 μm; globular	2–3 μm; globular	2 μm; globular	2 μm; globular	1.5 μm; globular	2 μm; globular	#	1 μm; globular	#
Hollow areas within granules	#	#	Internal	Peripheral	Peripheral	Peripheral	#	#	#
Other cells within the HO	#	Unspecific epith. cell	#	#	#	#	#	#	#
Stage of first appearance	25*	25*	23	25*	n.o.	n.o.	#.	n.o.	#
Degradation time**	~1 day	>2 days	<2 days	~1 day	n.o.	n.o.	#	n.o.	#

animals were imaged at high resolutions (1 μm voxelsize) using an Xradia MicroXCT system. This system uses a 90 keV/8 W tungsten X-ray source, a cooled 1k × 1k CCD camera, and switchable scintillator-objective lens units, which give fields of view from 5 mm down to a few hundred microns, with corresponding pixel sizes from 5 μm to less than 500 nm. The practical limit of resolution for images from this scanner is about 1 μm.

3. Results

In most investigated cephalopod species (except *Octopus vulgaris* and *Argonauta hians*) we could confirm the presence of a Hoyle organ (HO). In all cases it appears during the late embryonic development, is fully developed shortly before hatch and disappears after hatching. However, the time of the first and last appearance differs among the species as shown below and summarized in Table 1. An overview of the morphological characteristics is illustrated in Fig. 1.

3.1. *Idiosepius pygmaeus*

The HO in *Idiosepius* could clearly be separated morphologically in stage 25 and is fully developed at stage 29. About one day after hatch the hatching gland system in *Idiosepius* is degraded and disappeared. The HO consists of thin, slightly elevated bands and has an anchor-shaped appearance (Fig. 2A). One band is situated on the dorsal mantle side while the other two bands extend laterally to the fins. All three bands are laterally bordered by brush-like microvilli, about 1 μm in length. The epithelium has a height of 30–40 μm, only in the latest stages the HO cells overtop the epithelium cells by about 3–5 μm.

3.1.1. *Cell types*

The secretory cells are orientated in the centre of the HO bands (Fig. 3A). They have a triangular shape in cross section, with a diameter of 10 μm at their base down to 4 μm at the epithelium surface. The globular to oval nucleus (Ø 6–8 μm) is located basally and contains several nucleoli. Around the nucleus, typical cell compartments such as rough endoplasmic reticulum (rER), mitochondria, and Golgi bodies are located (Fig. 3B). The remaining cytoplasm is filled with globular granules (Ø 2 μm) of uniform density. The secretion pore of the glandular cells is covered by the microvilli border of the neighboring non-secretory cells (Fig. 3C). The secretion is effected by pinching off parts of the 'upper' cell areas, which subsequently pass the border.

Laterally, the glandular cells are bordered by conspicuous non-secretory cells. These cells can be distinguished from the regular epithelium cells by their dense cytoplasm and extra long microvilli (1.5 μm) (Fig. 3C), giving the HO the brush-like appearance. In contrast to the glandular cells, in the non-secretory cells the location of the nucleus varies but is frequently central. In addition, the cells contain a distinct Golgi network and cytoskeleton filaments.

3.1.2. *Egg-capsule description*

The total number of eggs ranges from 100 to 300 in *Idiosepius pygmaeus*. The eggs are spawned individually on any kind of surface during cultivation in aquaria (Fig. 4A). The globular eggs are translucent (Fig. 4B), about 1 mm in diameter and enclosed by a chorion and several nidamental layers. During embryonic development these nidamental layers condense so that at the time of hatch only a few layers remain visible (Fig. 4C). In the early developmental stages (up to stage 23) the embryo is strongly compressed within the egg, whereas during later development with further condensation of the layers and progressive enlargement of the perivitelline space, the embryos are able to move around freely (Fig. 4B).

3.1.3. *Behavioral observation of the hatching process*

We could not see with certainty whether the embryo of *Idiosepius* wipes with its HO in certain areas as does *Loligo* (see below). Rather, the animal apparently remains immobile with the HO located in a certain position of the egg membrane before hatching. The animal then hatches in this position of the egg. However, we have observed that in some cases, the hatching may take place in other parts of the egg membrane. During the hatching process the animals use their arms to push against the chorion and to disrupt the egg integument. At the time of hatch the eggs are inflated like a balloon and relatively firm to the touch. The moment the chorion is disrupted, the embryo is flushed out of the egg with the fluid. The hatching process is relatively fast (less than 30 s) (Film sequence 1).

Supplementary material related to this article found, in the online version, at http://dx.doi.org/10.1016/j.jcz.2013.04.001.

3.2. *Euprymna scolopes*

First indications of the HO could be observed latest at stage 25 and it is fully developed at stage 28–29. The degeneration of the HO is relatively slow; two days after hatch the organ is still visible even though progressively degraded. The HO in *Euprymna* is anchor-shaped, forming one dorsal and two lateral bands (Figs. 2B and 4F), and slightly elevated (more than in *Idiosepius* but less than in *Sepia*) (Fig. 5C). On the posterior mantle pole the bands merge, accompanied by a short conical spine (Fig. 5A and B).

The lateral boundary of the gland complex is less well demarcated than in the other observed species since the secretory cells are interspersed by non-secretory epithelial cells and because there are no particular bordering cells.

3.2.1. *Cell types*

The HO in *Euprymna* also possesses only one glandular cell type. These cells do not form a homogenous tissue, but are arranged individually between the non-secretory epithelium cells (Fig. 5D and F). The cells are column-shaped and do not taper towards the epithelium surface. The nucleus (globular to oval, Ø 10 μm) with several nucleoli is located basally and surrounded by several rER-layers. Synthesis occurs above the nucleus (Fig. 5E). The secretory granules are globular (Ø 2–3 μm), of uniform density and show no density gradient during gland development. The apical pole of the cells is encased in the epithelium and lacks a microvilli layer. Signs of secretion indicate that only the most apical part of the cell content is secreted, while the rest remains within the cells (Fig. 5F).

The non-secretory cells are randomly distributed between the glandular cells and are not limited to the HO but are also present in the normal, non-digestive epithelium. Within the HO, they are triangular in shape and seem to be restricted to the outermost third of the epithelium layer; a connection to the basal lamina could not be observed. The cells have a short microvilli layer (0.4 μm) on their apical surface and distinct cytoskeleton elements equally distributed within the cell in the HO as well as in the normal epithelium (Fig. 5F).

3.2.2. *Egg-capsule description*

The eggs of *Euprymna* are about 2 mm in diameter and spawned in clutches of 100–200 eggs to the bottom side of hard substrates (Fig. 4D). Furthermore, the females camouflage the eggs with a layer of sand. The eggs are enclosed by a chorion and several nidamental layers that are obviously sticky. The eggs are slightly milky in the beginning and become translucent during embryonic development. The thickness of the nidamental layers shrinks from stage 19 on while the perivitelline space swells. At stage 30 the embryos are able to rotate within the egg capsule, however the embryos are

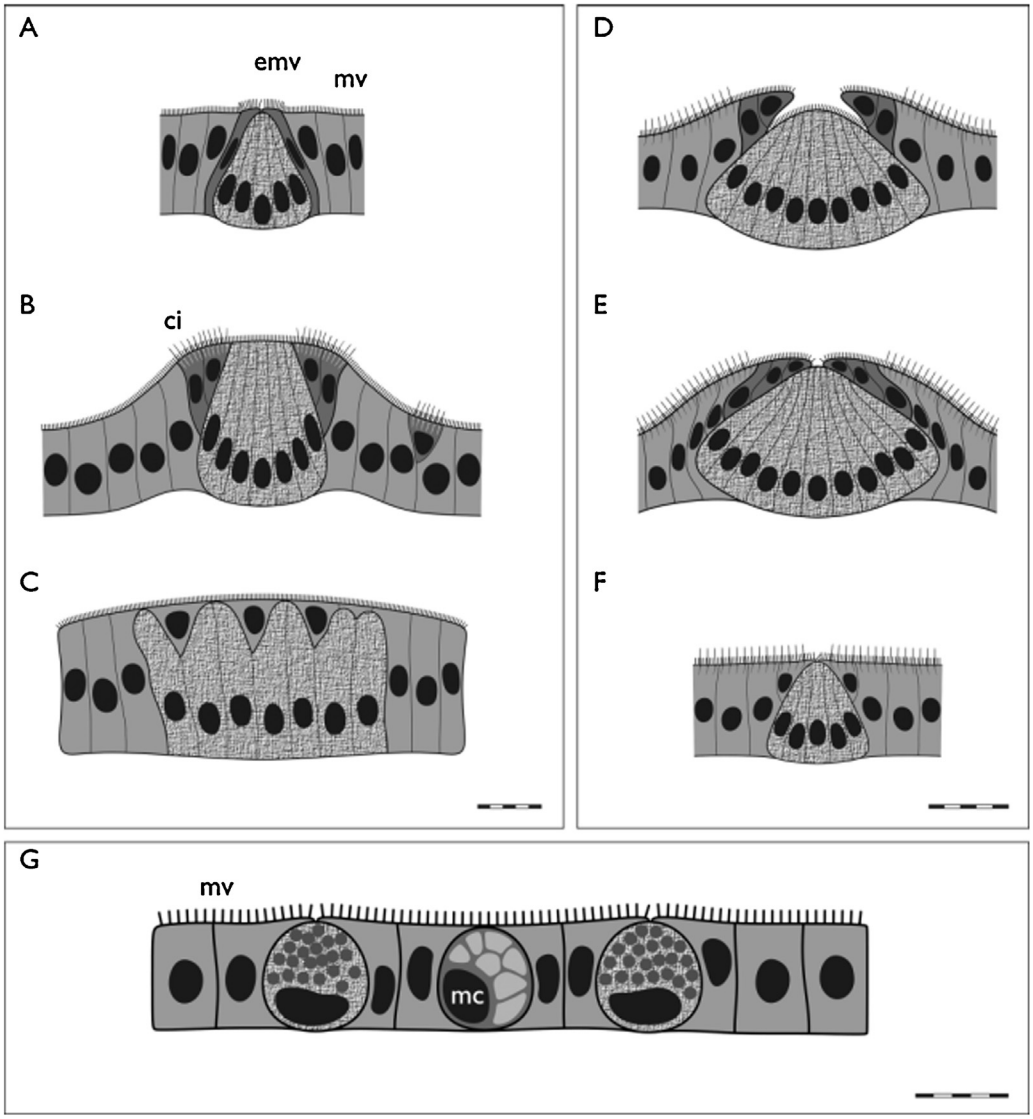

Fig. 1. Schematic illustration of the internal Hoyle organ architecture in cross section view. The textured central area in (A–C) (Sepiida), (D–F) (Loliginidae) and the left and right gland cell in (G) (Octopoda) represent the enzymatic secretory cells. The different epithelium cell types are labelled in homogenous shades of grey. (A) *Idiosepius pygmaeus*; (B) *Sepia officinalis*; (C) *Euprymna scolopes*; (D) *Loligo gahi*; (E) *Sepioteuthis lessoniana*; (F) *Architeuthis* sp; (G) *Tremoctopus gracilis*. ci, cilia; emv, elongated microvilli; mc, mucus cell; mv, microvilli. Scale bars: 20 μm (A–C); 50 μm (D–F); 10 μm (G).

tightly enclosed in the egg (Fig. 4E) and not able to swim around freely as those of *Idiosepius*.

3.2.3. Behavioral observation of the hatching process

During the hatching process the embryo strongly ventilates, pushing and wiping with its HO (Fig. 4F) and spine against the egg membrane. Nevertheless, it happens that the animal hatches afterwards through a different part of the egg membrane. The hatching process takes some minutes but sometimes the outer yolk sack inhibits the hatch for a while.

3.3. Sepia officinalis

The first hatching gland cells in *S. officinalis* could be observed at stage 23 and the maturity of the HO is reached in the embryonic stage 28. The degeneration of the HO in *Sepia officinalis* takes place in less than two days. As proposed in the literature (von Orelli, 1959), the HO has an anchor-like shape, of which one band lies on the middle dorsal line and the other two bands on the dorsal surface of each fin (Fig. 2C). As for *Idiosepius* the HO in *Sepia* is elevated from the epithelium surface and has a hump-like appearance in cross section (HO cell height: 45 μm vs. epithelium cell height: 20 μm) (Fig. 6A). The bands are laterally enclosed by ciliated epithelium cells.

3.3.1. Cell types

Also in *Sepia* only one secretory cell type occurs in the HO. In cross section the glandular cells appear located in the centre of the digestive hump, encased laterally by non-secretory ciliated cells. The cells are less tapered towards the surface than in *Idiosepius* but more oval in shape. The nucleus (globular to oval, 5–10 μm) with several nucleoli is likewise located basally and surrounded by rER. The synthesis of the secretory material, achieved by rER and Golgi bodies, is similar to that found in *Idiosepius*; in early HO developmental stages, the secretory granules are likewise globular (Ø 2 μm) and of low density (Fig. 6B). However, in mature HO (shortly before hatch) the granules shrink in size, their density increases and electron-transparent inclusions appear within the granules. These inclusions vary in size (up to 1 μm) and orientation; they are typically located in the centre of the granules, while the periphery stays

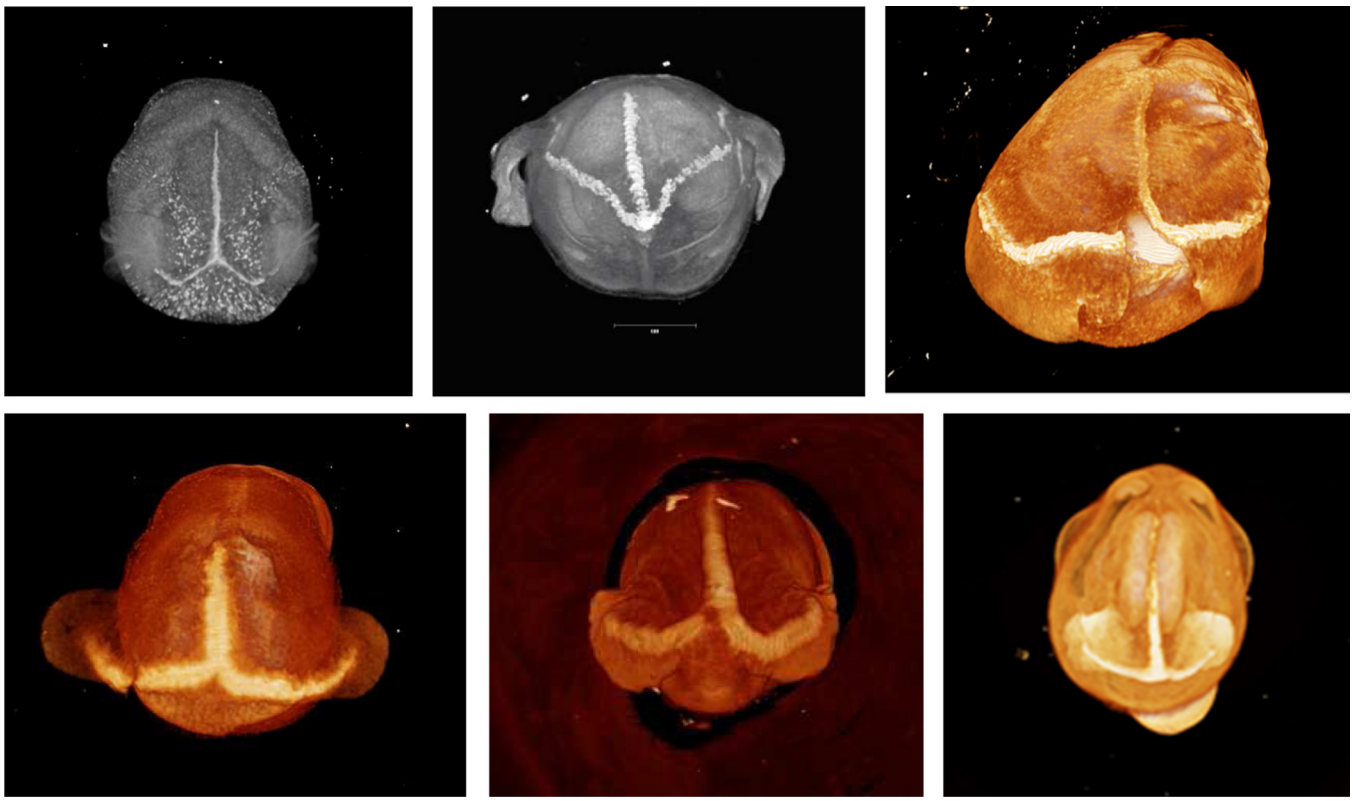

Fig. 2. μCT scans illustrating the distribution pattern of the Hoyle organ on the dorsal mantle surface. (A) *Idiosepius pygmaeus*; (B) *Euprymna scolopes*; (C) *Sepia officinalis*; (D) *Loligo gahi*; (E) *Sepioteuthis lessoniana*; (F) *Architeuthis* sp.
Image (B) was gratefully provided by Alexandra Kerbl from the University of Vienna.

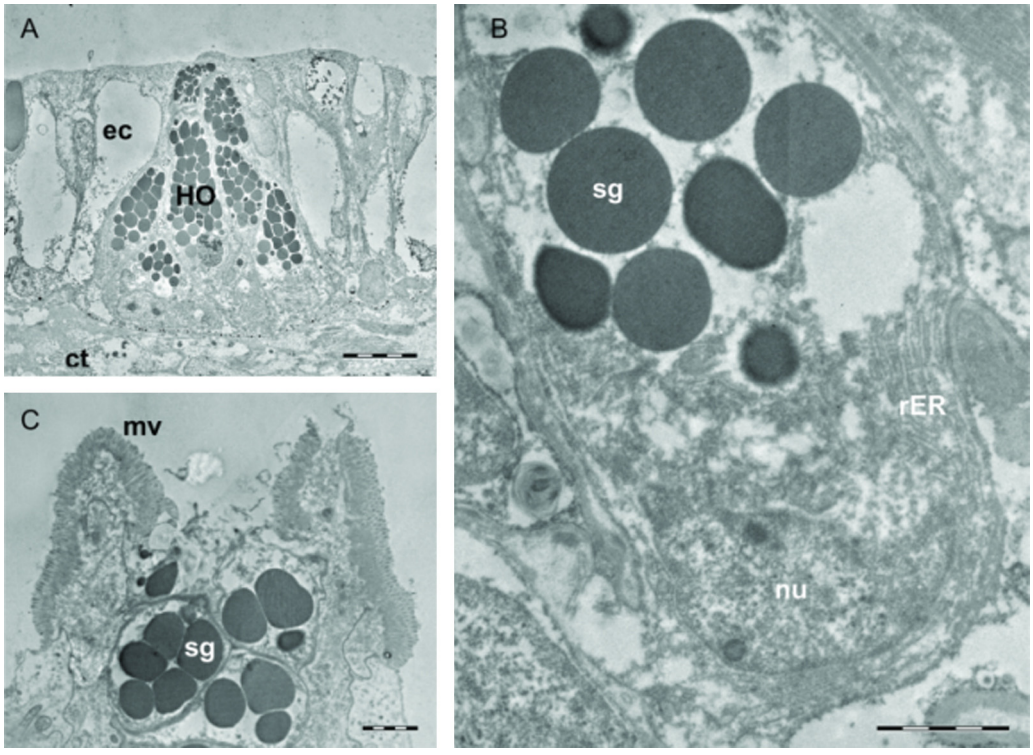

Fig. 3. *Idiosepius pygmaeus*. (A) In cross section the Hoyle organ appears triangular and is slightly protruding from the epithelium surface (stage 29). (B) Nucleus and synthesis organelles are basally located in the secretory cells (stage 29). (C) Surface area with the tips of secretory cells and the enclosing epithelium cells with the characteristic long microvilli fringe (stage 30). ec, epithelial cell; ct, connective tissue; HO, Hoyle organ; mv, microvilli; nu, nucleus; rER, rough endoplasmic reticulum; sg, secretory granules. Scale bars: 10 μm (A); 2 μm (B and C).

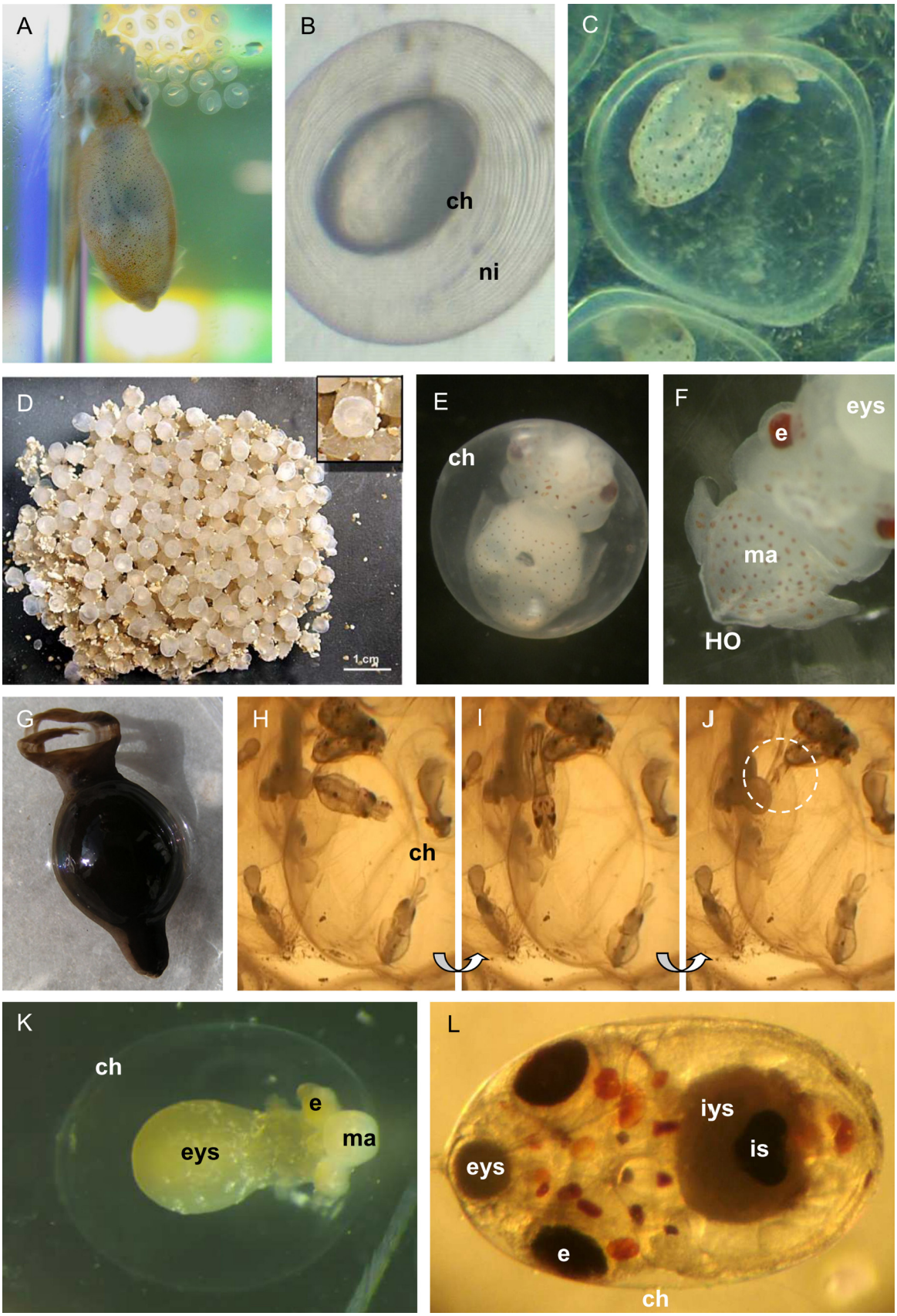

Fig. 4. Cephalopod eggs and embryos. (A) Female *Idiosepius pygmaeus* spawns the eggs singularly on any kind of surface during cultivation in aquaria. (B) The *Idiosepius* eggs are translucent, about 1 mm in size, enclosed by a chorion and several nidamental layers. (C) During the late embryonic development (about stage 29) the nidamental layers condense and the embryo is able to swim freely around. (D) Egg batch of *Euprymna scolopes*. (E) The *Euprymna* embryo is able to rotate within the egg but not to move freely. (F) Recently hatched *Euprymna*, showing its hatching gland. (G) Egg of *Sepia officinalis* with its typical dark appearance caused by the incorporated ink. (H) *Loligo* embryo disperses the enzymatic secretory material by sliding with its posterior tail along the chorion. (I) As soon as a gap is digested, it is widened by mantle contractions until

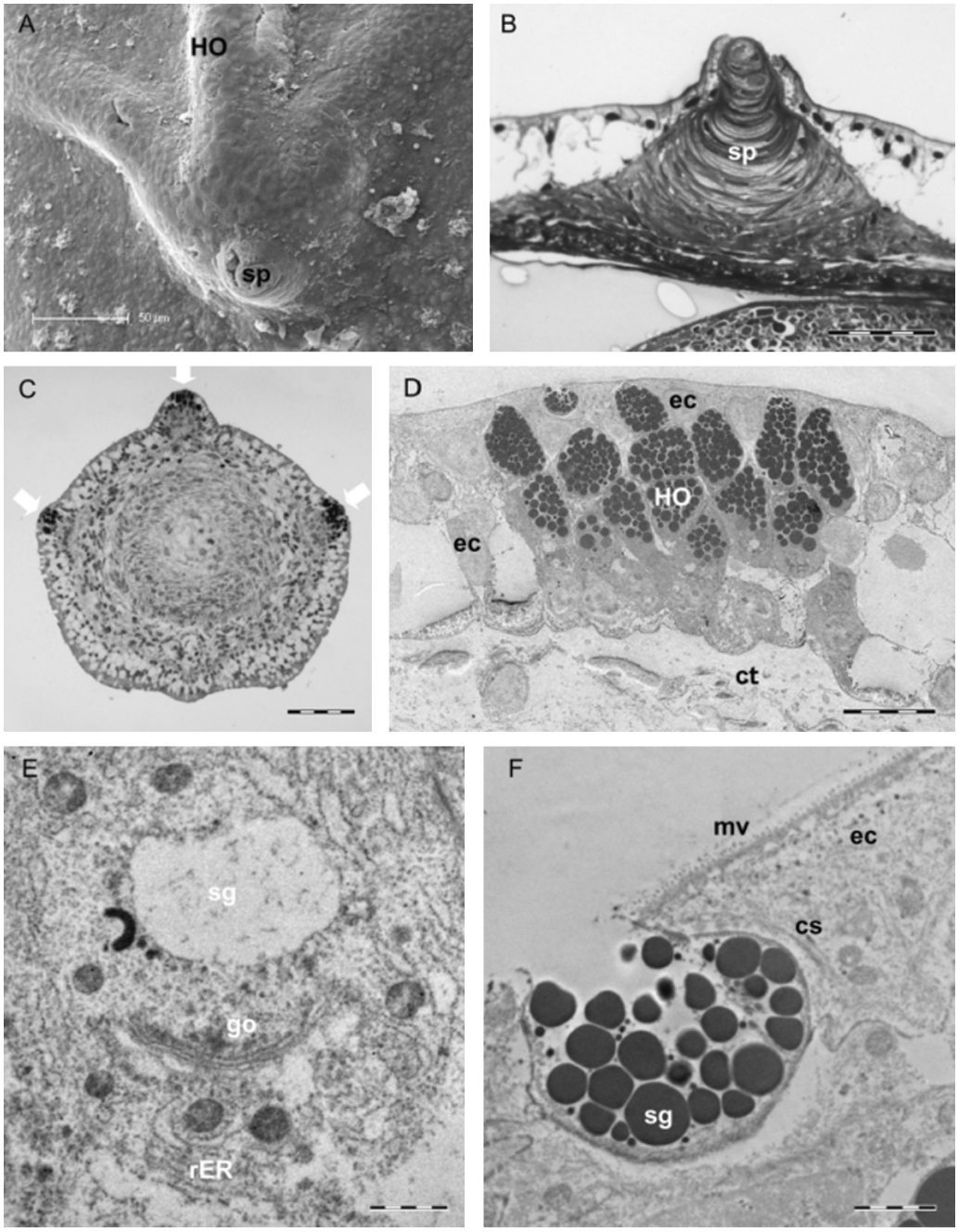

Fig. 5. *Euprymna scolopes*. (A) Convergence of the three bands of the gland on the posterior mantle pole, where the terminal spine breaks through the epithelium. (B) Cross section of the spine showing its internal architecture. (C) Overall cross section of the posterior mantle (stage 26) showing the three bands of the HO (arrows). (D) The secretory cells of the HO do not build an exclusionary complex but are interspersed with epithelium cells (stage 29–30). (E) Basally in the cells the secretory droplets are synthesized (stage 26). (F) At stage 29 releasing granules are observable. cs, cytoskeleton filaments; ct, connective tissue; ec, epithelial cell; go, Golgi bodies; HO, Hoyle organ; mv, microvilli; rER, rough endoplasmic reticulum; sg, secretory granules; sp, terminal spine. Scale bars: 50 µm (A and B); 100 µm (C); 20 µm (D); 1 µm (E); 2 µm (F).

globular (Fig. 6C). Between the secretory granules, microtubules are present, which proceed from above the nucleus up to the epithelial surface (Fig. 6D). The tips of the glandular cells are not covered by epithelium cells as in *Idiosepius* but are permanently exposed to the outer environment. Apically, the glandular cells possess microvilli, about 1 μm in length, which cover the cell surface. The secretory droplets seem to be released individually by exocytosis.

The non-secretory cells are clearly characterized by their densely arranged cilia (up to 10 μm in length) (Fig. 6E). Furthermore, the surface of the cells is covered by microvilli, similar to the

the embryo can pass through, (J) The gap is still visible after hatching (white circle). (K) The egg of *Architeuthis* allows the embryo to turn around without restrictions. (L) Embryonic stage 14 of *Argonauta hians* (shortly before hatch), showing that the embryo is tightly packed within the egg. Image (D) was gratefully provided by Dr. Patricia N. Lee from the Pacific Biosciences Research Center, USA, published in Lee et al. (2009). Image (L) was published in Sukhsangchan (2009) and re-used with permission of Dr. Charuay Sukhsangchan. ch, chorion membrane; e, eye; eys, external yolk sac; HO, Hoyle organ; is, ink sac; iys, internal yolk sac; ma, mantle; ni, nidamental membrane.

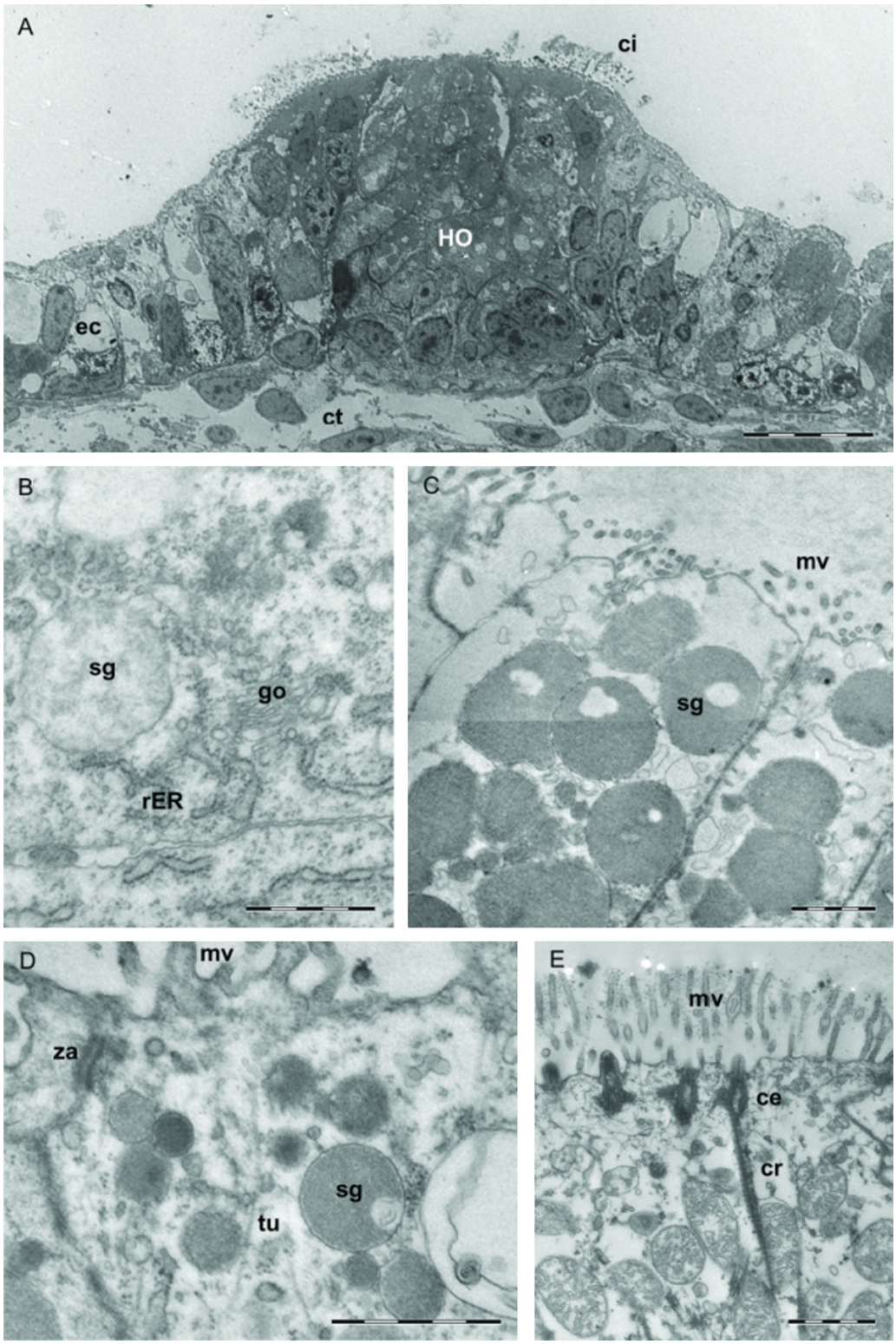

Fig. 6. *Sepia officinalis*. (A) Cross section of the Hoyle organ (stage 28); the gland is clearly protruding from the regular epithelium. Ciliated epithelium cells form a continuous band along the HO periphery. (B) The synthesized secretory material fuses to granules with initially low density (stage 26). (C) During migration towards the surface the granules condense, forming mostly central inclusions with a lower material density (stage 29). (D) Microtubules traverse the cells from the synthesis area to the surface, and are particularly visible in the earlier stages of the gland development. Apically the cells bear microvilli (stage 26). (E) The lateral border is achieved by epithelium cells with microvilli and rooted cilia (stage 30). ce, centriol; ci, cilia; cr, ciliary root; ct, connective tissue; ec, epithelial cell; go, Golgi bodies; HO, Hoyle organ; mv, microvilli; rER, rough endoplasmic reticulum; sg, secretory granules; tu, microtubules. Scale bars: 20 μm (A); 1 μm (B–E).

glandular cells. Apart from that, the non-secretory cells do not differ in their characterization from those found in other parts of the mantle epithelium.

3.3.2. Egg-capsule description

The egg morphology of *S. officinalis* is well known from the literature (Fioroni, 1978; von Boletzky et al., 2006), however for a better comparison we would like to repeat the most relevant features. The eggs of *S. officinalis* are attached individually to any object on the sea bottom by means of a fixation ring but are laid in batches comprising up to 400 eggs. The eggs are about 8 mm in diameter and consist of the inner chorion surrounded by several nidamental layers (Fig. 4G). In its outer layers, ink is incorporated, which gives the eggs the typical dark appearance. During late embryonic development the eggs swell and become increasingly fragile.

3.3.3. Behavioral observation of the hatching process

Not observed.

3.4. Loligo gahi

The HO in *Loligo* has the anchor-like shape as in *Sepia*. In contrast to the literature (Arnold and Singley, 1989), the HO could clearly be observed at stage 25 and is fully developed at stage 29 (Fig. 2D). As in *Idiosepius* the HO degenerates and disappears about one day after hatch. The gland in *Loligo* is embedded in an epidermal fold which partly covers the cell tips (Fig. 7A). While earlier studies proposed two glandular cell types (named alpha and delta cells) in *Loligo pealii* (Arnold, 1965, 1974; Arnold and Singley, 1989), we found only one glandular cell type.

3.4.1. Cell types

The glandular cells are close to each other, not intercepted by any other cell types. In cross section the secretory cells have a triangular shape, tapering towards the surface (Fig. 7A). The nucleus is located basally, containing several nucleoli, and is surrounded by rER. Synthesis takes place in the central cell area indicated by high amounts of rER and Golgi bodies (Fig. 7B). As described for *Sepia*, the granules (oval to round, Ø 2 μm) in *Loligo* also change their appearance with progression of HO-development. Initially, the secretory granules are of a uniform electron-dense material (Fig. 7C). In mature cells parts of the granules condense and low-density cavities arise (Fig. 7D). The majority of the cavities is circular shaped in cross section and frequently comprises substantial parts of the secretory droplets. As opposed to *Sepia*, they are not limited to the granular centre but also appear in the periphery. Although the epithelial fold partly covers the digestive gland, the apex of the glandular cells is exposed to the surface and bears microvilli (0.5 μm in length). Ultrastructural images indicate that the secretory granules pass individually through the cell surface (Fig. 7D).

Ciliated epithelium cells border the glandular cells laterally and partly cover the gland (Fig. 7A). The cells are small, cone-shaped, and mostly have a globular nucleus lacking nucleoli. Endoplasmic reticulum, ribosomes and mitochondria are rare. The cells form a continuous microvilli layer and possess long rooted cilia on their surface (Fig. 7E).

3.4.2. Egg-capsule description

Loligo gahi usually deposits one or two egg clusters with 50–70 eggs encapsulated in a conjoint gelatinous matrix. The eggs are about 1.5 mm in diameter and enclosed only by the chorion

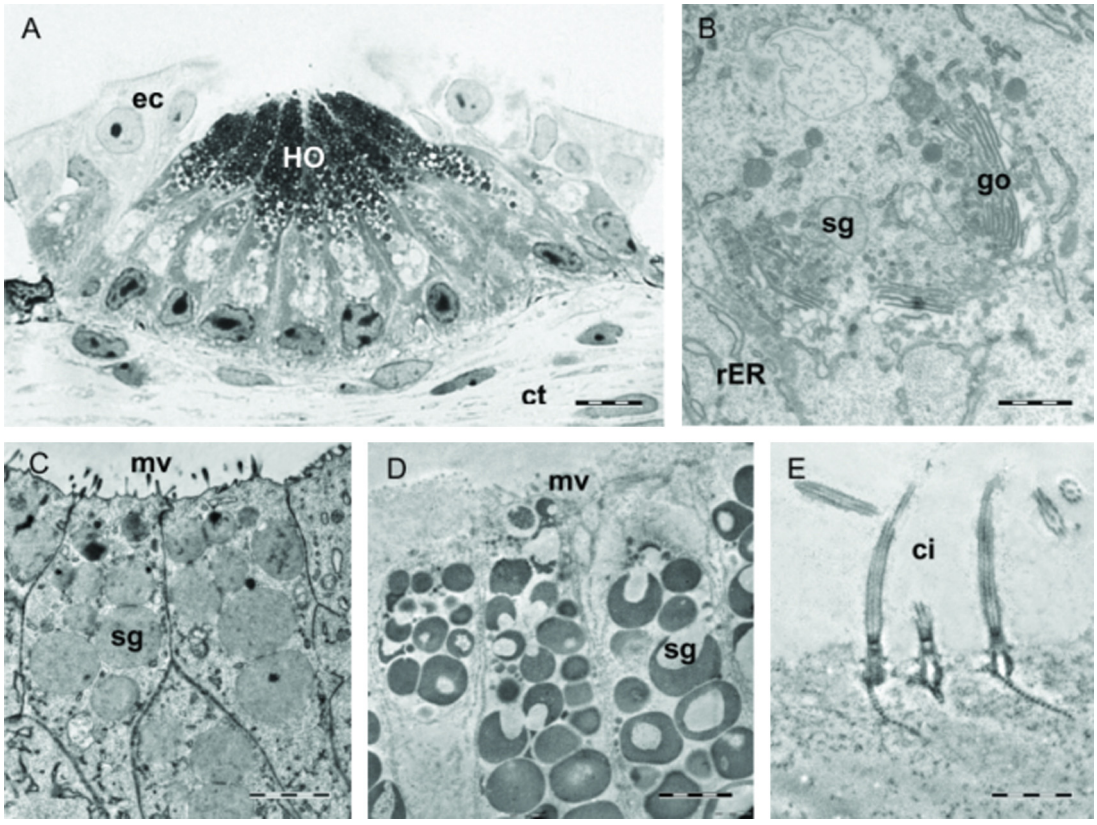

Fig. 7. *Loligo gahi*. (A) Glandular cells tapering towards the apical pole in cross section, forming a triangular shape. An epidermal fold covers partly the tips of the glandular cells (stage 29). (B) The synthesis is characterized by rER and a high amount of Golgi bodies (stage 25). (C) During the earlier development stage of the Hoyle organ the granules have a uniform, low density (stage 25). (D) In the mature secretory cells the granules are condensed and exhibit distinct low-density cavities (stage 29). (E) The bordering epithelium cells are characterized by their rooted cilia (stage 29). ci, cilia; ct, connective tissue; ec, epithelial cell; go, Golgi bodies; HO, Hoyle organ; mv, microvilli; rER, rough endoplasmic reticulum; sg, secretory granules. Scale bars: 20 μm (A); 1 μm (B); 2 μm (C and D); 1 μm (E).

membrane. The egg strands are light brown during female spawning and later embryonic development.

3.4.3. Behavioral observation of the hatching process

The embryo occupies about half the length of the egg and is clearly able to move around. Before hatch – during several hours up to one day – the animal starts to disperse secretory material on the chorion by sliding with its posterior tail along the egg membrane. As soon as a gap is digested, *Loligo* penetrates with its tail through the gap (takes about 10 min) (Fig. 4H–J), supported by strong mantle contractions and repulsive movements (Film sequence 2). Usually the hatchling immediately discards the remaining parts of the external yolk sac. Once leaving the egg, the embryo has to transit the matrix of the collective egg capsule. In a peripheral zone this takes a few minutes (cf. von Boletzky, 1978) but is delayed for embryos hatching in centrally located eggs, which have to squeeze their way through the closely spaced eggs.

Supplementary material related to this article found, in the online version, at http://dx.doi.org/10.1016/j.jcz.2013.04.001.

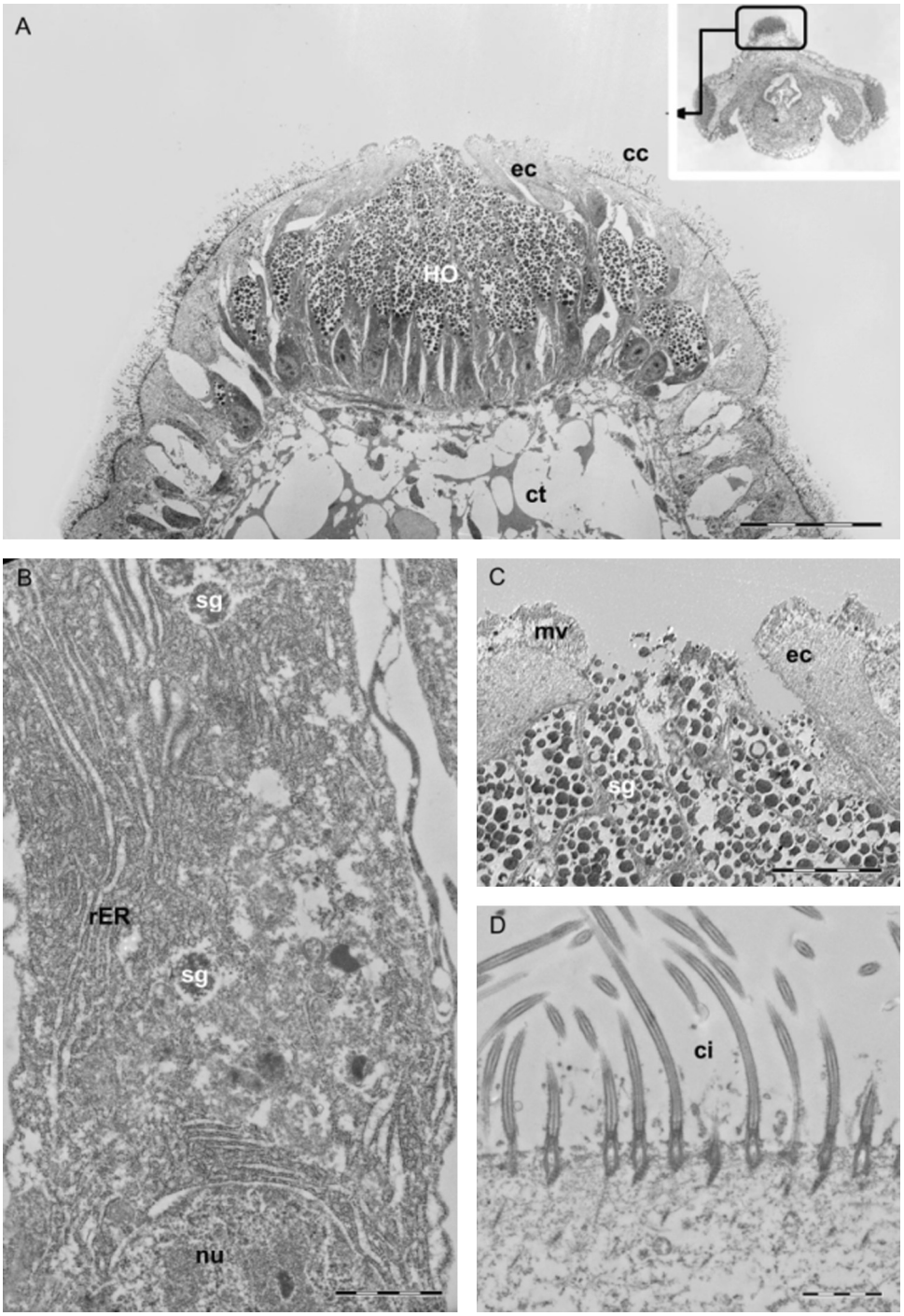

Fig. 8. *Sepioteuthis lessoniana.* (A) Cross section of the posterior mantle showing the prominent bands of the Hoyle organ. (B) Synthesis takes place above the nucleus, indicated by extensive rER. (C) Small peripheral epithelium cells are proximately adjoining to the glandular cells, followed (D) by the regular ciliated epithelium cells. cc, ciliated epithelium cells; ci, cilia; ct, connective tissue; ec, epithelial cell; HO, Hoyle organ; nu, nucleus; rER, rough endoplasmic reticulum; sg, secretory granules. Scale bars: 50 μm (A); 2 μm (B); 10 μm (C); 1 μm (D).

3.5. *Sepioteuthis lessoniana*

In comparison to the related loliginid species *Loligo gahi* as well as the other investigated cephalopod species, the HO of *S. lessoniana* is more prominent. This is due to the fact that the HO comprises more glandular cells, which are also larger in size. In addition, the gland system itself is considerably elevated (epithelial height 50 μm; HO 100 μm height) (Fig. 8A). In shape, the HO does not differ significantly from those of *Sepia* and *Loligo*: as in these two taxa it is anchor-shaped (Fig. 2E).

3.5.1. Cell types

The HO also consists only of one glandular cell type with a slender, columnar-shaped appearance. Cross-sections reveal that up to 20 cells are directly aligned with each other without interruption by other cell types. The cell nucleus is located basally, contains several nucleoli, and is surrounded by rER. The fixation with 50% isopropanol seems to be suboptimal for ultrastructural analysis; anyhow, remaining Golgi fragments in the cytoplasm indicate the presence of an earlier Golgi body within the gland cells (Fig. 8B) The secretory material consists of the round electron-dense granules

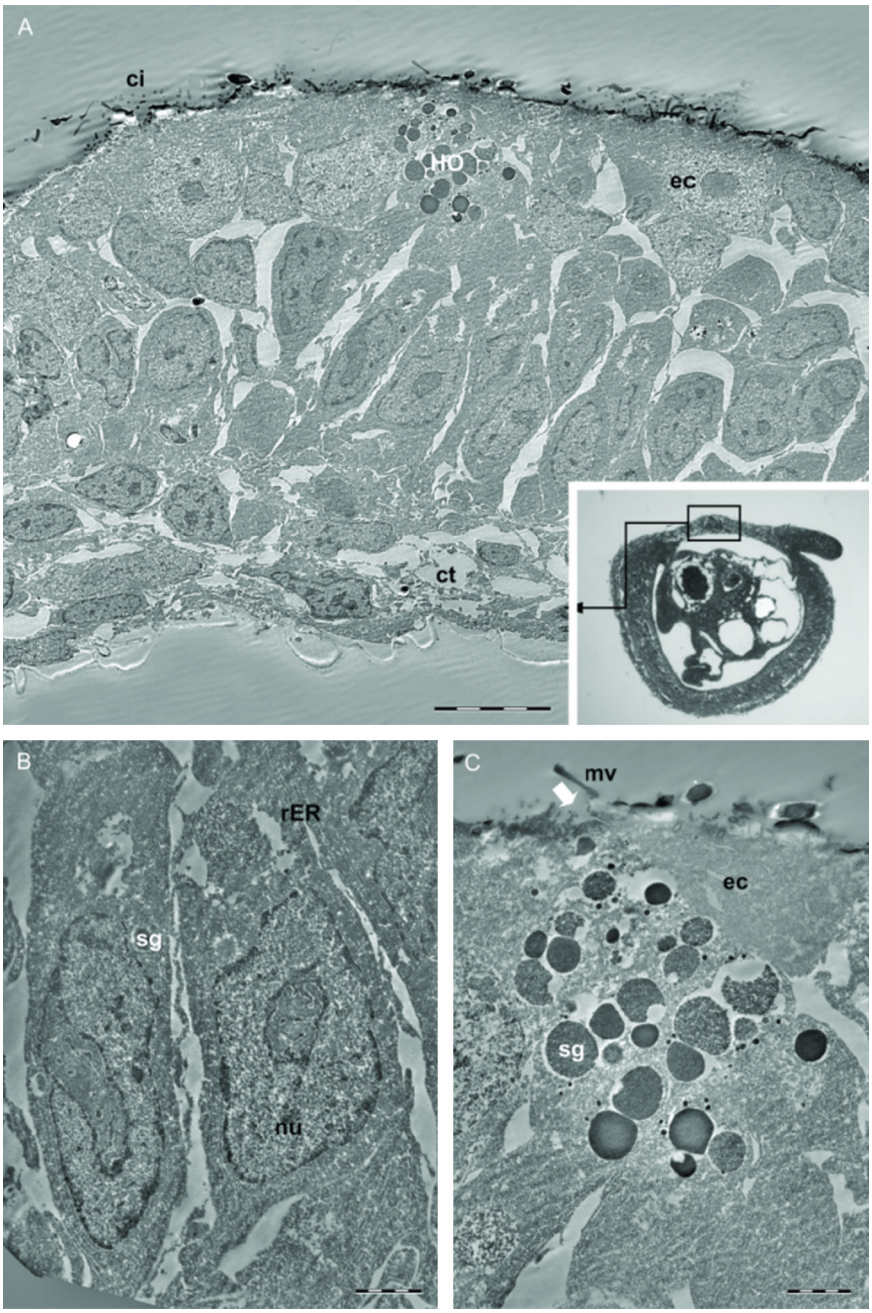

Fig. 9. *Architeuthis* sp. (A) The gland is inconspicuous in comparison to the other cephalopods; it is only weakly protruding from the surface and contains only a low number of cells. The few cells are only slightly filled with secretory granules. (B) Near the nucleus the secretory components are assembled and migrate to the cell surface. (C) As in the other Loliginids the granules are characterized by recessed areas. The epithelium cells cover the gland almost completely only leaving a narrow cleft (arrow). ci, cilia; ct, connective tissue; ec, epithelial cell; HO, Hoyle organ; mv, microvilli; nu, nucleus; rER, rough endoplasmic reticulum; sg, secretory granules. Scale bars: 10 μm (A); 2 μm (B); 2 μm (C).

(Ø 1.5 μm) with low density areas as also described for *Sepia* and *Loligo* (Fig. 8C).

Laterally to the HO gland cells, regular epithelium cells with rooted cilia (10 μm in length) are present and encase the HO (Fig. 8D). Their nuclei are mostly located in the centre or apically but never basally. This cell type is found throughout the epithelium. In contrast to this, a second, superficial epithelial cell type, is restricted to the outermost third of the epithelium and forms a lobe between the ciliated cells and the pore of the HO gland. The most prominent feature of this cell type is the presence of microvilli (2 μm in length) (Fig. 8C). All epithelial cell types are interconnected with each other via *zonulae adhaerentes*.

3.5.2. Egg-capsule description

Since we received only hatched embryos we could not follow the embryonic development and egg formation. As for *Octopus* we would like to refer to the pertinent literature for more information about the development of *Sepioteuthis* (Choe and Ohshima, 1961; Kondo, 1975; Shigeno et al., 2001b; Jackson and Moltschaniwskyj, 2002).

3.5.3. Behavioral observation of the hatching process

Not observed.

3.6. Architeuthis sp.

As seen from the outside, the HO has also an anchor-shaped appearance. The gland is only slightly elevated (35 μm cell height) in comparison to the normal epithelium (30 μm cell height). In cross section it is less clearly visible than in the other species (Fig. 2F). This may be related to the long fixation time in 10% formalin (~10 years) and/or that not the right stage was available.

3.6.1. Cell types

In cross-section, the organ is triangular in shape. Also, only one glandular cell type is present (Fig. 9A). The nucleus is located basally and surrounded by extensive rER layers (Fig. 9B). The secretory material of the *Architeuthis* HO consists of round electron-dense granules (Ø 2 μm), which condense frequently after secretion and display electron-bright cavities (Fig. 9C) as observed also in *Sepia*, *Loligo* and *Sepioteuthis*.

Ciliated epithelium cells cover almost entirely the tips of the glandular cells leaving only a small gap for secretion (Fig. 9C). In contrast to *Sepioteuthis*, no other cell types could be observed on the lateral boundaries of the HO.

3.6.2. Egg-capsule description

Eggs of *Architeuthis* are about 2 mm × 4 mm in size in late embryonic stages. The embryo itself measures about 2.5 mm in length (in elongated situation) and accordingly, it is able to move around freely (Fig. 4K).

3.6.3. Behavioral observation of the hatching process

Not observed.

3.7. Octopus vulgaris

Neither by means of μCT scans nor by light- and electron microscopical examinations we could detect any evidence of a HO.

3.7.1. Cell types

Instead, the entire mantle epithelium contains two different types of secretory cells: mucus cells with polygonal granules of

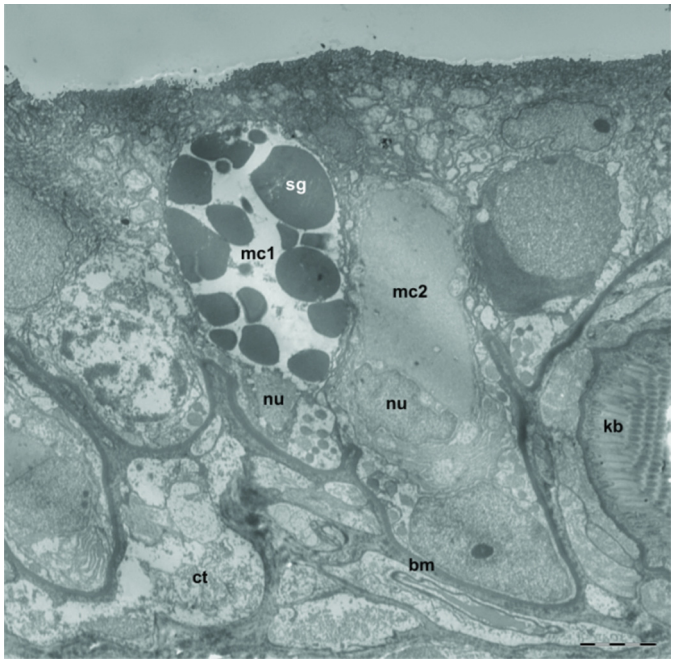

Fig. 10. *Octopus vulgaris*. Besides the regular epithelium cells the integument of *Octopus vulgaris* is dominated by two types of secretory cells. Mucus cells 1 contain polygonal granules, 2–3 μm in size, and mucus cells 2 are characterized by a homogenous fine grained material. A verification of the expected HO cells failed in the available specimens. bm, basal membrane; ct, connective tissue; kb, Kölliker bundle; mc1, mucus cell type 1; mc2, mucus cell type 2. Scale bar 2 μm.

2 μm in size and glandular cells with a homogenous, fine-grained content (Fig. 10). Both cell types have a polygonal nucleus in their base. Kölliker bundles are aligned all around the mantle.

3.7.2. Egg-capsule description

We received only fixed egg batches and therefore could not personally observe the embryonic development and hatching behaviour. Nevertheless, much is known about the egg development and position of the embryo during development in *Octopus*. For more information please consult the corresponding literature (Portmann, 1933; von Boletzky, 1966; Mather, 1984; Forsythe and Hanlon, 1985; Warnke, 1999; von Boletzky et al., 2001; Nepita Villanueva and Defeo, 2001; Ignatius and Srinivasan, 2006).

3.7.3. Behavioral observation of the hatching process

Not observed.

3.8. Tremoctopus gracilis

The HO is inconspicuous and can hardly be determined between the numerous mucus cells in the epithelium. We could identify two single rows of HO secretory cells crossing the posterior mantle pole (Fig. 11A). The cells have the same height as the remaining epithelium (up to 10 μm). Numerous Kölliker bundles are found in connective tissue and epithelium. In contrast to the decapods, *Tremoctopus* possesses a distinct basal membrane of 0.3–0.5 μm thickness along the epithelium base.

3.8.1. Cell types

The secretory cells belonging to the HO do not form cell aggregates as in the decapods but are individually arranged horizontally along the mantle end (Fig. 11A). Due to the low epithelium height, the cells have a more or less globular shape; almost half of the volume is claimed by the nucleus (Fig. 11B). The distal cell parts are

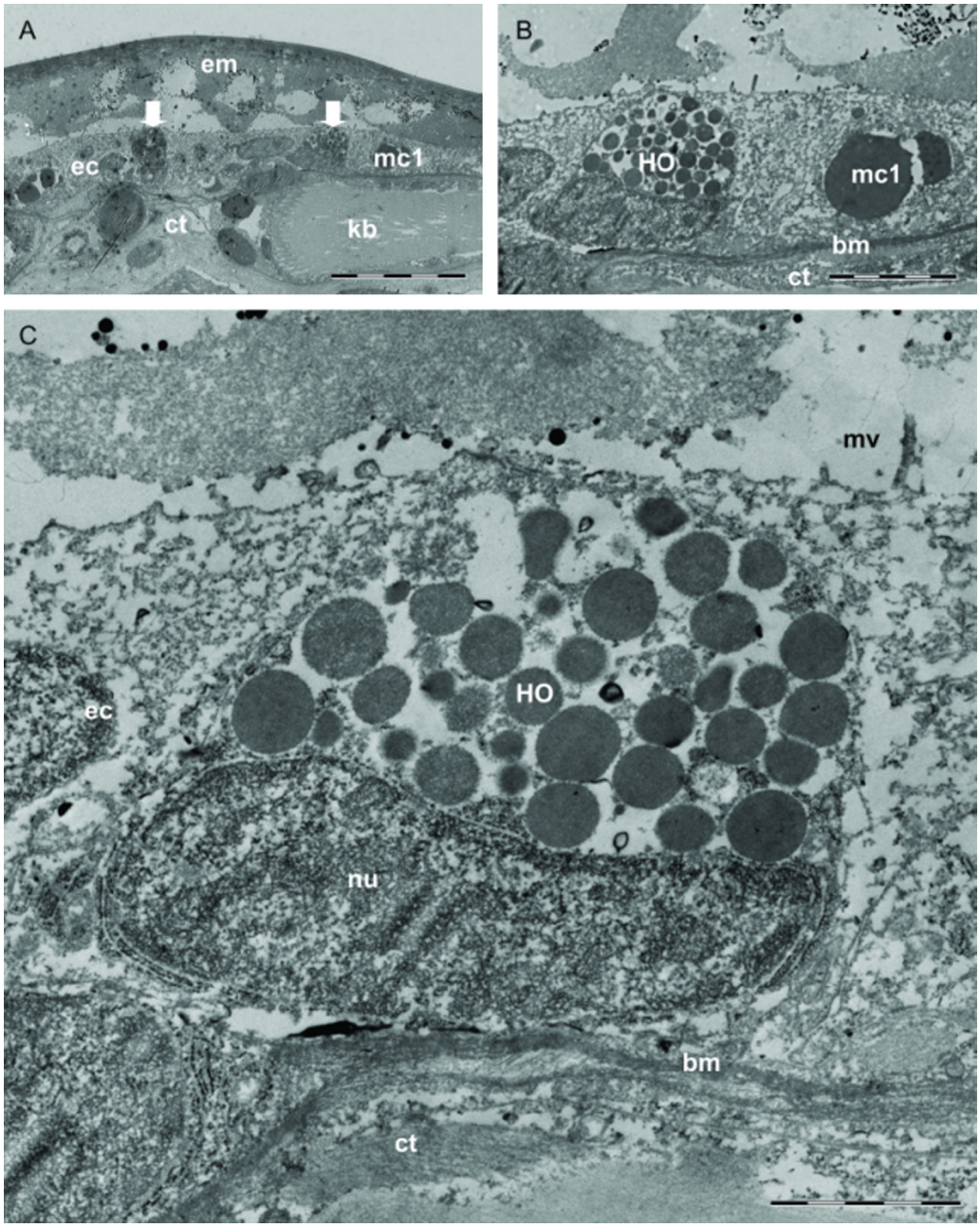

Fig. 11. *Tremoctopus gracilis*. The glandular cells of the Hoyle organ are much less abundant than in the decapods. (A) Only two solitary HO cells (arrows) are visible on the section close to the posterior mantle pole. (B) The majority of the epithelial glands are mucus cells with frequently fused secretory content. These cells are distributed along the entire mantle. (C) The Hoyle organ cells have a globular shape and are characterized by a flattened nucleus at their base and globular secretory granules of 1 μm in size. The epithelium is bordered basally by a basal membrane (0.3 μm thickness). bm, basal membrane; ct, connective tissue; ec, epithelial cell; em, egg membranes; HO, Hoyle organ cell; kb, Kölliker bundle; mc, mucus cell; mv, microvilli; nu, nucleus. Scale bars: 20 μm (A); 5 μm (B); 2 μm (C).

filled by globular granules of uniform density and a size of about 1 μm (Fig. 11C). Otherwise, the predominant mucus cells exhibit frequently amalgamated, amorphous granules, up to 4 μm in size (Fig. 11B). These cells are evenly distributed within the mantle epithelium. Both types of glandular cells are encased in epithelium cells covered by microvilli (0.5 μm length).

3.8.2. Egg-capsule description

Not observed.

3.8.3. Behavioral observation of the hatching process

Not observed.

3.9. Argonauta hians

The paper nautilus *Argonauta hians* lacks any external glandular structure, which might be linked to a hatching gland (Fig. 12A and B). Rather, the hatchlings bear Kölliker bundles on all parts of the body (Fig. 12C and D).

3.9.1. Cell types

The epithelium is rich in mucus cells: one type with polygonal secretory droplets and a second, less frequent type with a homogenous mucus (Fig. 12E–G).

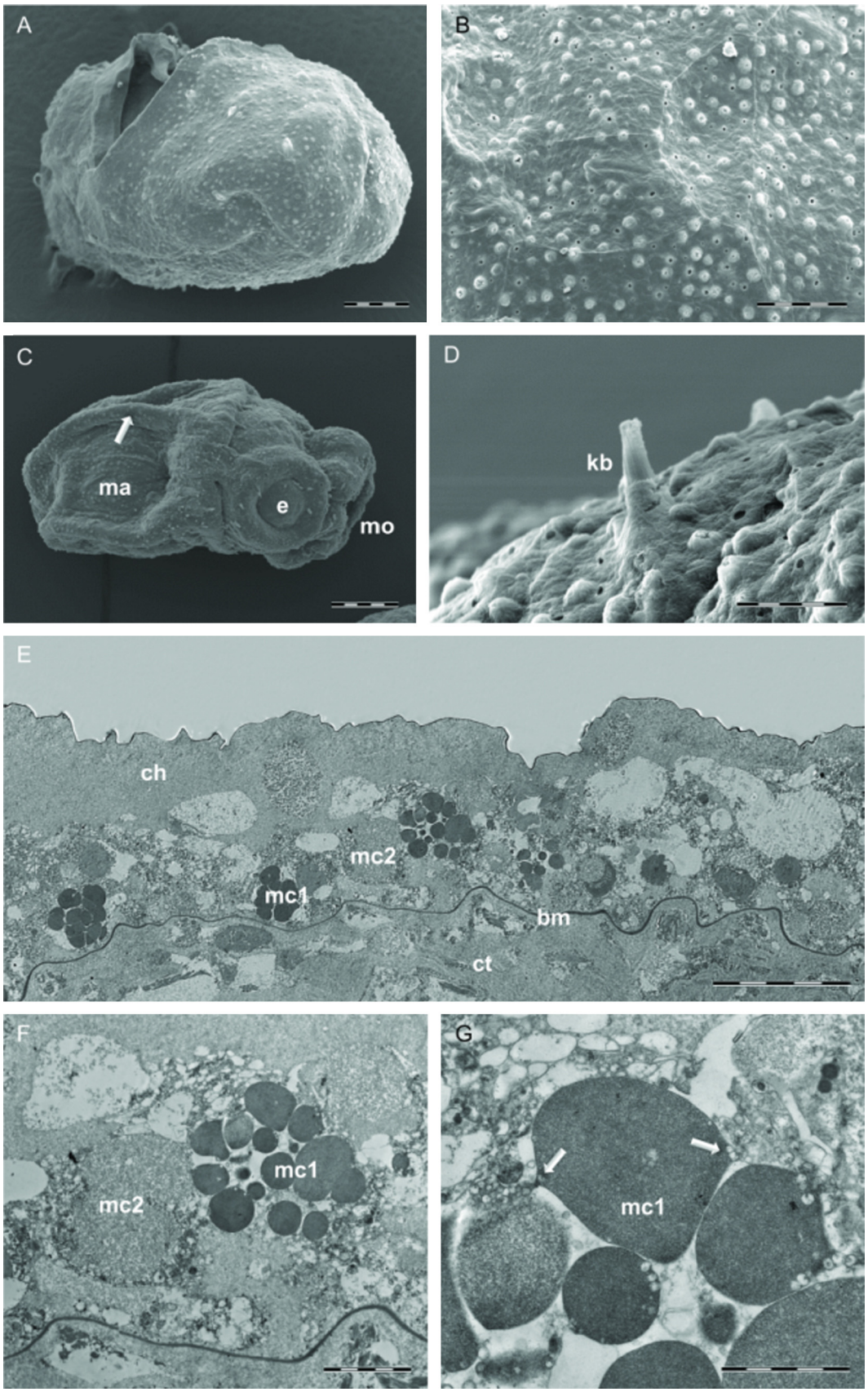

Fig. 12. *Argonauta hians*. (A) The external view on the posterior mantle part does not show a clearly visible hatching structure. (B) Higher magnification of the posterior mantle showing numerous gland pores. (C) Lateral view of the embryo. The elevations (white arrow) are decidedly dehydration artefacts. (D) Higher magnification of a Kölliker bundle present on all parts of the embryo's body. (E) Cross section of the posterior mantle epithelium with remaining parts of the chorion membrane. (F) The two occurring mucus cell types mc1 and mc2 are present in all parts of the mantle epithelium. (G) Some granules of mucus cells type1 appear to disintegrate, indicated by a release of foam like material from the granular periphery (white arrows). bm, basal membrane; ch, chorion membrane; ct, connective tissue; e, eye; kb, Kölliker bundle; ma, mantle; mc1, mucus cell type 1; mc2, mucus cell type 2; mo, mouth. Scale bars: 100 μm (A and C); 50 μm (B); 20 μm (D and E); 5 μm (F); 2 μm (G).

3.9.2. Egg-capsule description

The *Argonauta* female deposits several batches of fertilized eggs within its brood shell (less than 1 mm in size), whereas eggs in early development stages are located in the outer part of the brood shell aperture, those in late embryonic stages (13–15) in the inner part of the brood shell chamber. Furthermore, the egg batches can easily be separated visually by means of their colours, the early stages are white to yellow and those of the last embryonic stage are black. As typical for octopods the eggs of *Argonauta hians* are solitary and interconnected to each other by stalks; the embryos are covered by a chorion layer only, nidamental layers are absent. In late embryonic stages (around 12–15), according to the nomenclature by Sukhsangchan and Nabhitabhata (2007) and Sukhsangchan (2009), the embryos are tightly compressed within the egg and unable to move around (Fig. 4L).

3.9.3. Behavioral observation of the hatching process

Unfortunately it was impossible to observe the hatch of *Argonauta* embryos since they are permanently covered by the female in the brood shell. With isolated eggs it was possible to cultivate the embryos for some days; however during our analyses the embryos hatched exclusively at night and did not show any hatching behavior under artificial light.

4. Discussion

Earlier analyses of the hatching gland system in cephalopods focused on gland morphology (von Orelli, 1959; Arnold and Singley, 1989), cephalopod culture (von Boletzky, 1977, 1986, 2004; von Boletzky and Hanlon, 1983) and time of gland development (Fioroni, 1963; Arnold, 1965, 1974; Cardoso et al., 2005) but left a gap in our knowledge concerning a comparative cell type characterization. The present study aims to fill this gap and moreover to complement the morphological data with *in vivo* observations of the embryo within the egg. The results allow for direct comparison of the hatching enzymes of cephalopods with that of other invertebrates and vertebrates.

4.1. External morphology

This study largely corroborates the findings of von Orelli (1959). The Hoyle organ (HO) is located on the posterior mantle and consists of thin bands, which clearly differ from the normal epithelium. In the Decapodiformes (*Idiosepius*, *Euprymna*, *Sepia*, *Loligo*, *Sepioteuthis* and *Architeuthis*) the three bands are arranged in an anchor-like fashion: the median band is located on the dorsal side of the mantle and the two lateral ones extend to the fin bases.

In the Octopodiformes in contrast, the HO either appears as a single band horizontally along the mantle end (*Tremoctopus*) or is not externally visible (*Octopus* and *Argonauta*).

4.2. Internal morphology

In all decapods as well as *Tremoctopus*, only one glandular cell type represents the HO. These cells contain globular granules (1.5–3.0 μm in diameter) and are comparable among each other with regard to the amount of synthesis organelles, in particular the rER/Golgi-ratio. This observation indicates a similar composition of the secretory content in all observed species.

In *Sepia*, *Loligo*, *Sepioteuthis* and *Architeuthis* the secretory granules are modified in later stages by forming electron-lucent inclusions, named "bipartite dense granules" by Arnold and Singley (1989). In *Sepiella* the secretory granules have a similar bipartite appearance (Matsuno and Ouji, 1988). The function of bipartite dense granules remains questionable. We suppose a simple condensing artifact in most cases, occurring either native or caused by fixation.

The HO-bordering epithelium cells always lack secretory vesicles but frequently contain trans-Golgi network and cytoskeleton elements. In all observed species this cell type is apically covered with microvilli, and in all Decapodiformes it possesses cilia. In the most observed species (except for *Euprymna*) the glandular cell complex has a clearly defined lateral boundary. In *Idiosepius* only, the cell row next to the HO seems to be of a derived cell type, which has no counterpart in the mantle epithelium.

Our results are comparable with the observations by Arnold and Singley (1989), who proposed two cell types (named alpha and delta cells) in the HO of *Loligo pealei*. Based on the present results the glandular cells in *L. gahi* are related to the delta cells of *L. vulgaris*, which likewise contain secretory granules with electron-lucent inclusions. The non-secretory epithelium cells in *L. gahi* correspond with the alpha cell of *L. vulgaris*, whereas in *L. gahi* the fine filamentous material is absent.

4.3. Chemical composition

The glandular cells in the HO could produce a certain substance to support/improve the hatching process. Unfortunately, to-date it remains unclear what types of enzymes are involved in the chorion digestion of cephalopods. Arnold and Singley (1989) hypothesized that the digestive enzymes are of specific nature because weak acids, bases or proteases such as trypsin, pronase and protease K do not attack the chorion (Arnold and Singley, 1989).

Moreover, it remains unclear, if this secretory material contains only one enzyme or an enzyme complex as demonstrated for fishes as *Oryzias* (Yamagami, 1972, 1973, 1975; Yamamoto and Yamagami, 1975; Inohaya et al., 1995, 1997). Latest investigations have shown that the hatching gland of the frog *Xenopus* produce two enzymes, the first swells the eggs and partly digests the chorion (HCE with the isoforms HCE-1 and HCE-2), and the second completely digests the egg layers (LCE) (Yasumasu et al., 1989a,b).

In some cephalopod species (*Idiosepius*, *Euprymna*, *Loligo*) the perivitelline space starts to swell some days before hatching, indicating that an enzyme similar to HCE might be present.

The secretory droplets with heterogeneous electron-density in Loliginids. *Sepia* and *Sepiella* (Matsuno and Ouji, 1988) may be indications for the presence of an enzyme complex with at least two components. It remains unclear if this secreted material is produced by different enzymes or by density gradients generated by the chemical nature of a single enzyme. Secreted material in cephalopods does not usually react to any applied histochemical test (von Orelli, 1959; Matsuno and Ouji, 1988). It is therefore still challenging to analyze the components of the secreted material in the cephalopod's HO. Paulij et al. (1992) demonstrated that an extraction and basic characterization of the hatching enzymes from the perivitelline fluid is possible. However, the authors agree that it could not be excluded that enzymes from other organs might contaminate the extractions, leading to a false conclusion. Therefore, molecular and biochemical analyses are necessary (and under way) to provide more knowledge about the structure and components of the secreted material.

4.4. Egg capsule penetration and hatching behavior

Besides enzymatic support to hatching, some species use specialized structures or show a very active hatching behavior in order to penetrate the chorion and accelerate the hatching process.

Euprymna develops a short thick terminal spine on the posterior mantle pole which has been hypothesized to tap the chorion. Such a structure is also present in other Sepiolid species (*e.g. Rossia macrosoma*, *Sepiola affinis*) (von Boletzky, 1991). The spine of *Euprymna*

corresponds morphologically to those two species in size and form. As in *Euprymna* the degeneration of this hatching structure takes a while; in *Rossia* parts of the spine are still visible three month after hatching (von Boletzky, 1991). As in *Euprymna*, the spines of *Rossia* and *Sepiola* are of muscular nature, clearly distinguishable from the underlying mantle musculature and only marginally covered by epithelial cells. It remains to be known why the degradation of the hatching glands in *Euprymna* takes such a long time (more than 2 days after hatch) and if the spine degeneration plays a role in this extended degeneration process.

Idiosepius actively uses its arms to push with its posterior end of its mantle against the chorion. A similar behavior of penetrating the egg with the rear of the mantle could be observed in *Euprymna*. Besides the mechanical pushing against the chorion by the *Idiosepius* hatchling, the microvilli border along the three glandular bands of the HO might help to distribute the enzymes via a brush-function or by roughening the chorion.

A similar penetration behavior was also documented by von Orelli (1959) in *Loligo vulgaris*; this animal narrows the posterior end of its mantle and penetrates the chorion. Once part of the mantle fits through the chorion, the gap is widened by mantle expansion (von Orelli, 1959). In contrast, Arnold and Singley (1989) described that embryos of *L. pealei* attach "to the inside of the chorion to localize the effect of the digestive secretion onto one place on the chorion". Our observed specimens of *L. gahi* rather disperse the enzyme by gliding along a large membrane area (see Film sequence 2). It thus seems that the animals developed different strategies to achieve the best "outcome".

4.5. Comparison with other hatching systems

Hatching glands are not limited to cephalopods but are also present in other invertebrates and vertebrates. Although this structure and its function have been known for a long time, only a few morphological studies focusing on the gland system and the cellular composition have been carried out, most of them on fishes.

As far as documented in the literature, the hatching gland systems in other invertebrates (crustaceans as *Sesarma haematocheir*) (Saigusa and Terajima, 2000) and vertebrates (fishes as *Esox lucius*, *Oryzias latipes*, *Betta splendens*, *Clupea harengus* as well as amphibians as *Xenopus laevis*) (Yoshizaki, 1973; Rosenthal and Iwai, 1979; Schoots et al., 1982; Ishida, 1985; Mabee et al., 1998) consist of one glandular cell type only, mostly named hatching gland cell (HGC). The cells of this type are either separated or clustered but all synthesize granules of different size (*e.g.* in *Clupea harengus* 2–3 μm in diameter) (Rosenthal and Iwai, 1979) and different electron density. In *Oryzias latipes*, the granules coalesce in the late embryonic stage and gradually form a large rounded secretory mass (nothing similar is mentioned for the other hatching glands).

To date the total number of gland cells within hatching systems remains unknown, only for *Clupea harengus* were about 1500–2000 gland cells per embryo statistically calculated (Rosenthal and Iwai, 1979). This demonstrates that the embryos need a certain amount of enzymes for hatching.

While all systems possess only one glandular cell type, their granular components differ strongly regarding their enzyme numbers and types. While for *Oryzias latipes* (see above) two enzymes are needed, one to swell the egg (LCE) and the other to digest the chorion (HCE) (Yamagami, 1973, 1975, 1996; Yasumasu et al., 2010a), for *Esox lucius* and for the turtle *Pelodiscus sinensis* only one enzyme appears to be present (Schoots and Denuce, 1981; Schoots et al., 1982; Yasumasu et al., 2010b). In other animals only basic information about the hatching enzymes are known, *e.g.* trypsin in the moth *Antheraea* trypsin (Kafatos and Williams, 1964), serine protease in the frog *Xenopus laevis* (Carroll and Hedrick, 1974), serine esterase in the sea urchin *Strongylocentrotus purpuratus* (Barrett and Edwards, 1976) or chorionase in the fish *Salmo gairdneri* (Hagenmaier, 1974).

The present study provides a broad comparison of the hatching gland in different cephalopod groups. The characterization shows that only one glandular cell type is involved in the hatching process. However, since it is currently impossible to identify the secreted material by histochemical and biochemical methods, other techniques are required to verify if these materials are of the same nature in all cephalopods. Molecular biological analyses are necessary (and currently being undertaken) to characterize the secreted material and identify the genes involved in gland formation and degradation. The latter will help to provide a clearer picture of the Hoyle organ in cephalopods and allow further comparison with the hatching glands in other invertebrates and vertebrates.

Financial support

This work on the hatching system in cephalopods was supported by the Austrian Science Foundation FWF (Project No. P 21135-B17) and by the ASEA-UNINET University of Vienna Austria.

Acknowledgements

We like to thank Prof. Dr. Jaruwat Nabhitabhata from the Department of Biology (Cephalopod Research Unit), Faculty of Science, Prince of Songkla University, Thailand for critically reading the manuscript.

We are grateful to MSc. Jitima Suwanmala and Dr. Charuay Sukhsangchan from the Kasetsart University Bangkok, Thailand, for their assistance in collection, cultivating of *Idiosepius pygmaeus* and *Argonauta hians* and providing Fig. 4L for this study. The collection was permitted by the National Research Council Thailand (NRCT) Project No. 002.3/2999. Collection of *Sepia officinalis* was done together with Dr. Anna Palumbo and Teresa Mattiello from the Stazione Zoologica Anton Dohrn, Naples, Italy. Samples of *Euprymna scolopes* were provided by Dr. Marie Therese Nödl and Dr. Heinz Gert de Couet from the University of Hawaii, Manoa USA. Image 3D was gratefully provided by Dr. Patricia N. Lee from the Kewalo Marine Lab, Pacific Biosciences Research Center, USA, published in Lee et al. (2009). Fig. 1B of *Euprymna scolopes* was gratefully provided by Alexandra Kerbl from the Department of Integrative Zoology, Faculty of Life Sciences, University of Vienna, Austria. Hatchlings of *Loligo gahi* were cultivated by the first author under the supervision of Dr. Paul Brickle and Dr. Alexander Arkhipkin from the Falkland Islands Fisheries department, UK. Embryos of *Octopus vulgaris* were given by Dr. Pedro Domingues from the Instituto Español de Oceanografía in Spain. Hatchlings of *Sepioteuthis lessoniana* and *Tremoctopus gracilis* were given by Dr. Richard Young University of Hawaii, Manoa USA. Embryonic stages of *Architeuthis* sp. were provided from the collection of the Johann Wolfgang Goethe-Universität Frankfurt am Main, Germany.

References

Arnold, J.M., 1965. Normal embryonic stages of the squid, *Loligo pealii* (Lesueur). Biological Bulletin 128 (1), 24–32.

Arnold, J.M., 1974. Embryonic development. In: Arnold, J.M., Summers, W.C., Gilbert, D.L., Manalis, R.S., Daw, N.W., Lasek, R.J. (Eds.), A Guide to Laboratory Use of the Squid *Loligo pealei*. Woods Hole, pp. 24–44.

Arnold, J.M., Singley, C.T., 1989. Ultrastructural changes in the cells of the Hoyle organ during hatching of the squid *Loligo peali*. Journal of Cephalopod Biology 1 (1), 1–14.

Barrett, D., Edwards, B.F., 1976. Hatching enzyme of the sea urchin Strongylocentrotus purpuratus. In: Lorand, L. (Ed.), Methods in Enzymology. Vol. XLV: Proteolytic Enzymes Part B. Academic Press, New York, pp. 354–373.

Brocco, S.L., O'Clair, R.M., Cloney, R.A., 1974. Cephalopod integument: The ultrastructure of Kölliker's organs and their relationship to Setae. Cell Tissue Research 151, 293–308.

Cardoso, F., Baltazar, P., Bautista, J., 2005. The early development of the Patagonia squid Loligo gahi D'Orbigny, 1835 in Peruvian waters (Cephalopoda: Loliginidae). Revista Peruana de Biología 12 (3), 369–376.
Carroll, E.J., Hedrick, J.L., 1974. Hatching in the toad *Xenopus laevis*: morphological events and evidence for a hatching enzyme. Developmental Biology 38, 1–13.
Choe, S., Ohshima, Y., 1961. On the embryonal development and the growth of the squid *Sepioteuthis lessoniana* lesson. Venus, The Japanese Journal of Malacology 21 (4), 462–476.
Fioroni, P., 1962a. Die embryonale Entwicklung der Hautdrüsen und des Trichterorganes von *Octopus vulgaris* Lam. Acta Anatomica 50, 264–295.
Fioroni, P., 1962b. Die embryonale Entwicklung der Kölliker'schen Organe von *Octopus vulgaris* Lam. Revue Suisse de Zoologie 69 (30), 497–511.
Fioroni, P., 1963. Zur embryonalen und postembryonalen Entwicklung der Epidermis bei zehnarmigen Tintenfischen. Verhandlungen der Naturforschenden Gesellschaft in Basel 74 (2), 149–160.
Fioroni, P., 1978. Morphogenese der Tiere: Cephalopoda. VEB Gustav Fischer Verlag, Jena.
Forsythe, J.W., Hanlon, R.T., 1985. Aspects of egg development, post-hatching behavior, growth and reproductive biology of *Octopus burryi* Voss, 1950 (Mollusca: Cephalopoda). Vie Milieu 35 (3/4), 273–282.
Hagenmaier, H.E., 1974. The hatching process in fish embryos. V. Characterization of the hatching protease (Chorionase) from the perivitelline fluid of the Rainbow Trout, *Salmo gairdneri* Rich, as a metalloenzyme. Wilhelm Roux'Archiv 175, 157–162.
Hibbard, H., 1937. The hatching of the squid. Biological Bulletin 73 (385).
Ignatius, B., Srinivasan, M., 2006. Embryonic development in *Octopus aegina* Gray, 1849. Current Science 91 (8), 1089–1092.
Inohaya, K., Yasumasu, S., Araki, K., Naruse, K., Yamazaki, K., Yasumasu, I., Iuchi, I., Yamagami, K., 1997. Species-dependent migration of fish hatching gland cells that express astacin-like proteases in common. Development, Growth & Differentiation 39 (2), 191–197.
Inohaya, K., Yasumasu, S., Ishimaru, M., Ohyama, A., Iuchi, I., Yamagami, K., 1995. Temporal and spatial patterns of gene expression for the hatching enzyme in the teleost embryo, *Oryzias latipes*. Developmental Biology 171 (2), 374–385.
Ishida, J., 1985. Hatching enzyme: past, present and future. Zoological Science 2, 1–10.
Jackson, G.D., Moltschaniwskyj, N.A., 2002. Spatial and temporal variation in growth rates and maturity in the Indo-pacific squid *Sepioteuthis lessoniana* (Cephalopoda: Loliginidae). Marine Biology 140, 747–754.
Kafatos, F.C., Williams, C.M., 1964. Enzymatic mechanism for the escape of certain moths from their cocoons. Science 146, 538–540.
Kondo, A., 1975. The morphological observations on the Hoyle organ of a squid, *Sepioteuthis lessoniana*. Zoolological Magazine 84 (4), 480.
Lee, P.N., McFall-Ngai, M.J., Callaerts, P., de Couet, H.G., 2009. The Hawaiian bobtail squid (*Euprymna scolopes*): a model to study the molecular basis of eukaryote-prokaryote mutualism and the development and evolution of morphological novelties in cephalopods. Cold Spring Harbor Protocols 2009 (11), 1–13.
Mabee, P.M., Cua, D.S., Barlow, S.B., Helvik, J.V., 1998. Morphology of the hatching glands in *Betta splendens* (Teleostei: Perciformes). Copeia 4, 1021–1026.
Mather, J.A., 1984. Development of behaviour in *Octopus joubini* Robson, 1929. Vie Milieu 34 (1), 17–20.
Matsuno, A., Ouji, M., 1988. Ultrastructural studies on development of the tail gland of a cuttlefish, *Sepiella japonica*. Development, Growth & Differentiation 30 (6), 673–680.
Nepita Villanueva, M.R., Defeo, O., 2001. Growth of *Octopus maya* (Mollusca: Cephalopoda) of the Yucatan coast, Mexico: a long-term analysis. Revista de biología tropical 49 (1), 93–101.
Paulij, W.P., Verhoof, H.C.C.M., Denuce, J.M., 1992. Partial purification and characterization of *Loligo vulgaris* hatching enzyme obtained from hatching medium. Comparative Biochemistry and Physiology Series B 101 (4), 617–622.
Portmann, A., 1933. Observation sur la vie embryonnaire de la pieuvre (*Octopus vulgaris* Lam.). Archives de Zoologie experimentale et generale 76 (II), 24–36.
Reynolds, E.S., 1963. The use of lead citrate at high pH as an electron-opaque stain in electron microscopy. Journal of Cell Biology 17, 208–212.
Rosenthal, H., Iwai, T., 1979. Hatching glands in heering embryos. Marine Ecology Progress Series 1, 123–127.
Saigusa, M., Terajima, M., 2000. Hatching of an estuarine crab, *Sesarma haematocheir*: From disappearance of the inner (E3) layer to rupture of the egg case. Journal of Experimental Zoology 287, 510–523.
Schoots, A.F.M., Denuce, J.M., 1981. Purification and characterization of hatching enzyme of the pike (*Esox lucius*). International Journal of Biochemistry 13, 591–602.
Schoots, A.F.M., Opstelten, R.J.G., Denuce, J.M., 1982. Hatching in the pike *Esox lucius* L.: evidence for a single hatching enzyme and its immunocytochemical localization in specialized hatching gland cells. Developmental Biology 89, 48–55.
Shigeno, S., Kidokoro, H., Goto, T., Tsuchiya, K., Segawa, S., 2001a. Early ontogeny of the Japanese common squid *Todarodes pacificus* (Cephalopoda, Ommastrephidae) with special reference to its characteristic morphology and ecological significance. Zoological Science 18, 1011–1026.
Shigeno, S., Tsuchiya, K., Segawa, S., 2001b. Embryonic and paralarval development of the central nervous system of the loliginid squid *Sepioteuthis lessoniana*. Journal of Comparative Neurology 437 (4), 449–475.
Sukhsangchan, C., 2009. Behavior and life history of paper Nautilus (*Argonauta hians* Lightfood, 1786) in the Andaman Sea, Thailand., pp. 1–138.
Sukhsangchan, C., Nabhitabhata, J., 2007. Embryonic development of Muddy Paper Nautilus *Argonauta hians* Lightfood, 1786, from Andaman Sea, Thailand. Kasetsart Journal (Natural Science) 41, 531–538.
von Boletzky, S., 1966. Zum Schlüpfen von *Octopus vulgaris* Lam. Verhandlungen der Naturforschenden Gesellschaft in Basel 77, 164–170.
von Boletzky, S., 1977. Post-hatching behavior and mode of life in cephalopods. Symposia of the Zoological Society of London 38, 557–567.
von Boletzky, S., 1978. Ciliary locomotion in squid hatching. Experientia 35, 1051–1052.
von Boletzky, S., 1986. Encapsulation of cephalopod embryos: a search for functional correlations. American Malacological Bulletin 4 (2), 217–227.
von Boletzky, S., 1991. The Terminal spine of sepiolid hatchlings: its development and functional Morphology (Mollusca: Cephalopoda). Bulletin of Marine Science 49 (1–2), 107–112.
von Boletzky, S., 2004. A brief survey of cephalopod culture techniques. Turkish Journal of Aquatic Life 2 (2), 229–240.
von Boletzky, S., Erlwein, B., Hofmann, D.K., 2006. The *Sepia* egg: a showcase of cephalopod embryology. Vie et Milieu – Life & Environment 56 (2), 191–201.
von Boletzky, S., Fuentes, M., Offner, N., 2001. First record of spawning and embryonic development in *Octopus macropus* (Mollusca: Cephalopoda). Journal of the Marine Biological Association of the United Kingdom 81, 703–704.
von Boletzky, S., Hanlon, R.T., 1983. A review of the laboratory maintenance, rearing and culture of cephalopod molluscs. Memoirs of the Museum of Victoria 44, 147–187.
von Orelli, M., 1959. Über das Schlüpfen von *Octopus vulgaris*, Sepia officinalis und Loligo vulgaris. Revue Suisse de Zoologie 66 (18), 330–343.
von Querner, F.R., 1927. Die Köllikerschen Büschel jugendlicher Octopoden, nebst einigen Bemerkungen zur Histologie der Haut dieser Formen. Zeitschrift für Zellforschung und mikroskopische Anatomie 4, 237–265.
Warnke, K., 1999. Observations on the Embryonic Development of *Octopus mimus* (Mollusca: Cephalopoda) from Northern Chile. The Veliger 42 (3), 211–217.
Yamagami, K., 1972. Isolation of a choriolytic enzyme (Hatching enzyme) of the teleost, *Oryzias atipes*. Developmental Biology 29, 343–348.
Yamagami, K., 1973. Some enzymological properties of a hatching enzyme (chorionase) isolated from the fresh-water teleost, *Oryzias latipes*. Comparative Biochemistry and Physiology Series B Biochemistry & Molecular Biology 46 (3), 603–616.
Yamagami, K., 1975. Relationship between two kinds of hatching enzymes in the hatching liquid of the Medaka, *Oryzias latipes*. Journal of Experimental Zoology 192, 127–132.
Yamagami, K., 1996. Studies on the hatching enzyme (Choriolysin) and its substrate, egg envelope, constructed of the precursors (Choriogenesis) in *Oryzias latipes*: a sequel to the information in 1991/1992. Zoological Science 13, 331–340.
Yamamoto, M., Yamagami, K., 1975. Electron microscopic studies on choriolysis by the hatching enzyme of the teleost, *Oryzias latipes*. Developmental Biology 43, 313–321.
Yasumasu, S., Iuchi, I., Yamagami, K., 1989a. Isolation and some properties of low choriolytic enzyme (LCE), a component of the hatching enzyme of the teleost, *Oryzias latipes*. Journal of Biochemistry 105, 212–218.
Yasumasu, S., Iuchi, I., Yamagami, K., 1989b. Purification and partial characterization of high choriolytic enzyme (HCE), a component of the hatching enzyme of the teleost *Oryzias latipes*. Journal of Biochemistry 105, 204–211.
Yasumasu, S., Kawaguchi, M., Ouchi, S., Sano, K., Murata, K., Sugiyama, H., Akema, T., Iuchi, I., 2010a. Mechanism of egg envelope digestion by hatching enzymes, HCE and LCE in medeka, *Oryzias latipes*. Journal of Biochemistry 148 (4), 439–448.
Yasumasu, S., Uzawa, M., Iwasawa, A., Yoshizaki, N., 2010b. Hatching mechanism of the Chinese soft-shelled turtle *Pelodiscus sinensis*. Comparative Biochemistry and Physiology Series B Biochemistry & Molecular Biology 155, 435–441.
Yoshizaki, N., 1973. Ultrastructure of the hatching gland cells in the South African clawed toad, *Xenopus laevis*. Journal of the Faculty of Science Series 6, Zoology 18 (4), 469–480.

MECHANISMS OF DEVELOPMENT 135 (2015) 43–57

Available at www.sciencedirect.com

ScienceDirect

journal homepage: www.elsevier.com/locate/modo

Alterations in the mantle epithelium during transition from hatching gland to adhesive organ of *Idiosepius pygmaeus* (Mollusca, Cephalopoda)

Norbert Cyran [a,*], *Waltraud Klepal* [a], *Yannick Städler* [b], *Jürg Schönenberger* [b], *Janek von Byern* [c,d]

[a] *Faculty of Life Sciences, Core Facility Cell Imaging and Ultrastructural Research, University of Vienna, Althanstrasse 14, Vienna 1090, Austria*

[b] *Department of Structural and Functional Botany, Faculty Centre of Biodiversity, University of Vienna, Rennweg 14, Vienna 1030, Austria*

[c] *Center for Integrative Bioinformatics Vienna, Max F Perutz Laboratories, Dr. Bohr-Gasse 9, Vienna 1030, Austria*

[d] *Ludwig Boltzmann Institute for Experimental and Clinical Traumatology, Austrian Cluster for Tissue Regeneration, Donaueschingenstrasse 13, Vienna 1200, Austria*

ARTICLE INFO

Article history:
Received 5 September 2014
Received in revised form
27 November 2014
Accepted 28 November 2014
Available online 4 December 2014

Keywords:
Hatching gland
Hoyle organ
Adhesive organ
Cell degeneration
Programmed cell death

ABSTRACT

Epithelial gland systems play an important role in marine molluscs in fabricating lubricants, repellents, fragrances, adhesives or enzymes. In cephalopods the typically single layered epithelium provides a highly dynamic variability and affords a rapid rebuilding of gland cells. While the digestive hatching gland (also named Hoyle organ) is obligatory for most cephalopods, only four genera (*Nautilus*, *Sepia*, *Euprymna* and *Idiosepius*) produce adhesive secretions by means of glandular cells in an adhesive area on the mantle or tentacles. In *Idiosepius* this adhesive organ is restricted to the posterior part of the fin region on the dorsal mantle side and well developed in the adult stage. Two gland cell types could be distinguished, which produce different contents of the adhesive. During the embryonic development the same body area is occupied by the temporary hatching gland. The question arises, in which way the hatching gland degrades and is replaced by the adhesive gland.

Ultrastructural analyses as well as computer tomography scans were performed to monitor the successive post hatching transformation in the mantle epithelium from hatching gland degradation to the formation of the adhesive organ. According to our investigations the hatching gland cells degrade within about 1 day after hatching by a type of programmed cell death and leave behind a temporary cellular gap in this area. First glandular cells of the adhesive gland arise 7 days after hatching and proceed evenly over the posterior mantle epithelium. In contrast, the accompanying reduction of a part of the dorsal mantle musculature is already established before hatching. The results demonstrate a distinct independence between the two gland systems and illustrate the early development of the adhesive organ as well as the corresponding modifications within the mantle.

* Corresponding author. Cell Imaging and Ultrastructural Research, Faculty of Life Sciences, University of Vienna, Althanstrasse 14, UZA 1, A-1090 Wien, Austria. Tel.: +43 1 4277 54425; fax: 43-1-4277-876301.
E-mail address: norbert.cyran@univie.ac.at (N. Cyran).

http://dx.doi.org/10.1016/j.mod.2014.11.003
0925-4773/

1. Introduction

The characterization of adhesive systems and their glue in marine and terrestrial animals is currently the topic of many researchers (Smith and Callow, 2006; von Byern and Grunwald, 2010). While most studies focused on the gland morphology and glue analysis in adult animals, less is known about the formation and differentiation of such adhesive structures during embryonic development. Studying glandular growth and expansion is helpful to obtain a firmer understanding of the basic principles involved in the adhesive gland formation.

Idiosepiidae are a small taxon of cephalopods, represented by a single genus with eight species (Jereb and Roper, 2005) although a recent re-characterization assumes a reduction to four or five species (Nabhitabhata and Suwanmala, 2008; von Byern and Klepal, 2010; von Byern et al., 2012). One conspicuous morphological character of the family is the adhesive organ, which is restricted to the posterior part of the fin region on the dorsal mantle side. Structurally, the adhesive organ can be easily distinguished from the regular mantle epithelium by its rough-textured surface (Cyran et al., 2011; Sasaki, 1921; von Byern et al., 2008). The animals use the glue from the adhesive glands to stick to sea grass leaves or algae for camouflage and drift protection (Suwanmala et al., 2006b).

Morphological studies in adults confirm two distinct glandular cell types (columnar and granular cells) and one type of sensory cells (fusiform cells) composing the adhesive organ (Cyran et al., 2011; von Byern et al., 2008). Both glandular cell types contain neutral mucopolysaccharides (periodate-reactive substances) and basic proteins (Biebrich Scarlet test), but in a different ratio (von Byern et al., 2008). Obviously, substances secreted by these two glandular cell types are responsible for adhesion (Cyran and von Byern, 2010; Cyran et al., 2011; von Byern et al., 2008).

Previous observations of juvenile *Idiosepius* showed that the adhesive organ is not operational directly after hatching (Suwanmala et al., 2006a). First attachment behaviour seems to be visible around day 12 (J. von Byern, personal observations, 2008); however, other behavioural studies (Nabhitabhata, 1994) indicate a 30 day post-hatching phase before the animals attach with their adhesive organ.

von Byern et al. (2006) proposed that the adhesive organ arises during embryonic stage 24 as an anchor-shaped organ and continues its development after hatching. However, later re-characterization has shown that the pre-hatching anchor-shaped organ on the posterior mantle surface resembles the hatching gland (Arnold and Singley, 1989; Cyran et al., 2013; Matsuno and Ouji, 1988; von Orelli, 1959) rather than the adhesive gland.

The hatching glands (also termed Hoyle organ) occur in most cephalopods as a temporary organ, arising during late embryonic stages and degrading after hatching (Adam, 1939; Arnold, 1965; Arnold and Singley, 1989; Arnold and Williams-Arnold, 1980; Fioroni, 1963; Hibbard, 1937; Hoyle, 1889; Jecklin, 1934; Matsuno and Ouji, 1988; Shigeno et al., 2001; von Orelli, 1959). The function of the hatching gland is to digest the tough protective egg layers by means of choriolytic enzymes, synthesized in specific glandular cells. Following hatching, the production of secretory material ceases and the hatching gland degrades within hours or a few days (Cyran et al., 2013; von Orelli, 1959).

The rapid degradation of the hatching gland indicates a triggered disassembling mechanism, although of a hitherto undescribed type. The respective cells pass through a sequence of disintegrative cell alterations, obviously triggered by specific signal molecules. This process is referred to as programmed cell death. Traditionally three types can be distinguished: apoptosis, autophagy and necrosis (Wyllie et al., 1980). Generally, programmed cell death is essential for cell homeostasis in animal tissues, in particular during embryonic development, organogenesis and tissue remodelling (Zakeri and Lockshin, 2002).

In case of the hatching gland of cephalopods, cell death occurs twice: Several days before hatching, cells of the dorsal mantle epithelium disintegrate and make space for the arising gland cells. After hatching the hatching gland becomes obsolete. In the course of its autolysis the hatching gland cells undergo massive alterations and are finally eliminated. This study deals with the latter process.

With the present study we aim to describe the post hatching morphological modifications within the mantle epithelium of *I. pygmaeus*, in particular the transition from the hatching gland towards the adhesive gland. Although the origin and function of the adhesive gland in *Idiosepius* has been known for more than 90 years (Sasaki, 1921), details about its development still remain unknown. In the present study, ultrastructural analyses and X-ray microtomography imaging are used to characterize the hatching gland degradation and adhesive gland development during development of the juvenile *I. pygmaeus*.

The results will help to understand the formation of glandular structures in cephalopods and allow a detailed characterization of the immature gland cells. Comparison of the data with those recorded for the mature hatching gland (Cyran et al., 2013) and the adhesive organ in the adult *Idiosepius* species (Cyran et al., 2011) will serve to draw a complete picture of the morphological differentiation within the mantle epithelium during the transition from the hatching gland to the adhesive organ.

2. Results

The present findings cover the developmental activities between prehatching and juvenile stage. During the period of about 2 weeks we observed the morphological remodelling of the mantle epithelium, including the degradation of the hatching gland and the origin of the adhesive organ in *Idiosepius pygmaeus*.

2.1. *Hatching gland development and morphology*

At embryonic stage 25 all three bands of the hatching gland are well developed, showing its typical anchor shape (Fig. 1A,B). Externally the gland structure is slightly elevated from the normal mantle epithelium. The hatching gland boundary is lined by narrow, modified epithelial cells with long microvilli (Fig. 1B–D). Basally in the glandular cells the secretory

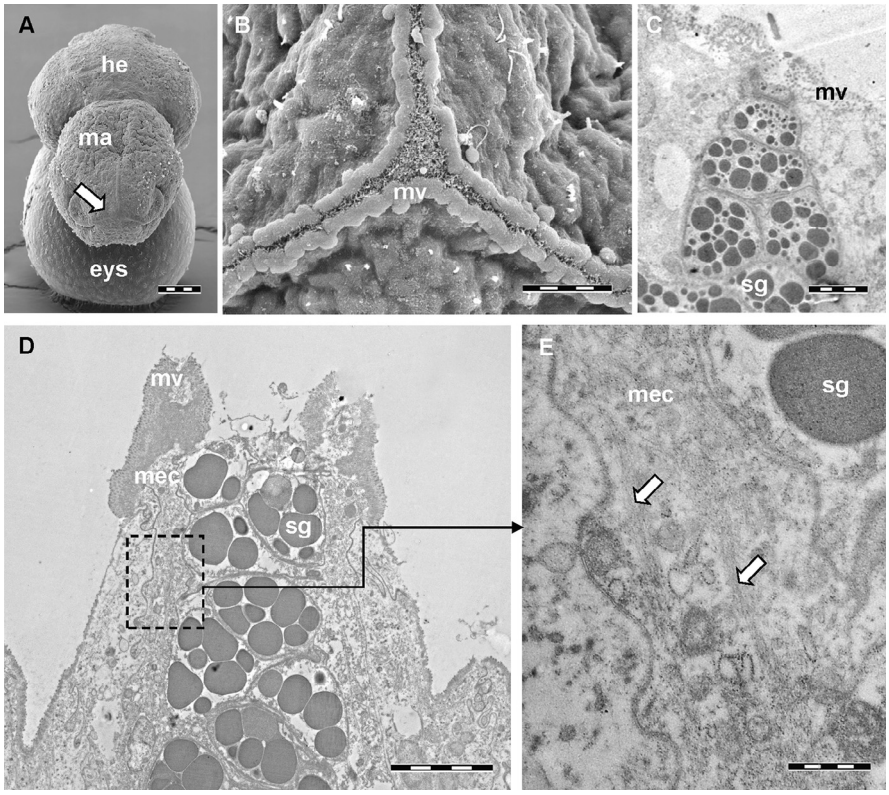

Fig. 1 – Early appearance of the hatching gland (embryonic stage 25, A–C) and stage of beginning secretion (embryonic stage 29, D, E). (A) SEM image of *Idiosepius pygmaeus*, showing the anchor-shaped hatching gland on the posterior mantle pole (arrow). (B) The elevated parts indicate the microvilli of the modified epithelium cells which delimit the secretory cells laterally. (C) In particular during the earlier hatching gland development the microvilli largely cover the tips of the secretory cells. (D) Later in development (embryonic stage 29) the bordering modified epithelium cells have a characteristic dense cytoplasm and (E) longitudinal filament bundles (arrows). eys, external yolk sac; he, head; ma, mantle; mec, modified epithelium cells; mv, microvilli; sg, secretory granules. Scale bars: 100 μm (A); 20 μm (B); 2 μm (C); 5 μm (D); 1 μm (E).

granules are assembled near the nucleus while the apical areas of the glandular cells are already packed with electron dense secretory granules. From stage 29 onwards, the secretory cells shrink in width, due to the beginning secretory process and the stagnating synthesis activity. The cytoplasm density of the gland cells increases considerably. Likewise the bordering modified epithelial cells become more compact, bundles of parallel cytoskeletal filaments become apparent in proximity of the epithelial surface (Fig. 1D,E) and the cell apices elevate more clearly from the surface than in earlier stages (Fig. 1D).

2.2. *Hatching gland degradation*

Post hatching, the organ degrades within approximately 1 day, whereby several stages of deterioration are distinguishable:

- The hatching gland cells start to disintegrate immediately after hatching. Initially, the endoplasmic reticulum swells and agglutinates with the premature secretory vesicles (Fig. 2A).
- Subsequently, the organelles degrade in an apparently unspecific manner, beginning at the cell bases, while the mature secretory droplets in the cell tips remain intact at first (Fig. 2B,C). The secretory cells regress further, leaving behind an increasing furrow. Concurrently, the modified epithelial cells recede, as well (Fig. 3). Merely remnants of the microvilli border, the apical cell areas and the nucleus are existent, while the bulk of the once compact cytoplasm no longer exists.
- Clumped compartments of the secretory cells containing secretory material and organelles appear to be ingested by neighbouring epithelial cells (Fig. 3). So far the nuclei of the secretory cells are not essentially affected by the degradation. They still look like the nuclei of other cells.
- The surrounding epithelium finally replaces the secretory cells. After 24 hours the epithelial cells form a mantle surface without any evidence of the vanished hatching gland.

2.3. *Mantle epithelium of the paralarvae*

The mantle epithelium has a height of about 40 μm dorsally and 20 μm ventrally at the time of hatching. During the first 2 weeks of the planktonic stage it grows to a height of 50–60 μm dorsally and 25 μm ventrally. The basement membrane between the epithelium and the connective tissue is 0.35 μm thick. Basal cells, goblet cells and saccular cells resembling in shape and content those of the adult stage are present in the mantle epithelium of the late embryonic stage 29 (Fig. 4A).

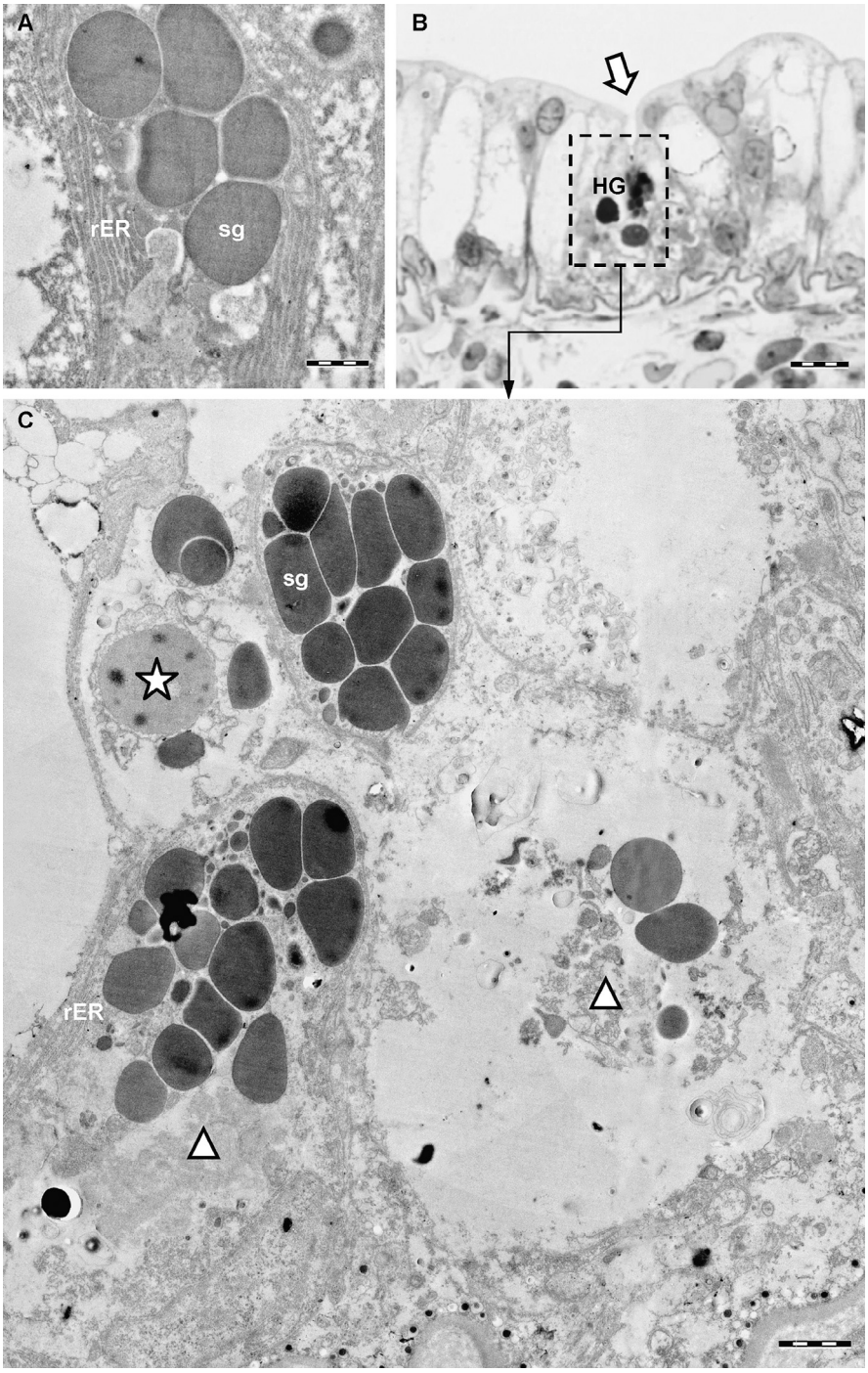

Fig. 2 – Degradation of the hatching gland after hatch. (A) A few hours after hatch the endoplasmic reticulum swells and agglutinate with the circumjacent granules. (B) The secretory cells shrink and lead to the formation of a longitudinal groove along the extension of the hatching gland (arrow). (C) In the distal cell regions the secretory granules fuse (asterisk) while in the basal cell regions degradation of organelles and secretory material is evident (triangles). HG, hatching gland; rER, rough endoplasmic reticulum; sg, secretory granules. Scale bars: 1 μm (A); 10 μm (B); 2 μm (C).

The **basal cells** form a continuous slender cell layer (about 3–5 μm high) along the basement membrane (Fig. 4B) over the entire mantle epithelium. **Goblet cells** contain a homogeneous secretory material of different density, according to their degree of maturity. Some cells with lower density content synthesize material while others, tightly packed cells show evidence of secretion (Fig. 5A,B). The cells contain parallel microtubules in longitudinal direction along the lateral cell border. These tubules condense before the cells release their content.

Saccular cells occur in different stages, determined by the appearance of the secretory material. Some cells are full of homogenous material (Fig. 5C) and sporadic flocculent

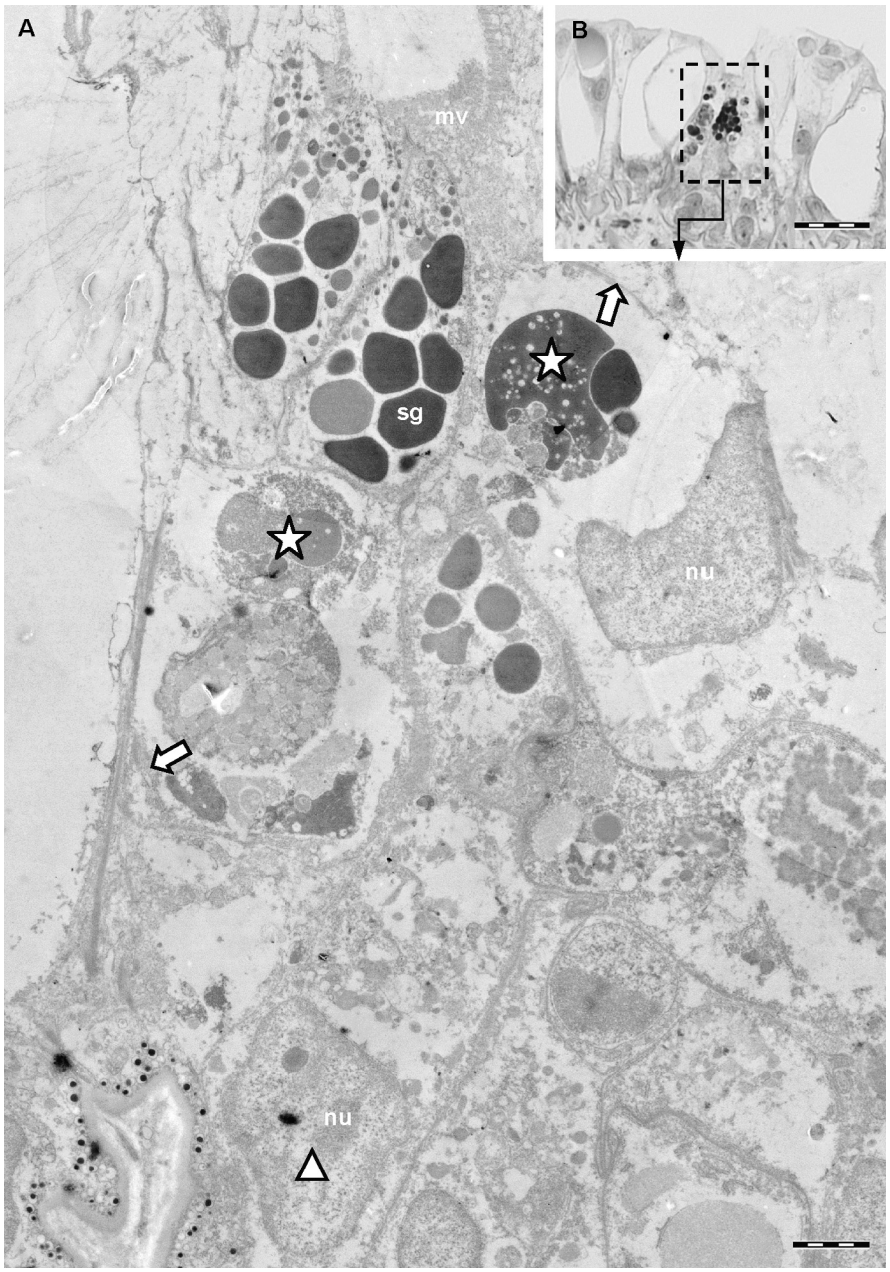

Fig. 3 – Degradation of the hatching gland. The clumped secretory material (asterisks) and other organelle remnants of the secretory cells are obviously incorporated by the neighbouring epithelium cells. This is indicated by properties of the respective cell as the distal location of the nucleus, parallel filament bundles (arrows) and in particular the microvilli on the cell surface. The nuclei of the secretory cells (triangle) appear still intact, even containing nucleoli. mv, microvilli; nu, nucleus; sg, secretory granules. Scale bar: 2 μm (A) 20 μm (B).

agglomerations. In others, only partly filled cells, the secretory content appears coarsely-grained or flocculent (Fig. 5D). In general the saccular cells contain a narrow area (about 0.5 μm wide) of cytoplasm along the lateral cell border, composed of endoplasmic reticulum, mitochondria and longitudinal filaments. Frequently, almost empty cells with more or less disintegrated cytoplasm can be found (Fig. 5E). While the nucleus of the saccular cells with remaining lateral cytoplasm has a roundish shape, it is flattened in empty cells (without lateral cytoplasm) (Fig. 5E). In hatchlings and paralarvae the saccular cells are more often empty than in embryos.

Interstitial cells as unspecific, non-secretory epithelial cells fill the space between the glandular cells. The shape of the cells and location of the nucleus comply with the shape of the neighbouring cells.

Only the goblet cells exhibit a distinct distribution pattern within the epithelium: In late embryonic stages the goblet cells are concentrated around the posterior mantle pole and in two angular lines each crossing the dorsal and ventral mantle side (Fig. 6A, B). The dorsal bands proceed along the border of the emerging adhesive organ. Beyond these areas the concentration of the goblet cells is lower. In early juveniles this

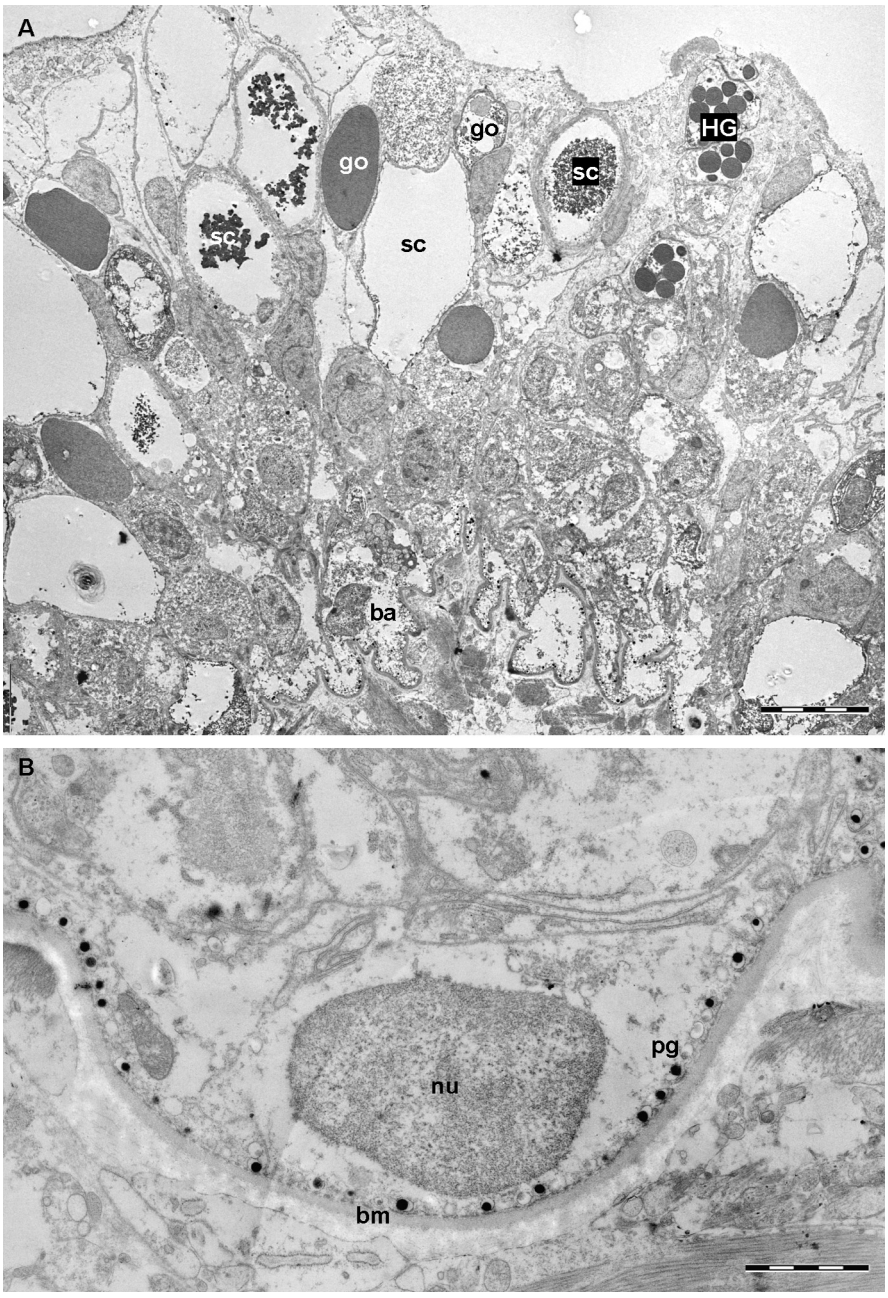

Fig. 4 – Mantle epithelium of the paralarvae (embryonic stage 29). (A) Overview of the cell types in the mantle epithelium. (B) Basal cell with pigment granules aligned along the basal membrane. ba, basal cell; bm, basal membrane; go, goblet cell; HG, hatching gland; nu, nucleus; pg, pigment granules; sc saccular cell; pg, pigment granules. Scale bars: 10 μm (A); 2 μm (B).

arrangement becomes even more conspicuous (7 day old animal in Fig. 6C–F). In particular the high abundance around the posterior pole is obvious.

2.4. *Adhesive organ development in the juvenile* Idiosepius

The distribution of the adhesive organ-related gland cells is random within the entire subsequently occupied area of the mature organ. A clearly orientated development (e.g. from the centre of the gland area to its periphery or opposite) could not be observed.

First indications for gland cells, belonging to the adhesive organ, appear about 7 days after hatching (Fig. 7). Columnar cells originate between the epithelial cells adjacent to the basement membrane, initially containing a roundish nucleus surrounded by rough endoplasmic reticulum. Rapidly the columnar cells extend towards the epithelial surface. Secretory granules, delivered by the endoplasmic reticulum in the cell base, migrate towards the apical cell pole where they accumulate. Thereby the granules apparently track along microtubules (Fig. 7B) by overcoming a still remaining central bottleneck. The columnar cells, always occurring in clusters in

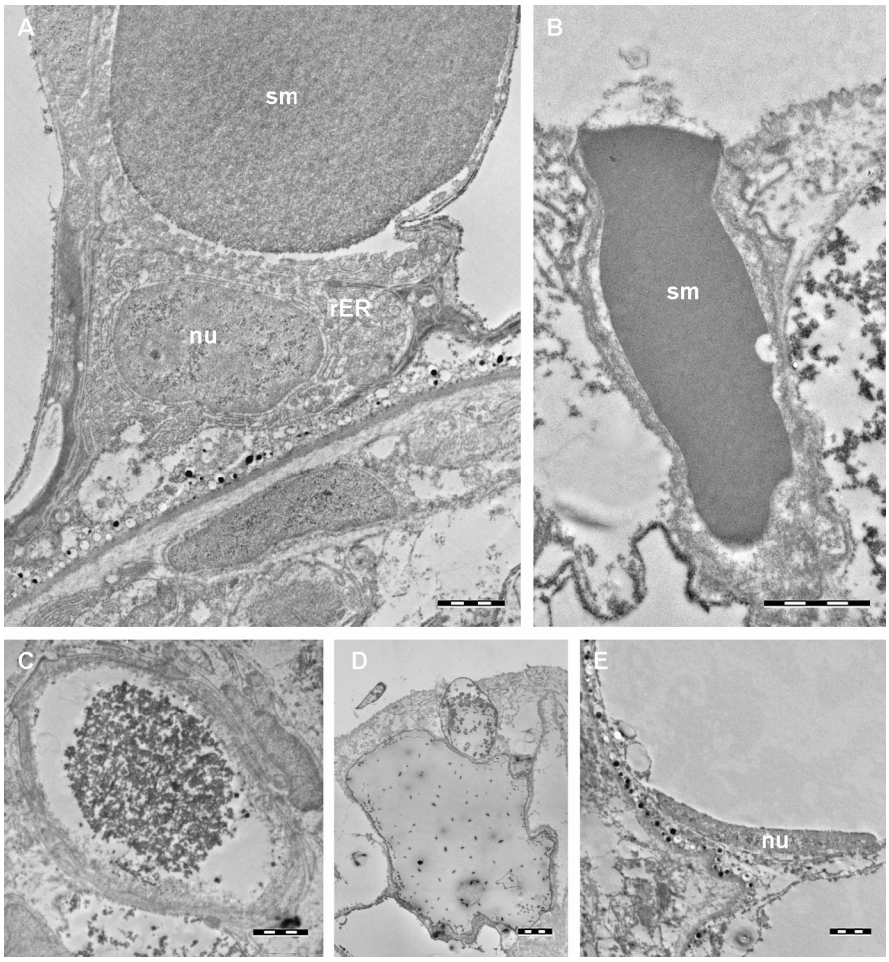

Fig. 5 – Cells of the regular epithelium at embryonic stage 29 (A–B, goblet cells; C–E, saccular cells). (A) In this goblet cell the secretory material fuses to a uniform mass above the nucleus. (B) A later maturity stage of a goblet cell with densified content. Saccular cells were observed in different physiological stages; (C) containing condensed aggregations of flocculent material and a distinct lateral cytoplasm area, (D) containing homogeneous fine-grained material of low density, (E) or appearing as completely discharged cells with a highly flattened and obviously inactive nucleus. nu, nucleus; rER, rough endoplasmic reticulum; sg, secretory granules; sm, secretory material. Scale bars: 2 μm (A, B, C, E); 5 μm (D).

the mature adhesive organ, likewise develop simultaneously with the other cells of the cluster. However, the columnar cells are not yet separated from each other by intermediate epithelial cells but have still direct contact with the other columnar cells in the cluster.

Ten days after hatching the first columnar cells are almost completely filled with secretory material (Fig. 8A). Meanwhile spacing epithelial cells have emerged between the glandular cells and separate them from each other. However, so far we could not find any indication of fusiform cells, which are obligatory in each columnar cell cluster in the adults. In addition, the first granular cells arise (Fig. 8B). As for the columnar cells the secretory granules initially agglomerate at the apical cell pole.

The accompanying modification of the dorsal mantle musculature, described in an earlier study by Cyran et al. (2011) and comprising an almost complete reduction of a drop shaped area (in top view) (Fig. 9B) near the posterior pole, is already finalized before hatching at embryonic stage 29 (Fig. 9): The anterior half of the mantle muscles is arranged in a closed circle (in cross section) as usual for cephalopods (Fig. 9C). The majority of the posterior dorsal parts of the mantle muscles are disconnected from the mantle epithelium. A muscle free area is forming, roughly displaying the distribution of the adult adhesive organ. Within this area the musculature is no longer arranged in a closed circle. Instead, the open ends of the muscle ring are connected with the intestinum (Fig. 9D–G,I).

3. Discussion

This study illustrates the rapid reorganization in the post hatching mantle epithelium of *Idiosepius pygmaeus* and illuminates the chronological succession of hatching gland degradation and rise of the adhesive organ. It should be pointed out that the embryonic development as well as the juvenile growth is strongly influenced by water temperature and therefore the time measurements may differ from earlier observations.

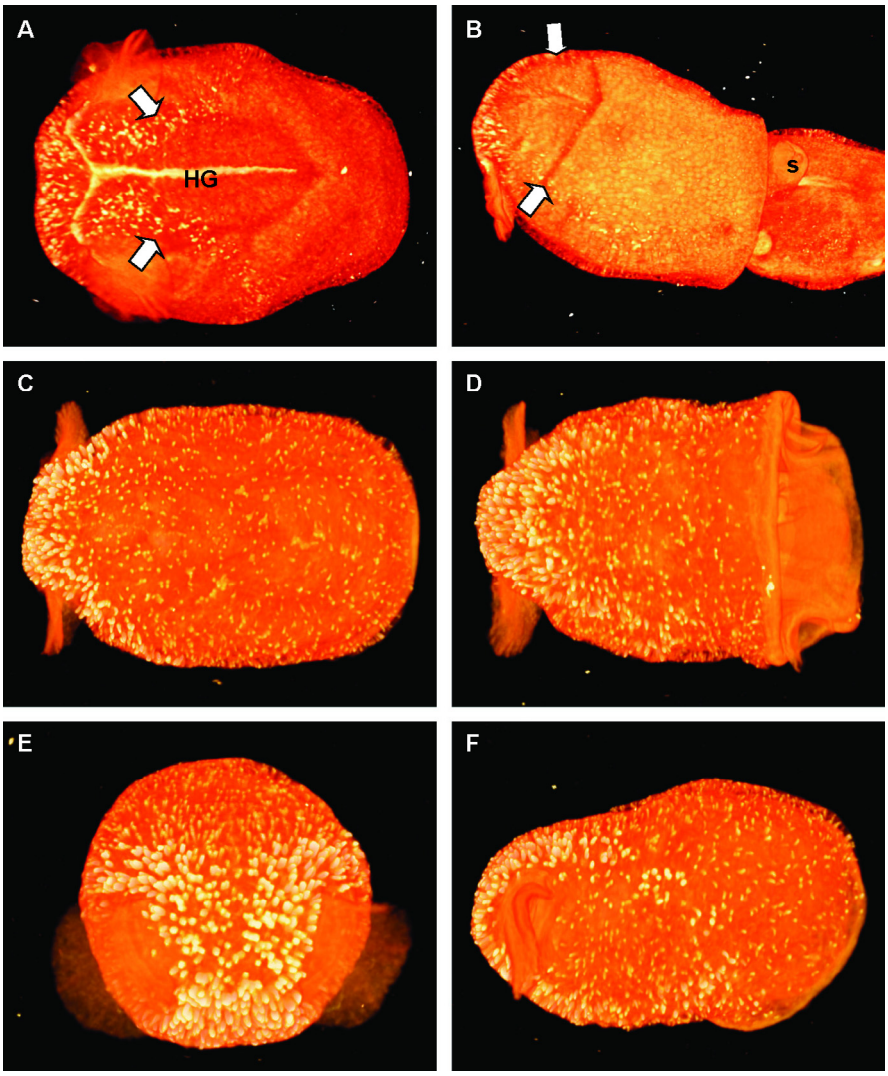

Fig. 6 – Microcomputer tomographic illustrations of the goblet cells distribution during the late embryonic and the early juvenile stages. The cells were stained with phosphotungstic acid. (A and B) Embryonic stage 29 (dorsal and ventral mantle side). In particular the posterior mantle pole provides a high abundance of goblet cells. Moreover two distinct diagonal bands are visible dorsally and two slight bands ventrally (arrows). (C–F) Seven day old hatchling (dorsal, ventral, posterior and sagittal view). The concentration of goblet cells is considerably higher than in the embryonic stages. HG, hatching gland; s, sipho.

3.1. *Relationship between the hatching gland and the adhesive organ*

Since the hatching gland of the embryo and the adhesive organ of the adult *I. pygmaeus* require the same area on the mantle surface, a possible relationship between the two organs was thought in the past (von Byern et al., 2006). However, our present results clearly disprove this presumption by showing that the first cells relating to the adhesive organ arise several days after the hatching gland disappears. Moreover, although the location is comparable, the distribution pattern of the two gland systems differs strongly. Furthermore, a functional shift of glandular cells is unlikely. Therefore it is assumed that the referred glands are two independent structures and represent different developmental stages of the animal.

3.2. *Hatching gland morphology*

Morphologically the hatching gland of *I. pygmaeus* resembles widely that of *L. pealei* (Arnold and Singley, 1989), except for the granules of the digestive cells, which are bipartite in *Loligo pealei* but not in *Idiosepius*. A detailed comparison of the different hatching glands in cephalopods was already done in a previous study (Cyran et al., 2013). At this point we want to emphasize a special cell type occurring in *Idiosepius* and *L. paelei*, which has not been described for other cephalopods so far.

As in *Loligo pealei* (Arnold and Singley, 1989) the hatching gland cells in *I. pygmaeus* are flanked along the edges by cells (referred to as alpha cells in *L. pealei*) with a distinct microvilli margin, abundant small vesicular and tubular content as well as longitudinal cytoskeletal filaments. Likewise, this type

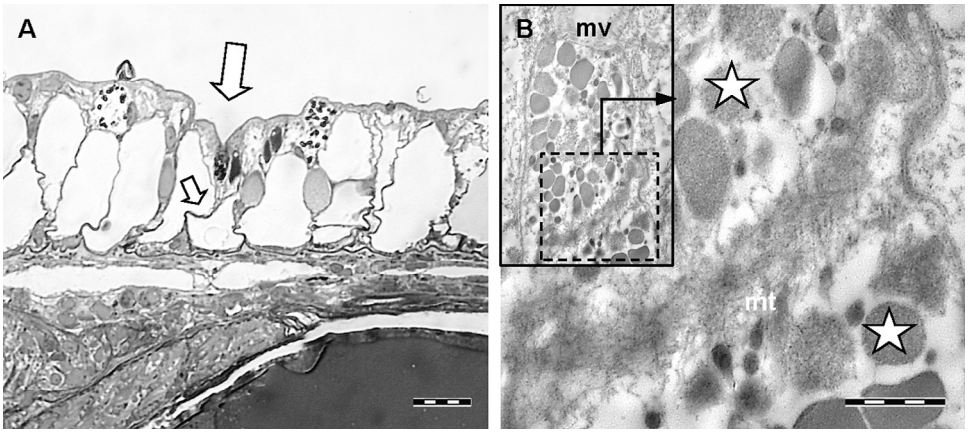

Fig. 7 – Seven day old hatchling. (A) The first distinct appearance of columnar cells (large arrow) is noticeable. The cells are still largely empty and have a central bottleneck (small arrow). (B) Secretory granules accumulate in the apical cell areas. Microtubules are aligned alongside the cell borders. The image shows two adjacent columnar cells (asterisks) without spacing interstitial cells, indicating their conjoint development as a cell cluster. In this state the columnar cell are still adjacent to each other. mt, microtubules; mv, microvilli. Scale bars: 20 μm (A); 1 μm (B).

of cells emerges with the developing hatching gland cells and disappears coincidently with the degrading hatching gland. Numerous Golgi bodies in the central cell area as well as the dense trans-Golgi network and scores of small vesicles right next to the cell surface indicate a high secretory activity.

Similarly as supposed for the alpha cells in *L. pealei* (Arnold and Singley, 1989), the modified epithelial cells may play a role in localizing the effect of the digestive secretion not only by inhibiting a lateral dispersion beyond the microvilli margin. As outlined by Arnold and Singley (1989), these cells release an adhesive, responsible for the attachment behaviour of *L. pealei*. This attachment behaviour also applies to *I. pygmaeus* (Cyran et al., 2013). To what extent a real adhesive substance or possibly a sucker effect causes the attachment remains unanswered.

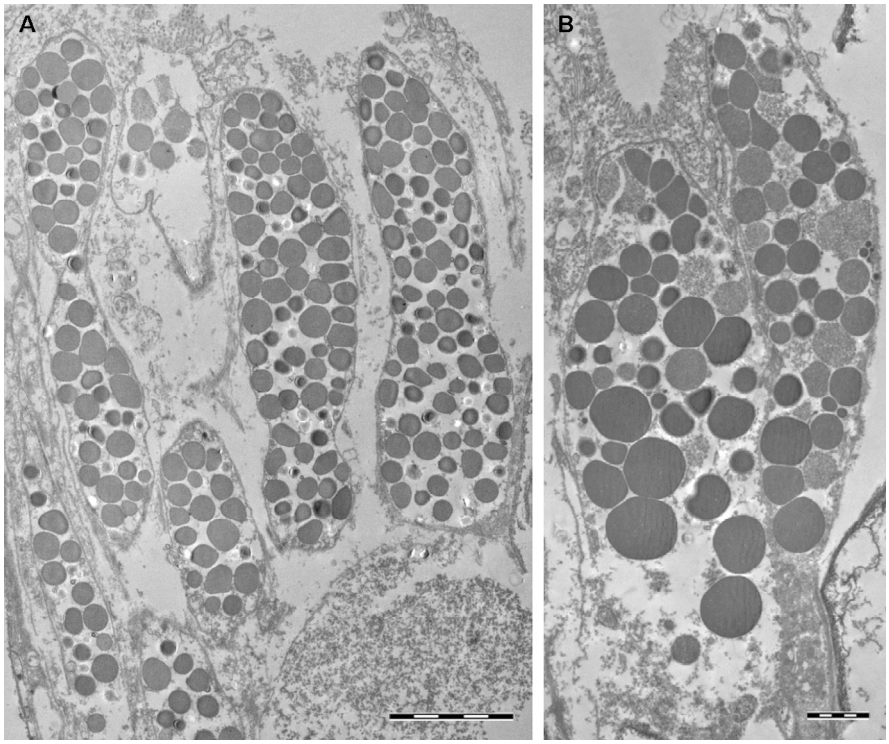

Fig. 8 – Sample from a 10 day old hatchling. (A) The columnar cells already separate from each other by spacing epithelial cells. (B) The first granular cells emerge between the epithelium cells, containing initial aggregations of secretory droplets near the distal cell pole. Scale bars: 5 μm (A); 2 μm (B).

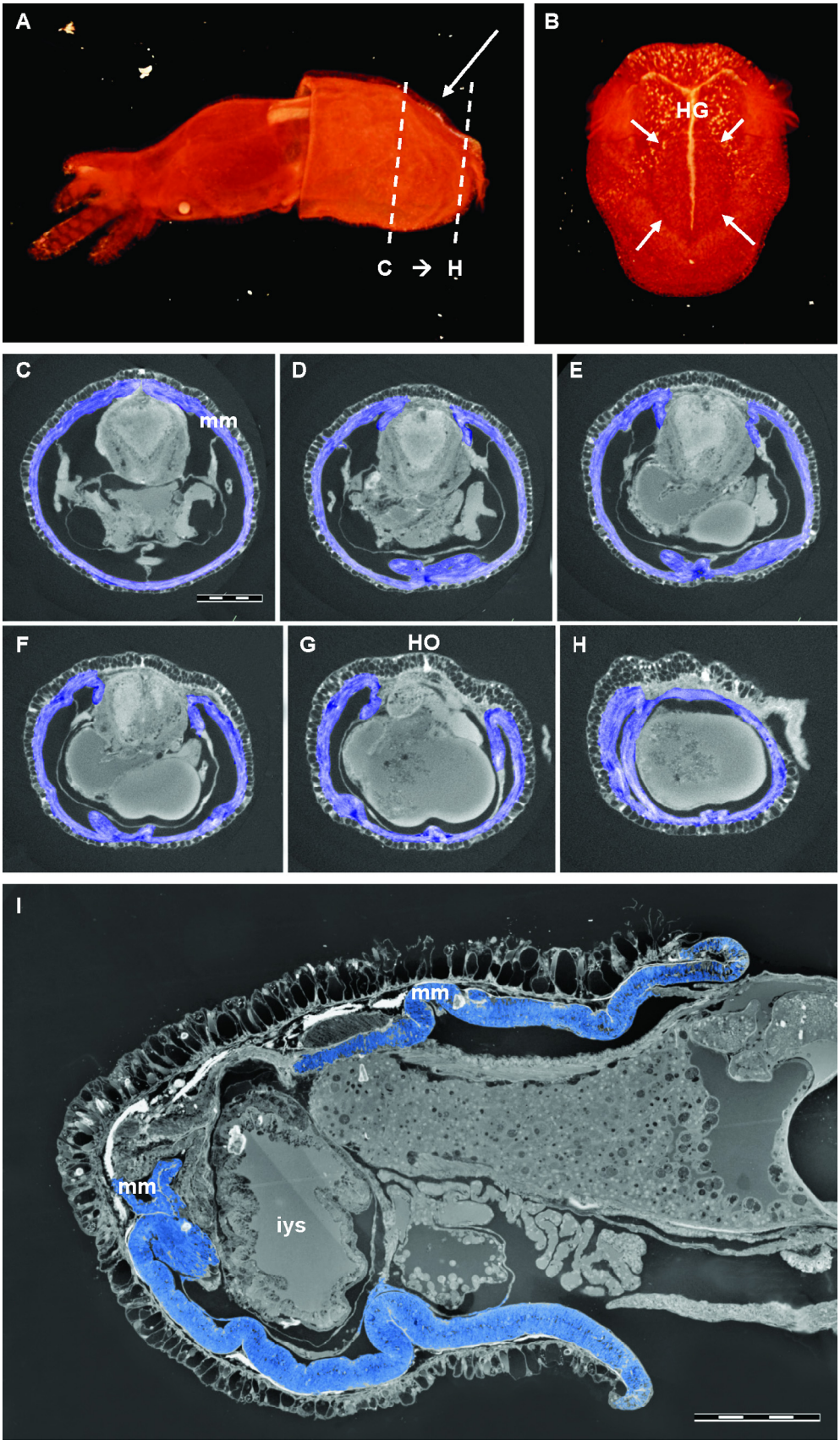
A
C → H
B
HG
C
mm
D
E
F
G
HO
H
I
mm
mm
iys

Remarkable is the occurrence of apparently the same sort of modifications in epithelial cells in the adult *I. pygmaeus*. In that case, the cells (referred to as interstitial cells) were found spacing the columnar cells within the adhesive organ (Cyran et al., 2011; von Byern et al., 2008). Likewise the microvilli of these cells create an elevated area around the glandular cells to warrant a punctuate secretion and as in *L. pealei* (Arnold and Singley, 1989) and in the present observations they contain compact longitudinal filament bundles. As Arnold and Singley (1989) and Cyran et al. (2011) suspected a possible contraction capacity, this possibility cannot be ruled out for the hatching gland of *Idiosepius*. This presumption would require the participation of a motor protein, which is unproved yet. Apparently, comparable adaptations of epithelial cells, as observed for the hatching gland as well for the adhesive organ (Cyran et al., 2011), are common to specific glandular cells in Idiosepiidae. We never observed the existence of this cell type without relationship to glandular cells. This fact underlines its role as glandular supporting cell.

3.3. *Hatching gland degradation*

Once hatched, the degradation of the hatching gland cells of *Idiosepius* starts immediately with the swelling of synthesizing organelles at the cell bases. The rough endoplasmic reticulum merges with the immature secretory droplets and subsequently disintegrates to amorphous flocculent material. Similar observations were made for *L. pealei* (Arnold and Singley, 1989) and *Sepiella japonica* (Matsuno and Ouji, 1988). The cell volume shrinks considerably and the remaining mature secretory droplets disintegrate leaving behind areas of blank cytoplasm, just as in *L. pealei* (Arnold and Singley, 1989) and *S. japonica* (Matsuno and Ouji, 1988). As described for *L. pealei*, also in *I. pygmaeus* epithelial cells adjacent to the hatching gland ingest some organelle remnants (referred to as HGRs – hatching gland residues in *L. pealei*). Due to the quick degradation within around 1 day (Cyran et al., 2013) the shrinkage of the gland cells is faster than the filling of the emerging space by neighbouring epithelial cells. This circumstance leads to the temporary formation of a distinct furrow along the area of the degraded hatching gland.

3.4. *Comparison with the cell depletion sequences in other hatching glands and embryonic tissues*

Epithelial hatching glands, producing enzymes to digest the egg envelopes, are also well studied in fishes and amphibians, referred to as hatching gland cells (HGC) (Yoshizaki, 1973). Only a few studies on hatching glands consider the morphological changes during their degradation (Rojo et al., 1997; Schoots et al., 1983; Yamamoto et al., 1979; Yoshizaki, 1973) and allow a direct comparison of the cell alterations.

Unlike the typical solitary digestive cells in teleosts (Schoots and Denuce, 1981; Willemse and Denuce, 1973; Yamamoto et al., 1979; Yokoya and Ebina, 1976), in amphibians they tend to form cell groups (Yoshizaki, 1973; Yoshizaki and Katagiri, 1975), while in cephalopods a continuous tissue is developed. The mode of cell clusters formation in the latter two groups seems to be crucial for the cell death pathway they follow:

As isolated cells are typically affected by apoptotic cell decay (Kerr et al., 1972; Wyllie et al., 1980), teleosts show typical apoptotic nuclear changes as peripheral chromatin condensation and a highly indented outline (Rojo et al., 1997; Schoots et al., 1983; Yamamoto et al., 1979). Furthermore, cell shrinkage immediately after secretion, multivesicular bodies and spherical hatching gland remnants ingested in adjacent epithelial cells (Schoots et al., 1982; Yamamoto et al., 1979), confirm this presumption.

To the contrary, the degrading digestive cells in *Idiosepius* as well as in amphibians (Yoshizaki, 1973) do not display significant nuclear changes. Likewise in *Xenopus laevis*, the synthesis of enzymes declines before hatch, expressed by granules agglomeration in the apical cell regions and significantly reduced Golgi bodies (Yoshizaki, 1973). Post hatching the cell volume decreases as in *Idiosepius* in height instead of laterally. Other than in *Idiosepius* and other cephalopods, which never exhibit clear indications of a controlled resorption of cell organelles by lysosomes, the basal cytoplasm in the HGCs of the frogs *Xenopus laevis* (Yoshizaki, 1973) and *Rana chensinensis* (Yoshizaki and Katagiri, 1975) contains lysosomes with incorporated fragments of membranes, mitochondria and other residues.

Generally, the degradation of the hatching gland takes place within a few days in cephalopods (Arnold and Singley, 1989; Cardoso et al., 2005; Cyran et al., 2013; Matsuno and Ouji, 1988), which is considerably shorter than in vertebrates, where it lasts up to several weeks (Rojo et al., 1997; Schoots and Denuce, 1981; Yokoya and Ebina, 1976; Yoshizaki and Katagiri, 1975).

3.5. *Pathways of programmed cell death*

Control mechanisms and pathways of cell death in metazoa are still far from being thoroughly understood. Since programmed cell decay in higher organisms have a high level of complexity and numerous interdependencies (Chautan et al., 1999; Oppenheim et al., 2001), current studies mostly focus on

Fig. 9 – Microcomputer tomographic illustrations of the mantle musculature of *Idiosepius pygmaeus*. In Idiosepiidae the mantle musculature shows a typical modification in connection with the adhesive organ. In order to strengthen the adhesive force by fitting the mantle surface to the substratum surface, the adhesive area is free of the mantle musculature. (A) Sagittal view of the animal (embryonic stage 29). The arrow points to the modified area (dented part) and additionally indicates the angle of view for B. The dashed lines mark the forward and backward limitations of the muscle modification, sequentially illustrated in cross sections in C–H. (B) Inclined dorsal view (according to the arrow in A) showing the drop shaped area (darker zone, indicated by arrows) of the lacking mantle musculature. (C–H) Sequence of cross sections of the same region, ranging between the dashed lines in A. The mantle musculature is coloured blue (embryonic stage 29). (I) Sagittal section showing the front/back – extension of the mantle muscles, coloured blue (12 day old hatchling). HG, hatching gland; iys, internal yolk sac; mm, mantle musculature. Scale bars: 200 μm (C, I).

the observation of single cells as a manageable model to learn more about trigger molecules and possible cell alterations. Of course, the obtained results are only partially applicable on contiguous tissues of organisms.

Studies of embryogenesis in invertebrates as well as vertebrates confirm the role of apoptosis (Kerr et al., 1972) as decisive mechanism, in particular in case of replacement of individual cells (Abrams et al., 1993; Coles et al., 1993; Gohlke et al., 2007; Voyron et al., 1999). The current knowledge about control mechanisms and morphological alterations of complete organ depletion in invertebrates is rather limited and does not provide an adequate reference for the hatching gland degradation in cephalopods.

As a preliminary remark, it should be emphasized that since the degradation of the organ is part of the embryonic development, it has to be seen as 'developmental programmed' cell death (Lockshin and Zakeri, 2001), regardless of the observed cell death characteristics.

Certainly **apoptosis** as cell death pathway can be excluded because of the lack of some typical indications as chromatin condensation, nuclear fragmentation, plasma membrane blebbing, or membrane coated cytoplasm fragments and stacks of membranes (Altmann and Bannasch, 1966; Kerr et al., 1972; Klepal et al., 2008).

There is no clear evidence for an **autophagic pathway** either. Indeed a weak vacuolization of the cytoplasm is obvious in the degrading HGCs, but there is no presence of distinct membrane enclosed autophagic vacuoles (Levine and Klionsky, 2004). On the other hand, the relatively well-preserved nucleus, as long as the bulk of cytoplasm is not removed, is typical for autophagic cell death (Bursch, 2001; Kitanaka and Kuchino, 1999). Moreover, autophagy is typical for massive removal of cells within developmental programmes (Baehrecke, 2002; Bursch, 2001; Levine and Yuan, 2005). An uptake of organelle remnants by adjacent cells or phagocytes was observed in both the apoptotic and the autophagic pathway (Beaulaton and Lockshin, 1982; Bursch, 2001; Levine and Klionsky, 2004).

Some of the most conspicuous characteristics in the dying cells correspond to attributes described in association with **necrotic cell death** (Clarke, 1990; Kerr et al., 1972, 1995; Wyllie et al., 1980): swelling organelles and loss of intracellular contents. Contrary is the observation of obligatory cell shrinkage in *Idiosepius*, whereas the literatures mostly indicate a gain in cell volume by inactivation of membrane ionic channels (ion pumps failure by lack of ATP) (Barros et al., 2001; Hetz et al., 2005; Majno and Joris, 1995). But this attribute rather matches the accidental necrosis and less the concept of necrosis-like programmed cell death, defined as PCD (programmed cell death) without chromatin condensation (Guimaraes and Linden, 2004; Leist and Jaattela, 2001).

The concept of **oncosis** (Majno and Joris, 1995; Trump et al., 1997; von Recklinghausen, 1910; Van Cruchten and Van den Broeck, 2002) specifies the prelethal alterations of a usually programmed but nonapoptotic cell death mode. According to this definition the term necrosis comprises only the postmortem degradative changes which always represent the final states of cell depletion, even after apoptosis. Most observed properties of the dying hatching gland cells correspond to the description of oncosis, as swelling of organelles, break up into vesicles and subsequently clumping (Majno and Joris, 1995; Trump and Berezesky, 1998). Likewise a progressive formation of organelle-free areas is evident (Trump et al., 1997). Instead of the indicated cytoplasmatic swelling and cell expansion, provoked by de-energization of Na+, K+-ATPase accompanied by water influx, the degrading hatching gland cells shrink. A fixation-related alteration of the original conditions cannot be excluded in this respect, e.g. by osmotic activity. Otherwise, since it is not clear in which degradation stage the 'point of no return' is exceeded, a clear division between oncotic alterations and the necrotic disintegration is difficult and the shrinking could be a consequence of the necrotic plasma membrane disruption already. Anyhow, oncosis is known to affect broad zones of cells (Trump et al., 1997) instead of individual cells, making this cell death pathway reasonable for degradation of entire organs.

Ultimately the observed morphological characteristics cannot be coherently related to one single described cell death mode since (1) the degrading HGCs display features suiting to more than one defined cell death type and (2) even the classified types have several overlapping characteristics. It is also evident that apoptosis and autophagy can occur simultaneously in the same tissue or even in the same cell (Bursch, 2001; Klepal et al., 2008).

In conclusion we propose a kind of hybrid cell death mode which is clearly triggered. A more precise classification would require immune histochemical and molecular biological analyses with focus on distinct signal molecules as caspases, RIP and others. But even then the interpretation remains difficult since e.g. caspases, typically responsible for triggering the apoptotic pathway, are found also participating in other cell death modes than apoptosis and therefore do not sufficiently prove apoptosis (Kroemer and Martin, 2005).

3.6. *Adhesive organ*

While the first columnar cells could be observed in 7 day old hatchlings and appear completely filled in 10 day old hatchling, the development of the granular cells starts apparently some days later. The first clear evidence of granular cells was detected not until day 10 after hatching.

Our observations point to an obligatory conjoint development of columnar cells as cell clusters as they appear in the mature adhesive organ (Cyran et al., 2011; von Byern et al., 2008) whereas the granular cells always develop solitarily. Fusiform cells and modified epithelial cells as an obligatory part of the columnar cell clusters (Cyran et al., 2011) could not be observed until day 12.

Although the adhesive organ is still not fully developed yet, behavioural observations of *Idiosepius pygmaeus* revealed first attachment behaviour at the aquarium glass wall in 12 day old juveniles (J. von Byern, personal observations). This is contrary to the quoted 30 days without attachment in *Idiosepius pygmaeus*, observed by Nabhitabhata (1994). This discrepancy may have various reasons: First, the water temperature in the study of Nabhitabhata (1994) was 28 °C, in our study it was 32 °C. Since the temperature is crucial for the growth rate in Idiosepiidae (Tracey et al., 2003), the difference of 4 °C could be relevant. Second, it is unclear to what extent the artificial environment biases the natural behaviour. Therefore a direct correlation between attachment behaviour and developed state of the adhesive organ may fail. We cannot rule out that our

observations of the supposedly attachment after 12 days illustrates a hereditary behaviour of the juvenile even before the adhesive organ is functioning properly. The observed attachment in this case, may be a result of partly a sucker effect of the flattened part of the dorsal mantle, partly generated by jet propulsion and partly by the early adhesive organ. We moreover have no data about the dietary intake of the individuals which also could play an important role for the speed of development.

It remains unclear so far, at which juvenile stage the development of the adhesive organ is completed and whether a fully functioning bonding behaviour is required for capturing prey by ambushing them. Anyway, considerable amounts of the internal yolk sac are remaining in the observed 12 day old juveniles as indicated in Fig. 9I.

3.7. *Collateral modifications related to the adhesive organ*

As shown by Cyran et al. (2011) the mantle musculature of adult Idiosepiidae exhibits a dorsal gap that enables flattening during attachment. This unique peculiarity can be observed already during late embryonic development (at stage 29). Another referring characteristic of *Idiosepius*, the different thickness of the dorsal and ventral mantle epithelium, is obvious at embryonic stage 29 as well, whereas in earlier embryonic stages this is not the case.

3.8. *Occurrence of the regular epithelial tissue*

The cells of the regular epithelium (basal, interstitial, goblet and saccular cells) are already present in the embryonic epithelium and correspond structurally and in their arrangement to those in the adult (Cyran et al., 2011). However, while the saccular cells in adults almost lack secretory material, in juveniles this cell type is frequently at least partially filled with secretory content, whereas the role of this specific secretion is not clear yet. A stress-induced release of the content during cultivation cannot be excluded. We have moreover no explanation for the distinct distribution pattern of the goblet cells along the posterior mantle pole so far.

4. Experimental procedures

4.1. *Collection and rearing*

Males and females of *Idiosepius pygmaeus* were collected in the mangrove rivers Mudong and Bangrong in Phuket Island, Thailand (Suwanmala et al., 2006b). They were reared at 32 °C in small glass aquaria in the Phuket Marine Biological Center. After spawning the adults were removed and the eggs were kept until the embryos hatched. All hatchlings of the same days were isolated and fed with Nauplii (stage 4) of *Litopenaeus vannamei*, provided by a local shrimp farm (South Sea Farm in Southern Phuket Island). For this research project we used animals between embryonic stages 25 and 30 and hatchlings up to 12 days old. The assignation of the embryonic stage numbers was done according to the concept of Yamamoto (1988), defining 30 embryonic stages before hatching in *Idiosepius pygmaeus*. The rearing of *Idiosepius* hatchlings in artificial systems is still difficult (Boletzky et al., 2005; Nabhitabhata, 1998; Suwanmala, 2007; von Byern et al., 2006). Consequently we were able to rear only a few individuals to day 8 and only 1–2 specimens to day 12. Because of this sample limitation we used also animals (older than 7 days) which died overnight. This explains the partially poor structure-preserving in some samples.

4.2. *Fixation and sample processing*

For ultrastructural analyses the embryos and paralarvae were fixed in 2.5% glutaraldehyde with 0.1 M sodium-cacodylate buffer (pH 7.4, plus 10% sucrose) for 6 h at 25 °C. For post-fixation, carried out at the University of Vienna, the samples were immersed for 1.5 h in 1% osmium tetroxide with the same buffer solution and dehydrated in a graded series of ethanol.

For transmission electron microscopy (TEM) examination, the samples were embedded in epon; ultrathin sections (50–70 nm) were mounted on copper slot grids coated with formvar in dioxane, stained with uranyle acetate and lead citrate, and examined in Zeiss Libra 120 and Zeiss EM 902 electron microscopes.

For scanning electron microscopy (SEM) examination, the samples were washed several times in 100% acetone after ethanol dehydration, dried with a critical point dryer Leica CPD 300, mounted on stubs, coated with gold in a Polaron 5800 sputter coater, and viewed in the SEM Philips XL 20.

For Microcomputer tomography (μCT) the fixed samples were washed and stored in EtOH. Subsequently, the samples were contrasted for 36 h in 1% (w/v) phosphotungstic acid (PTA) in EtOH and transferred to water for scanning. The animals were imaged with a resolution of 1 μm on an Xradia MicroXCT-200 (90 keV/8 W tung-sten X-ray source) with a cooled 1k CCD camera.

Acknowledgements

We are grateful to MSc. Jitima Suwanmala and Dr. Ratree Suksuwan, Director of the Phuket Aquarium, Phuket, Thailand, for their assistance in collection and cultivating of *Idiosepius pygmaeus*. The collection was permitted by the National Research Council Thailand (NRCT). Project No. 002.3/2999.

Financial support

This work on the hatching system in cephalopods was supported by the Austrian Science Foundation FWF (Project No. P 21135-B17) to Janek von Byern as well as the ASEA-UNINET University of Vienna Austria to Norbert Cyran.

REFERENCES

Abrams, J.M., White, K., Fessler, L.I., Steller, H., 1993. Programmed cell-death during drosophila embryogenesis. Development 117, 29–43.

Adam, W., 1939. The cephalopoda in the Indian Museum, Calcutta. Rec. Ind. Mus. 41, 61–110.
Altmann, H.W., Bannasch, P., 1966. Die intravitale karyorrhexis der exokrinen pankreaszelle im elektronenmikroskopischen bild. Z. Zellforsch. Mikrosk. Anat. 71, 53.
Arnold, J.M., 1965. Normal embryonic stages of the squid, *Loligo pealii* (Lesueur). Biol. Bull. 128, 24–32.
Arnold, J.M., Singley, C.T., 1989. Ultrastructural changes in the cells of the Hoyle organ during hatching of the squid *Loligo peali*. J. Ceph. Biol. 1, 1–14.
Arnold, J.M., Williams-Arnold, L.D., 1980. Development of the ciliature pattern on the embryo of the squid *Loligo pealei*: a scanning electron microscope study. Biol. Bull. 159, 102–116.
Baehrecke, E.H., 2002. How death shapes life during development. Nat. Rev. Mol. Cell Biol. 3, 779–787.
Barros, L.F., Hermosilla, T., Castro, J., 2001. Necrotic volume increase and the early physiology of necrosis. Comp. Biochem. Phys. A 130, 401–409.
Beaulaton, J., Lockshin, R.A., 1982. The relation of programmed cell death to development and reproduction: comparative study and an attempt at classification. Int. Rev. Cytol. 79, 215–235.
Boletzky, S., Nishiguchi, M.K., Nabhitabhata, J., Nugranad, J., 2005. *Idiosepius*: ecology, biology and biogeography of a mini-maximalist. Phuket Mar. Biol. Cent. Res. Bull. 66, 11–22.
Bursch, W., 2001. The autophagosomal-lysosomal compartment in programmed cell death. Cell Death Differ. 8, 569–581.
Cardoso, F., Baltazar, P., Bautista, J., 2005. The early development of the Patagonia squid *Loligo gahi* D'Orbigny, 1835 in Peruvian waters (Cephalopoda: Loliginidae). Rev. Peru. Biol. 12, 369–376.
Chautan, M., Chazal, G., Cecconi, F., Gruss, P., Golstein, P., 1999. Interdigital cell death can occur through a necrotic and caspase-independent pathway. Curr. Biol. 9, 967–970.
Clarke, P.G.H., 1990. Developmental cell-death – morphological diversity and multiple mechanisms. Anat. Embryol. 181, 195–213.
Coles, H.S.R., Burne, J.F., Raff, M.C., 1993. Large-scale normal-cell death in the developing rat-kidney and its reduction by epidermal growth-factor. Development 118, 777–784.
Cyran, N., von Byern, J., 2010. Idiosepius. In: von Byern, J., Grunwald, I. (Eds.), *Biological Adhesive Systems: From Nature to Technical and Medical Application – Chapter "Characterization of the Adhesive Systems in Cephalopods"*. Springer Verlag, Wien/New York, pp. 61–66.
Cyran, N., Klepal, W., von Byern, J., 2011. Ultrastructural characterization of the adhesive organ of *Idiosepius biserialis* and *Idiosepius pygmaeus* (Mollusca, Cephalopoda). J. Mar. Biol. Assoc. UK 91, 1499–1510.
Cyran, N., Staedler, Y., Schonenberger, J., Klepal, W., von Byern, J., 2013. Hatching glands in cephalopods – a comparative study. Zool. Anz. 253, 66–82.
Fioroni, P., 1963. Zur embryonalen und postembryonalen Entwicklung der Epidermis bei zehnarmigen Tintenfischen. Verh. Naturforschenden Ges. Basel 74, 149–160.
Gohlke, J.M., Griffith, W.C., Faustman, E.M., 2007. Computational models of neocortical neuronogenesis and programmed cell death in the developing mouse, monkey, and human. Cereb. Cortex 17, 2433–2442.
Guimaraes, C.A., Linden, R., 2004. Programmed cell deaths – apoptosis and alternative deathstyles. Eur. J. Biochem. 271, 1638–1650.
Hetz, C.A., Torres, V., Quest, A.F.G., 2005. Beyond apoptosis: nonapoptotic cell death in physiology and disease. Biochem. Cell Biol. 83, 579–588.
Hibbard, H., 1937. The hatching of the squid. Biol. Bull. 73, 385.
Hoyle, W.E., 1889. VI. On a tract of modified epithelium in the embryo of *Sepia*. P. Roy. Soc. Edinb. A 10, 58–60.
Jecklin, L., 1934. Beitrag zur Kenntnis der Laichgallerten und der Biologie der Embryonen decapoder Cephalopoden. Mathematisch-Naturwissenschaftlichen Abteilung der Philosophischen Fakultät der Universität Basel. 595–673.
Jereb, P., Roper, C.F.E., 2005. *Cephalopods of the World – An Annotated and Illustrated Catalogue of Cephalopod Species Known to Date. No. 4, Volume 1: Chambered Nautiluses and Sepioids (Nautilidae, Sepiidae, Sepiolidae, Sepiadariidae, Idiosepiidae and Spirulidae)*. Food and Agriculture Organization of the United Nations, Rome.
Kerr, J.F., Wyllie, A.H., Currie, A.R., 1972. Apoptosis: a basic biological phenomenon with wide-ranging implications in tissue kinetics. Br. J. Cancer 26, 239–257.
Kerr, J.F., Gobé, G.C., Winterford, C.M., Harmon, B., 1995. Anatomical methods in cell death. Method Cell Biol. 46, 1–27.
Kitanaka, C., Kuchino, Y., 1999. Caspase-independent programmed cell death with necrotic morphology. Cell Death Differ. 6, 508–515.
Klepal, W., Gruber, D., Pflugpfelder, B., 2008. Natural cyclic degeneration by a sequence of programmed cell death modes in *Semibalanus balanoides* (Linnaeus, 1767) (Crustacea, Cirripedia, Thoracica). Zoomorphology 127, 49–58.
Kroemer, G., Martin, S.J., 2005. Caspase-independent cell death. Nat. Med. 11, 725–730.
Leist, M., Jaattela, M., 2001. Four deaths and a funeral: from caspases to alternative mechanisms. Nat. Rev. Mol. Cell Biol. 2, 589–598.
Levine, B., Klionsky, D.J., 2004. Development by self-digestion: molecular mechanisms and biological functions of autophagy. Dev. Cell 6, 463–477.
Levine, B., Yuan, J.Y., 2005. Autophagy in cell death: an innocent convict? J. Clin. Invest. 115, 2679–2688.
Lockshin, R.A., Zakeri, Z., 2001. Programmed cell death and apoptosis: origins of the theory. Nat. Rev. Mol. Cell Biol. 2, 545–550.
Majno, G., Joris, I., 1995. Apoptosis, oncosis, and necrosis. An overview of cell death. Am. J. Pathol. 146, 3–15.
Matsuno, A., Ouji, M., 1988. Ultrastructural studies on development of the tail gland of a cuttlefish, *Sepiella japonica*. Dev. Growth Differ. 30, 673–680.
Nabhitabhata, J., 1994. Rearing of Thai pygmy cuttlefish, *Idiosepius thailandicus* Chot., Okut. & Chait., I.: some biological aspects. Technical Paper, Rayong Coastal Aquaculture Station, 13.
Nabhitabhata, J., 1998. Distinctive behaviour of Thai pygmy squid, Idiosepius thailandicus Chotiyaputta, Okutani & Chaitiamvong. Phuket Mar. Biol. Cent. Spec. Publ. 18, 25–40.
Nabhitabhata, J., Suwanmala, J., 2008. Reproductive behaviour and cross-mating of two closely related pygmy squids *Idiosepius biserialis* and *Idiosepius thailandicus* (Cephalopoda: Idiosepiidae). J. Mar. Biol. Assoc. UK 88, 987–993.
Oppenheim, R.W., Flavell, R.A., Vinsant, S., Prevette, D., Kuan, C.Y., Rakic, P., 2001. Programmed cell death of developing mammalian neurons after genetic deletion of caspases. J. Neurosci. 21, 4752–4760.
Rojo, M.C., Blanquez, M.J., Gonzalez, M.E., 1997. Ultrastructural evidence for apoptosis of pavement cells, chloride cells, and hatching gland cells in the developing branchial area of the trout Salmo trutta. J. Zool. 243, 637–651.
Sasaki, M., 1921. On an adhering habit of a pygmy cuttlefish, *Idiosepius pygmaeus* Steenstrup. Annot. Zool. Japon. 10, 209–213.
Schoots, A.F.M., Denuce, J.M., 1981. Purification and characterization of hatching enzyme of the pike (*Esox lucius*). Int. J. Biochem. 13, 591–602.
Schoots, A.F.M., De Bont, R.G., van Eys, G.J.J.M., Denuce, J.M., 1982. Evidence for a stimulating effect of prolactin on teleostean hatching enzyme secretion. J. Exp. Zool. 219, 129–132.

Schoots, A.F.M., Evertse, P.A.C.M., Denuce, J.M., 1983. Ultrastructural changes in hatching-gland cells of pike embryos (*Esox lucius* L.) and evidence for their degeneration by apoptosis. Cell Tissue Res. 229, 573–589.

Shigeno, S., Kidokoro, H., Goto, T., Tsuchiya, K., Segawa, S., 2001. Early ontogeny of the Japanese common squid *Todarodes pacificus* (Cephalopoda, Ommastrephidae) with special reference to its characteristic morphology and ecological significance. Zool.Sci. 18, 1011–1026.

Smith, A.M., Callow, J.A., 2006. *Biological Adhesives*. Springer-Verlag, Heidelberg.

Suwanmala, J., 2007. Some Aspects on Life History and Behaviour of Two-Row Pygmy Squid, Idiosepius biserialis Voss, 1962 (Master's thesis). Kasetsart University, Bangkok, Thailand, Department of Marine Science,

Suwanmala, J., Szaffich, C.A., von Byern, J., Nabhitabhata, J., 2006a. Ultrastructural insights in the embryonic development of *Idiosepius biserialis* (Mollusca, Cephalopoda). In: Moltschaniwskyj, N.A., Pecl, G.T., Semmens, J., Jackson, G.D. (Eds.), *Cephalopod International Advisory Council Symposium 2006*. Hobart, Tasmania, p. 106.

Suwanmala, J., von Byern, J., Nabhitabhata, J., 2006b. Observation of *Idiosepius pygmaeus* (Cephalopoda, Idiosepiidae) at Klong Bangrong, Phuket Island, Thailand. Phuket Mar. Biol. Cent. Res. Bull. 67, 49–51.

Tracey, S.R., Steer, M.A., Pecl, G.T., 2003. Life history traits of the temperature mini-maximalist *Idiosepius notoides* (Cephalopoda:Sepioidea). J. Mar. Biol. Ass. UK 83, 1297–1300.

Trump, B.F., Berezesky, I.K., 1998. The reaction of cells to lethal injury: oncosis and necrosis – the role of calcium. In: Lockshin, R.A., Zakeri, Z., Tilly, J.L. (Eds.), *When Cells Die*. Wiley-Liss, New York, pp. 57–96.

Trump, B.F., Berezesky, I.K., Chang, S.H., Phelps, P.C., 1997. The pathways of cell death: oncosis, apoptosis, and necrosis. Toxicol. Pathol. 25, 82–88.

von Byern, J., Grunwald, I., 2010. *Biological Adhesive Systems: From Nature to Technical and Medical Application*. Springer Verlag, Wien/NewYork.

von Byern, J., Klepal, W., 2010. Re-evaluation of taxonomic characters of Idiosepius (Cephalopoda, Mollusca). Malacologica 52, 43–65.

von Byern, J., Shigeno, S., Klepal, W., Kasugai, T., 2006. Postembryonic development of the adhesive organ in *Idiosepius* under artificial conditions. In: Moltschaniwskyj, N.A., Pecl, G.T., Semmens, J., Jackson, G.D. (Eds.), *Cephalopod International Advisory Council Symposium, 2006*. Hobart, Tasmania, p. 54.

von Byern, J., Rudoll, L., Cyran, N., Klepal, W., 2008. Histochemical characterization of the adhesive organ of three *Idiosepius* spp. species. Biotech. Histochem. 83, 29–46.

von Byern, J., Söller, R., Steiner, G., 2012. Phylogenetic characterization of the genus Idiosepius (Cephalopoda; Idiosepiidae). Aquatic Biol. 17, 19–27.

von Orelli, M., 1959. Über das Schlüpfen von *Octopus vulgaris*, *Sepia officinalis* und *Loligo vulgaris*. Rev. Suisse Zool. 66, 330–343.

von Recklinghausen, F., 1910. *Untersuchungen über Rachitis und Osteomalacie*. Gustav Fischer Verlag, Jena.

Van Cruchten, S., Van den Broeck, W., 2002. Morphological and biochemical aspects of apoptosis, oncosis and necrosis. Anat. Histol. Embryol. 31, 214–223.

Voyron, S., Giacobini, P., Tarozzo, G., Cappello, P., Perroteau, I., Fasolo, A., 1999. Apoptosis in the development of the mouse olfactory epithelium. Dev. Brain Res. 115, 49–55.

Willemse, M., Denuce, J.M., 1973. Hatching gland in the teleosts, *Brachydanio rerio*, *Danio malabaricus*, *Moenkhausia oligolepis* and *Barbus schuberti*. Dev. Growth Differ. 15, 169–177.

Wyllie, A.H., Kerr, J.F., Currie, A.R., 1980. Cell death: the significance of apoptosis. Int. Rev. Cytol. 68, 251–306.

Yamamoto, M., 1988. Normal embryonic stages of the pygmy cuttlefish, *Idiosepius pygmaeus paradoxus* Ortmann. Zool.Sci. 5, 989–998.

Yamamoto, M., Iuchi, I., Yamagami, K., 1979. Ultrastructural changes of the teleostean hatching gland cell during natural and electrically induced precocious secretion. Dev. Biol. 68, 162–174.

Yokoya, S., Ebina, Y., 1976. Hatching glands in salmonid fishes, *Salmo gairdneri*, *Salmo trutta*, *Salvelinus fontinalis* and *Salvelinus pluvius*. Cell Tissue Res. 172, 529–540.

Yoshizaki, N., 1973. Ultrastructure of the hatching gland cells in the South African clawed toad, *Xenopus laevis*. J. Fac. Sci. Tokyo Univ. 6, 18, 469–480.

Yoshizaki, N., Katagiri, C., 1975. Cellular basis for the production and secretion of the hatching enzyme by frog embryos. J. Exp. Zool. 192, 203–212.

Zakeri, Z., Lockshin, R.A., 2002. Cell death during development. J. Immunol. Methods 265, 3–20.

The short life of the Hoyle organ of *Sepia officinalis* - Formation, differentiation and degradation by programmed cell death

Authors

Norbert Cyran[1], Anna Palumbo[2], Waltraud Klepal[1], Erica A. G. Vidal[3], Yannick Staedler[4], Jürg Schönenberger[4] and Janek von Byern[5, 6]

Addresses

[1] University of Vienna, Faculty of Life Sciences, Core Facility Cell Imaging and Ultrastructural Research, Vienna, Austria

[2] Stazione Zoologica Anton Dohrn, Department of Biology and Evolution of Marine Organisms, Naples, Italy

[3] Center for Marine Studies. University of Parana - UFPR, Pontal do Parana, Brazil

[4] Div. of Structural and Functional Botany, Dept. of Botany and Biodiversity Research, University of Vienna, Vienna, Austria

[5] Centre for Integrative Bioinformatics Vienna, Max F Perutz Laboratories, University of Vienna, Medical University of Vienna, University of Veterinary Medicine, Vienna Austria

[6] Ludwig Boltzmann Institute for Experimental and Clinical Traumatology, Austrian Cluster for Tissue Regeneration, Vienna, Austria

Corresponding author: norbert.cyran@univie.ac.at Tel. 0043 1 4277 57903

Abstract

Cephalopods encapsulate their eggs in protective egg envelopes. To hatch from this enclosure, most cephalopod embryos release egg shell-digesting choriolytic enzymes produced by the Hoyle organ (HO). After hatching, this gland becomes inactive and rapidly degrades by programmed cell death. We aim to characterize morphologically the development, maturation and degradation of the gland throughout embryonic and first juvenile stages in *Sepia officinalis*. Special focus is laid on cell death mechanisms and the presence of nitric oxide synthase during gland degradation. Hatching enzyme has been examined in view of metallic contents, commonly amplifying enzyme effectiveness. HO gland cells are first visualized at embryonic stage 23; secretion is observed from stage 27 onwards. Degradation of the HO occurs after hatching within two days by the rarely observed autophagic process, recognized for the first time in cephalopods. Nitric oxide synthase immunopositivity was not found in the HO cells after hatching, suggesting a possible NO role in cell death signaling. Although the HO 'life course' chronology in *S. officinalis* is similar to other cephalopods, gland degradation occurs by autophagy instead of necrosis. Eggs that combine a large perivitelline space and multi-layered integument seem to require a more complex and large gland system.

Keywords

hatching gland; autophagy; nitric oxide; nitric oxide synthase

Introduction

Cephalopods have a great variety of egg encapsulation mechanisms that can consist of from a single chorionic coat without protective jelly envelopes in octopodiforms to a multi-layer spirally coiled jelly coat in most decapodiforms (Boletzky, 1986). Eggs can be released individually or in egg masses, which size, shape, structure and consistency also vary substantially among species (Boletzky, 1986, 1998).

The hatching gland in cephalopods, referred to as the HO (Hoyle organ) (Wintrebert, 1928; Yung Ko Ching, 1930) represents a co-adaptation of the embryo to overcome the barrier imposed by the egg envelopes, across which it has to move freely during hatching. A close association is expected between egg encapsulation design and the morphology of the HO (Boletzky, 2012). Therefore, detailed information on the morphology and the process of formation and degradation of the HO should have special value in clarifying how the gland system has evolved among species with assorted encapsulation mechanisms. This in turn would provide a foundation for the understanding of the ecological and evolutionary significance of the HO.

In cephalopods, the HO is an epithelial organ restricted to the posterior part of the dorsal mantle surface. Shortly before hatching, the HO is fully developed and releases proteolytic enzymes (Denuce & Formisano, 1982) that weaken the egg integument so that it becomes permeable to water, resulting in an increase in osmotic pressure within the perivitelline space (Boletzky, 2003). Instantly after hatching, a bulk degradation of the gland takes place and is accomplished within a few hours to a few days (Orelli, 1959).

The HO generally consists of only one type of glandular cells, which synthesize electron-dense granules, spherical to polygonal in shape (depending on the charging level) (Cyran et al., 2013). In several decapodiform species (e.g. *Sepiella japonica*, *Sepia officinalis*, *Loligo* sp., *Sepioteuthis lessoniana*, *Architeuthis* sp.) these granules differ in the later stage of development by containing electron-lucent inclusions (Arnold & Singley, 1989; Cyran et al., 2013; Matsuno & Ouji, 1988) named “bipartite dense granules” (Arnold & Singley, 1989).

No information is available on the metal ion content of the hatching enzyme of cephalopods and the environmental and biological factors that regulate its availability. Detailed examinations of hatching enzymes have been carried out for teleosts (Ogawa & Ohi, 1968; Yamagami, 1973; Yasumasu et al., 1988). The fish-hatching enzyme, referred to as chorionase (Yamagami, 1973), was found to be composed of two distinct components, a chorion swelling HCE (high choriolytic enzyme) and a subsequent chorion-digesting LCE (low choriolytic enzyme); both enzymes contain Zn, Mg and Ca (Yasumasu et al., 1988;

Yasumasu et al., 1989a; Yasumasu et al., 1989b). Marine trace metal concentrations and their availability are strongly influenced by anthropogenic effects such as ocean acidification that has the potential to cause chances in trace metals solubility (Gledhill et al., 2015). Even small changes in essential trace metal availability can have a significant impact on organism function (Eide, 1998; Morel et al., 2003; Stockdale et al., 2016). Moreover, changes in pH have the potential to severely impact the aerobic performance of cephalopods (Pörtner & Zielinski, 1998), with late embryos and paralarvae being certainly more susceptible. Low pH values can even cause an ionic and acid–based imbalance that leads to changes in the biocumulation of metals (D'Aniello et al., 1989; Lacoue-Labarthe et al., 2011).

The three most common types of cytoplasm-degradative processes are apoptosis, necrosis and autophagy (Berry & Baehrecke, 2007; Clarke, 1990; Kerr et al., 1972; Wyllie et al., 1980). In cases of bulk degradation of tissues or organs mostly autophagic cell death (Arbeitman et al., 2002; Berry & Baehrecke, 2007; Mcphee et al., 2010) or necrosis-like programmed cell death (Guimaraes & Linden, 2004; Leist & Jaattela, 2001) have been observed. However, genetically triggered cell death strategies are complex and exhibit overlapping characteristics, which moreover flexibly diverge according to environmental and metabolic influence (Galluzzi et al., 2012).

Currently, the HO-degradation process has not been satisfactorily investigated with respect to the executing cell death strategy. In *Idiosepius* sp., characterization of the degradation process to a specific cell death mode was first attempted (Cyran et al., 2015). The authors identified an unspecific degradation of the entire cytoplasm and the loss of desmosomes between the glandular cells (Cyran et al., 2015) and hypothesized that this occurred via a hybrid cell death mode with an almost necrotic appearance. Similar characteristics were described earlier in *Loligo pealei* (Arnold & Singley, 1989) and *Sepiella japonica* (Matsuno & Ouji, 1988). Since the HO in *Sepia officinalis* is large in comparison to the aforementioned species and the egg is encapsulated in a thick multi-layer envelope (Boletzky, 1986), we suppose to witness the rather effective autophagic cell death strategy, observed for instance several times during *Drosophila* development (Arbeitman et al., 2002; Berry & Baehrecke, 2007).

Among the physiological mediators, nitric oxide (NO) has been reported to be involved in different processes in metazoans (Castellano et al., 2014; Comes et al., 2007; Migliaccio et al., 2014; Palumbo, 2005). This gaseous molecule, synthesized from L-arginine by the enzyme NO synthase (NOS), plays key roles in neurotransmission, defence system and development in *Sepia officinalis* (Di Cristo et al., 2007; Fiore et al., 2004; Mattiello et al.,

2010, 2012, 2013; Palumbo et al., 2000). The spatial pattern of NO and NOS is very dynamic during cuttlefish development (Mattiello et al., 2012). An initial weak NO signal and NOS immunopositivity have been detected in the HO area at embryonic stage 26 (Mattiello et al., 2012). As development proceeds (stages 28-29), the NO signal is amplified in the anchor-shaped HO area. Also the density of NOS-immunopositive cells increases in the HO between stages 28 and 29. Considering the role of NO as cell death inhibitor (Leise et al., 2004), an increase in NO-levels in the HO at late stages would ensure enzyme synthesis until hatching occurs. In this context, we would expect a dramatic decline in NO concentration after hatching and consequently, activation of cell death signals and glandular degradation.

The aim of this study is to determine the first morphological indications for cell proliferation associated with the HO, to track the morphological differentiation of the HO cells and the associated ciliary cells throughout their lifetime and to characterize and define the cell death processes by means of morphological criteria. Additionally, NOS-detection by immunohistochemistry has been carried out on the HO to examine the NO presence during HO degradation. A first enquiry into the involvement of metallic components in hatching enzymes in cephalopods also has been performed on mature gland content (embryonic stage 29) and contrasted to available data for metal ions in hatching enzymes of teleosts. We use *Sepia officinalis* as a "model" because its embryonic development is well described (Boletzky et al., 2016; Fioroni, 1990; Nixon & Mangold, 1998; Orelli, 1959) and both the embryo and the hatching gland structure are relatively large compared to those of loliginids and octopods.

Material and Methods

Embryo collection

Fertilized eggs laid by *S. officinalis* females were allowed to develop in tanks with oxygenated sea water (20°C; pH 8.1; salinity 38 ppt) at the Marine Resources for Research service of the Zoological Station Anton Dohrn. Different embryonic stages (from 20 to 30, according to Lemaire (1972) as well as 1 and 2-day old juveniles were selected. The embryos were isolated from the egg capsule, vitelline layers and chorion and anesthetized in 3% ethanol.

Fixation and microscopy

For ultrastructural analyses, the egg layers and animals were fixed in 2.5% glutaraldehyde with 0.1M sodium-cacodylate buffer (pH 7.4, plus 10% sucrose) for 5 hrs at 25°C and post-fixed for 1.5 hrs in 1% osmium tetroxide with 0.1 M buffer solution and dehydrated in a graded series of ethanol. For TEM (transmission electron microscopy), the samples were

embedded in Epon (Agar 100 resin); ultrathin sections (50-70 nm) were mounted on copper slot grids coated with formvar in dioxane, stained with gadolinium triacetate (Nakakoshi et al., 2011) and lead citrate (Reynolds, 1963) and examined in a Zeiss Libra 120 with LaB_6 filament and a bottom mount camera Olympus Sharp:eye TRS (2x2 k). For SEM (scanning electron microscopy), the samples were washed several times in 100% acetone, dried in a critical point drier (Leica EM CPD 300), mounted on stubs, coated with gold in a sputter coater (JEOL JFC 2300 HR), and viewed in a JEOL IT 300.

For analyses of the elemental composition, semithin sections (2.5 µm) of the resin blocks were prepared for EDX (energy dispersive X-Ray tomography) with an EDAX System (Software Team, Version 4.3, Co. Ametek Germany) on the SEM. Additionally, sections of 40 nm thickness were mounted on copper grids for EELS (electron energy loss spectroscopy) measurements and EFTEM (energy filtered TEM) mapping on the TEM Zeiss Libra 120 with an in-column Omega filter.

For µCT (micro computer tomography), the glutaraldehyde-fixed samples were washed in aqua bidest and dehydrated in a graded series of ethanol. Subsequently, the samples were contrasted for 36 hours in 1% (w/v) PTA (phosphotungstic acid) in EtOH. The animals were imaged with an Xradia MicroXCT system (90 keV/8 W tungsten x-ray source, cooled 1 k × 1 k CCD camera).

Nitric oxide synthase detection

Tissue of just hatched juvenile were prefixed in 4% PFA (paraformaldehyde) in PBS (phosphate buffered saline, 0.1 M, pH 7.4 for 2 h at 25°C), washed three times in PBS and then embedded in albumin-gelatine. After fixation overnight in 4% formalin and several washings in distilled water, slices of 100 µm sections were obtained using the vibratome Leica VT1200S (Leica Biosystems GmbH, Germany). Primarily, an antibody against universal NO synthase (uNOS) (Co. Thermo Scientific USA, Cat. Nr. PA1-039) was used at a dilution of 1:300; then the secondary Alexa Fluor-labelled antibody (Invitrogen USA, Cat. Nr. A 11008) was used at a dilution of 1:500 (see protocol in Wollesen et al., 2009). Imaging was carried out with a laser confocal microscope Leica TCS SP5X with a white light laser (excitation wavelength 488 nm, detected at 510-530 nm).

Results

Morphological transformation of the egg and its integument during development

The eggs of *S. officinalis* consist of the chorion membrane, several vitelline layers (Fig. 1A) and a multi-layered egg capsule with a fixation ring. All layers show a filamentous organization with a strand diameter of about 10 nm. The layers of the egg capsule as well as the vitelline layers contain ink droplets and other exogenous inclusions (Fig. 1B-D). The outermost capsule layers seem to exhibit the highest abundance of ink (Fig. 1B). A section through the entire egg integument did not reveal any morphological differences between the vitelline layers and those of the capsule.

Up to embryonic stage 24 the egg integument exhibits a predominantly uniform density (Fig. 1B), while before hatching the individual layers are compressed and clearly distinguishable (stage 30, see Fig. 1D). Areas with material of lower density appear between the vitelline layers, which are not observable between the capsule layers (Fig. 1D). These less dense areas almost lack ink and other inclusions.

During the last 2-3 days prior to hatching, the egg integument expands by about 30 %. The vitelline layers and internal parts of the egg capsule disintegrate increasingly until at hatching only the outermost capsule layers and the chorion membrane remain, while the layers in-between lose their cohesion completely. Steady body movements of the embryo before hatching finally lead to a collapse of the egg integument.

HO development

The following section describes the chronological sequence of the formation and differentiation of the HO cells, the synthesis and secretion of the glandular content and the subsequent cellular decay of the organ. The development of the HO appears to be asynchronous: initially, the lateral bands arise, starting from the central crossing point of the anchor (Fig. 2A, D) at stage **23**. The dorsal band occurs later (not before stage 24) while the lateral bands continuously extend sideways (Fig. 2D). As a clear indication of gland development, the epithelium height increases locally from 15 to 30 µm (Fig. 2A, B). In the apical cell area, accumulations of electron-dense secretory droplets appear in the emerging HO cells. Basally and centrally within the secretory cells, the synthesis of the hatching enzymes takes place, as evidenced by the presence of the rough endoplasmic reticulum and Golgi bodies. The first secretory granules, accompanied by microtubules, can already be observed at this early stage (Fig. 2C).

At stage **24** a high abundance of dividing cells signalizes an epithelial reorganization, also at the distal ends of the dorsal band (Fig. 2D-F). In contrast to the arising gland cells, neighbouring epithelial cells show signs of apoptosis such as nuclear chromatin condensation as well as cytoplasm compression and vacuolization (Fig. 2F). At this stage, near the HO crossing point a local heightening of the epithelium, twice of that of the regular cells, can be observed (Fig. 2D, G), as was seen earlier for the lateral bands. In cross section, the secretory cells of the gland form a triangular shape. The secretory material accumulates in membrane-bound spherical granules (1-1.5 µm in diameter) apically in the cells (Fig. 2H). Abundant microtubules illustrate the migratory movements of the granules from the basal synthesis region towards the apical cell surface (Fig. 2I). On the apical pole of the secretory cells are numerous microvilli (approximately 1 µm in length, sometimes branched). Beside numerous scattered ciliary fields across the mantle surface, a continuous lateral boundary of the secretory cells by ciliated epithelial cells starts to be present (Fig. 2G).

With ongoing embryonic development (stages **25-26**) (Fig. 3A), the apical cell areas show large accumulations of secretory granules (Fig. 3B). Furthermore, increasing condensation leads to ‘empty areas’ in the granules, termed earlier as ‘bipartite granules’. As the replenishment with fresh material decreases within the cell apices, the previously dominant microtubules are not evident anymore. Within the cell base, the enzyme synthesis is proceeding as observable by means of active protein synthesis, vesicular transport and obvious assembling of secretory droplets. (Fig. 3C).

Around stage **27** (Fig. 3D-F) the upper two thirds of the gland cells are largely filled with granules and the ongoing condensation intensifies their bipartite character, especially in the distal cell areas (Fig. 3F). While the synthesis of granules in the basal cell parts continues unchanged, the first indications of secretory activity are observable as cell content is found deposited outside the body surface (Fig. 3F).

At stage **28** the glandular area of the HO reaches its largest dimension (in cross section) (Fig. 4A) with a height of 50 µm, twice that of the regular epithelium cells, and a width of 40 µm. The ciliated lateral boundary cells as well as their glycocalix are particularly pronounced at this stage (Fig. 4A, B). In cross section, around five gland cells are neighbouring each other within a band and are tightly filled with secretory material up to their distal poles (Fig. 4B). The gland appears at this stage to be more barrel-shaped than triangular in cross section. No evidence of an interuption in the synthesis process was observable (Fig. 4C).

The following embryonic stages are characterized by a regression of the HO, caused by continuous secretion in combination with a reduced synthesis rate. At stage **29** (Fig. 4D-F) the

secretory cells are substantially condensed and increasingly narrower (Fig. 4E). Major parts of the remaining secretory material are released during stage **30** (Fig. 4J) before hatching occurs. The rough endoplasmic reticulum below the nucleus still appears intact (Fig. 4K), although indications of material synthesis could no longer be observed.

HO degradation

After hatching, the remnants of the secretory material and cell organelles degrade. The secretory cells, with an overall width of 40 µm at stage 28, are collapsed to a joint width of 10 µm (Fig. 5A). They contain numerous distinct single-membraned autophagic vacuoles (autolysosomes) enclosing cytoplasmic elements such as membrane stacks, mitochondria, ribosomes and secretory granules (Fig. 5B). Concomitantly, the increase of Golgi bodies and an abundant budding of Golgi vesicles are evident (Fig. 5C).

Two days after hatching, the previously prominent elevation of the HO has disappeared almost entirely and only a slightly elevated (about 20 µm) ridge is left, provoked by the still thickened connective tissue (Fig. 6A). The cellular residues are further reduced and restricted to a narrow area in the basal parts of the cells (Fig. 6B). Ingested organelles in the autolysosomes have been degraded almost beyond recognition (Fig. 6C), and the recently emerging Golgi bodies have already disappeared.

Nitric Oxide Synthase

Newly hatched embryos showed no NOS immunopositivity within the gland cells of the HO (Fig. 7). By contrast, immunofluorescence could be observed in some individual epithelial cells in close proximity to the HO and with a scattered dispersion within the connective tissue.

Related modification of the normal mantle epithelium

From stage 28 onwards an increasing erosion of the regular epithelial cells could be observed on the dorsal mantle surface. Apart from a few residues of secretory material the cells are empty (Fig. 4E) in contrast to earlier stages (Fig. 2G, 3E, 4A). Numerous epithelial cells appear abraded or even completely etched off (Fig. 4D, 4F-I), in particular those close to the dorsal band of the HO (Fig. 4H). However, indications for a triggered cell degradation mechanism pertaining to the epithelial cells could not be observed in this study.

Ciliated epithelium cells and their alterations

Ciliated epithelium cells make up the abundant ciliary tufts (Fig. 8A) on the mantle and head, as well as the ciliated HO boundary. Those cells differ from the regular epithelial cells

by exhibiting a denser cytoplasm, a more electron-dense nucleus with sharply bounded nucleoli, numerous Golgi bodies and mitochondria but with a lower amount of cytoskeleton elements (Fig 8B). The nucleus is frequently located in the apical cell region near the epithelial surface and the cytoplasm is then reduced to a thin margin. In some cells, ciliary roots appear to be connected to the outer membrane of the mitochondria (Fig 8C). On the mantle surface a glycocalix (pronounced at stage 29 and later) with branching fibrous appendices adheres to the microvilli. Only the length of the microvilli differs between the cilia from the tuft (10 µm) and those that are associated with the HO (5 µm).

After hatching, both types of ciliated cells disappear simultaneously with the HO. While one day after hatching just a few remaining ciliated cells could be found, there is no evidence of the latter after two days.

SEM observations discovered an alteration in the pattern of ciliated cells on the mantle surface during embryonic development:

- HO periphery

Along the secretory cells, the ciliary border appears at stage 24, after the secretory cells assemble the first secretory droplets. Initially, a small band of cilia is established on each side of the gland. Beginning from stage 26 onwards, the ciliated area along the HO is no longer aligned in parallel to the secretory cells, but expands laterally in several short lines (50-100 µm length) in an increasing angle to the secretory cell bands (15° at stage 27, 20° at stage 29, 90° at stage 30), resulting in a feather-like pattern which is clearly visible from stage 27 onwards (Fig. 3D, E; 4A, F, I).

- Ciliary tufts

The ciliary tufts on the mantle surface have a relatively constant size of about 10 µm and each of them belongs to one or a few epithelial cells. We observed changes in the number and distribution of these tufts. In the earliest observed stage (23), only the head is evenly covered with them. Dorsally, the mantle is almost free of ciliary tufts, except for some sporadic tufts along the anterior mantle edge. A band of these structures is present on the ventral mantle surface, beginning at the posterior pole (Fig. 2A). Later in development, the ciliated areas rapidly spread around the mantle. Up until stage 24 the whole mantle is uniformly covered with ciliary tufts (Fig. 2D).

Trace metals in the embryonic tissue

In both the secretory cells of the hatching gland as well as in the subepithelial connective tissue, small amounts of copper (0.24% / 0.13%) and iron (0.21 % / 0.15%) (Table 1, Fig. 9)

could be measured at embryonic stage 29; none of these metals were present in the regular epithelium cells. Measurements on the egg integument at embryonic stage 24 revealed approximately half the value for copper and a quarter of the value for iron in relation to the HO. Detailed EFTEM mapping shows the distribution of copper in the secretory granules of the gland (Fig. 9C).

Discussion

This study provides the first comprehensive information on the processes of formation, differentiation and degradation of the HO in *Sepia officinalis*. It indicates that the rarely observed autophagic cytoplasm-degradative process is responsible for the disappearance of the entire HO within two days after hatching. By nature, hatching and the days that follow represent a critical transitional period in the early life history of cephalopods pointed out by high mortalities (Boletzky, 2003; Vidal et al., 2014). During this very short period, *S. officinalis* hatchlings go through complex morphological, ecological and behavioural milestones, such as the transition from endogenous (yolk) to exogenous (prey) food sources accompanied by maturation of the digestive gland and mastering predatory and swimming abilities (Boucaud-Camou et al., 1985; O'Brian, 2017). Thus, it is of significance that concurrently with these major events, the HO goes through complete degradation.

The HO in *S. officinalis* late embryos is an anchor-shape conspicuous feature, containing relatively large amounts of enzymes to digest a multi-layer thick egg integument with large perivitelline space. These seem to be the main congruent features of the HO in all decapodiform cephalopods studied so far (Boletzky, 2012; Cyran et al., 2013). The gland system, however, differs between species in its outer morphology. It is elevated in *S. officinalis* and most studied species, infolded in *Loligo* and accompanied by a terminal spine in *Euprymna scolopes* and *Rossia macrosoma* (Boletzky, 1991; von Byern et al., 2016).

It is of evolutionary relevance, however, that substantial morphological dissimilarities occur between taxonomic groups. In octopodiforms, represented by *Tremoctopus gracilis, Octopus vulgaris* and *Argonauta hians* the HO gland system consists of a discreet single horizontal band with relatively few glandular cells, while in the later two species, it is not even clearly visible (Cyran et al., 2013). The eggs in this group lack protective envelopes and show limited chorionic expansion and thus perivitelline space, making late stage embryos tightly surrounded by the chorion, what perhaps facilitates the action of HO enzymes. In comparison, in decapodiforms, the perivitelline space is in general large and there are many jelly layers to be also digested. A combination of large perivitelline space and a multi-layer egg integument seems to be a necessary prerequisite for a more complex and large gland system. In this regard, the HO seems to have evolved high complexity and importance in decapodiforms in general and in *S. officinalis* in particular.

Egg integument

The disintegration of the egg capsule and the vitelline layers appears to take place from the centre outwards in accordance with the proposed effect of the hatching enzymes. The first changes in the egg integument occur concomitantly with the first secretion of enzymes at stages 27-28. It has been shown that the increase of the chorionic space during late embryonic development leads to the shrinkage of the inner egg envelopes (Cyran et al., 2013; Gomi et al., 1986; Jecklin, 1934), whereby the individual layers become clearly visible in contrast to earlier developmental stages (Fig. 1D). The observed lower density areas between the vitelline layers are almost devoid of the inclusions located in the dense areas such as ink and bacteria. Since such inclusion-free areas were not observed at earlier embryonic stages, they apparently arise in the course of the reorganization of the egg integument.

Enzyme production

Initial alterations in the mantle epithelium with respect to the upcoming HO take place relatively early in embryonic development (embryonic stage 23) compared to other cephalopods (Arnold & Singley, 1989; Cyran et al., 2013; Orelli, 1959). This may be related to the large embryo and large perivitelline space of the egg. A large embryo size (Fioroni, 1978) should induce a comparatively large spatial expansion of the gland in relation to other teuthid or octopod species. A higher amount of egg shell weakening enzymes also should be required in view of the large perivitelline space (Orelli, 1959) and the many-layered egg integument (Boletzky, 1986).

Our observations confirm that the synthesis of enzymes occurs until shortly before hatching, as also observed for *Loligo* and *Sepiella* (Arnold & Singley, 1989; Matsuno & Ouji, 1988). The fact that unspent secretory material remains in the cells during hatching is due to the supposed high redundancy in enzyme volume to ensure hatching under all circumstances (Boletzky, 2012; Orelli, 1959).

Bipartite granules

We suppose that the less electron-dense areas in the secretory granules (Fig. 3B, F) appear as a consequence of the incremental material density. The condensed secretory material requires less volume, leaving voids in the granules. In contrast, Matsuno & Ouji (1988) assumed the existence of two discriminative components as an explanation for the bipartity in granules of *Sepiella japonica*. We could not find any evidence for the synthesis of two different secretory products within the HO cells of *S. officinalis*.

Evidences for autophagic cell death in the degrading HO

Before the knowledge of the numerous metabolic triggering molecules within the cells (Thumm et al., 1994; Tsukada & Ohsumi, 1993), electron microscopic imaging was the only way to investigate cellular degradation events in detail (Ashford & Porter, 1962; Clark, 1957; Novikoff & Essner, 1962). This technique is still reliable to classify cell death strategies by their morphological features before performing the subsequent molecular pathways analyses (Eskelinen, 2008; Eskelinen et al., 2011).

Previous observations of the degradation of the HO cells in cephalopods revealed a rather unspecific cellular degradation without any clear reference to a specific cell death type. The morphological features of the observed degradation suggest that a necrotic cell death mechanism is most probable in *Loligo*, *Idiosepius* and *Sepiella* (Arnold & Singley, 1989; Cyran et al., 2015; Matsuno & Ouji, 1988).

In the present study, the HO cells of *S. officinalis* display during their degradation the typical vacuolated appearance as commonly described for autophagy (Levine & Klionsky, 2004). An autophagic vacuole can be morphologically distinguished according to its degradation level in either: a) a double-membraned **AVi** (initial autophagic vacuole) before lysosome fusion and yet without evidence of degradation, b) a single-membraned **AVd** (degradative autophagic vacuole) with highly degraded content or c) an intermediate level (**AVi/d**) (Dunn, 1990a, 1990b; Liou et al., 1997). In the present study we observed exclusively single membraned **AVd**'s in the HO (Fig. 5B, 6C). Furthermore, there were partly degraded but still recognizable organelles, which can be referred to as type **AVi/d**, shortly after fusion with lysosomes.

A similar degradative autophagic process could also be observed in other molluscs (Kiss, 2010) associated with cell degradation (Folkis et al., 1984), antiviral response (Green et al., 2015), depletion of reactive oxygen species-damaged proteins and organelles during oxidative stress (Abele et al., 2009; Moore et al., 2007, 2008) or as protection against microbial infection (Moreau et al., 2015).

Although autophagic activity is not intended to eliminate whole cells or even organs in the majority of cases (Kroemer & Levine, 2008), in the present case the extinction of the entire HO is clear evidence for the rather seldom observed autophagic cell death (ACD) (Berry & Baehrecke, 2007; Galluzzi et al., 2008; Levine & Yuan, 2005). The ultrastructural observations further confirm the expected accompanying features relating to ACD, such as the secondary enlarged Golgi bodies and the loss of microvilli and junctional complexes (Berry & Baehrecke, 2007; Clarke, 1990; Klepal et al., 2008).

Since autophagic activities require an unimpaired cellular metabolism to assemble phagophores and lysosomes, the following question arises: 'What happens with the remaining cell compartments (nucleus, Golgi, lysosomes) after the autophagic depletion of the cytoplasm?' Our observations did not provide answers to this outstanding issue; perhaps this final degradative period is of markedly short duration. Several studies provide indications that in the case of bulk cells degradation the expression of autophagic genes can induce caspase-dependent apoptotic features (Maiuri et al., 2007; Scott et al., 2007; Yousefi et al., 2006) to clean up cell remnants. In the salivary gland degradation of *Drosophila* larvae, the steroid hormone ecdysone plays an important role for inducing the expression of both the ATG genes and caspases during tissue remodelling (Berry & Baehrecke, 2007).

Another observed ACD pathway leads to the activation of RIPK3 (receptor-interacting protein kinase) - dependent necroptosis (Basit et al., 2013; Bonapace et al., 2010). Alternatively, phagocytes are implied to eliminate the remaining cellular parts (Tsujimoto & Shimizu, 2005). Autophagy also leads to the degradation of catalase, a key enzyme in eliminating reactive oxygen species (ROS) (Mates et al., 1999; Sohal & Orr, 1992); the subsequent ROS accumulation causes membrane peroxidation, the loss of membrane integrity and cell death (Yu et al., 2006).

Apparently, the different molecular pathways have numerous crossing points and collaborate in various combinations, depending on species and requirements as well as the current physiological and metabolic conditions. Current studies on the molecular pathways of ACD and participating molecules (Johansen & Lamark, 2011; Klionsky et al., 2011, 2012) in several model organisms provide opportunities for upcoming investigations. Future efforts should focus on setting up the protocols for cephalopods.

Nitric Oxide Synthase

Our results show that after hatching the HO cells do not exhibit any NOS immunopositivity, which might be the consequence of cell degradation by programmed cell death. On the other hand, this finding together with the presence of NOS and NO in the HO at later developmental stages before hatching (Mattiello et al., 2012) could also suggest a possible involvement of NO in preventing cell death signalling (CDS). The action of NO as a cell death inhibitor has likewise been reported in the apical ganglion of the gastropod *Ilyanassa obsoleta*, whereby this structure disappears by apoptosis at metamorphosis induction (Leise et al., 2004). Moreover, the increasing NO levels in the HO before hatching also could be related to the metabolism of the gland and NO might positively affect the

activity of the gland in producing the lytic enzymes necessary to digest the chorion (Fioroni, 1990). Concurrent evaluation of NO and CDS on embryos before, during and after the hatching phase may be helpful to correlate an antagonistic presence in the different tissue regions and at a specific embryonic stage.

Eroded epithelial cells

The content of the epithelial cells is mainly discharged, both in late embryonic stages (stage 27 onwards) (Fig. 4E), and in hatchlings (Fig. 5A, 6A). This phenomenon has been repeatedly described for other cephalopods (Cyran et al., 2015; Faussek, 1901; Fioroni, 1963) and imaged in further studies (Boletzky, 1982; Orelli, 1959; Shigeno et al., 2001). Moreover, epithelial abrasions were observed in late embryonic stages on the posterior and dorsal mantle (Fig. 4D, G, H). Other areas as head, ventral and lateral mantle remained intact. Similar observations of a "individual or groups of epithelial cells loss" in relationship to the HO-degradation were made for *Loligo pealei* (Arnold & Singley, 1989; Arnold & Williams-Arnold, 1980). Although a fixation-related artefact cannot be excluded, a collapse of the epithelium due to the absence of internal cell content and the insufficient intercellular stability (Fioroni, 1963) in connection with a sliding behaviour of the HO along the chorion also has to be taken into account.

Ciliary tufts and the ciliated HO border

The presence of numerous ciliary tufts on the mantle surface have been associated with the continuous flow in the perivitelline fluid in particular during late embryonic development (Arnold & Williams-Arnold, 1980; Boletzky, 1979, 1986), whereas the ciliated bands along the HO with their short cilia are supposed to provide a locomotory aid during hatching (Boletzky, 1986) or even a kind of adhesion effect (Arnold & Singley, 1989). The feather-like expansion of those ciliated bands from stage 26 onwards (Fig. 3D, 4F, I) is suspected to provide a more efficient dispersion of the enzymes along the chorion, similar to the microvilli border in Idiosepiidae (Cyran et al., 2011). The complete regression of both types of ciliary cells within about one day after hatching fits well with their ascribed role in supporting hatching.

Such continuous alterations in the pattern of ciliated cells are related to the changing conditions and requirements during embryonic development such as the growing perivitelline space and the required flow of the perivitelline fluid. Similar observations were made for other decapods such as *Loligo pealei* (Arnold & Williams-Arnold, 1980), where the ciliated

cells increasingly form longitudinal bands as the embryo gets closer to hatching. This arrangement generates a flow towards the head, giving support to hatching (Arnold & Williams-Arnold, 1980). Functionally, the emerging ciliated branches along the dorsal band of *Sepia officinalis* HO seem to resemble the ciliary bands in *Loligo* and may thus be responsible for the hatch-supporting current.

The close association of the ciliary rootlets with the outer membranes of mitochondria (Fig. 8C) illustrates the high energy requirement for generating the perivitelline flow and is strongly reminiscent of the observations in *Loligo vulgaris* yolk sac envelope (Boletzky, 1973).

Metallic contents in the hatching gland enzymes

The present study confirms the presence of metals such as Fe and Cu within the HO and connective tissue. The normal mantle epithelium lacks these elements; a metal contamination by the surrounding water could thus be excluded. Also, it is proposed that Fe and Cu cannot pass through the egg integument (Boletzky, 1966, 1973; Paulij et al., 1990), excluding an accumulation during embryonic development. The digestive gland (hepatopancreas) of cephalopods is considered to be the storage site of metals (Bustamante et al., 2002; Miramand & Bentley, 1992). Measurements of metal concentrations in this gland in *Sepia officinalis* (Miramand & Bentley, 1992; Miramand et al., 2006) and *Octopus vulgaris* embryos (Villanueva & Bustamante, 2006) indicate that Fe and Cu as well as Zn occur in significantly higher concentrations than other metals. Also, high amounts of Cu and Cu-containing proteins are found in mature *S. officinalis* eggs extracted directly from females ovaries, although the Cu belongs to a large extent to the Cu-cored hemocyanin (Wolf & Decleir, 1980). Due to the lack of data, comparison with hatching enzyme-associated metals of other cephalopods is currently not possible. However, in the teleost *Orizias latipes* a catalytic effect of the metals Zn and Mg (1.24 µg/mg and 1.64 µg/mg) occur in the hatching enzymes (Yasumasu et al., 1989a). In *Sepia officinalis* the detected Fe and Cu ions may achieve a comparable catalytic effect. The assumption of metalloproteases contribution in the HO of cephalopods is being strengthened by successful inhibition of the enzymatic activity of the hatching medium by the metal chelator EDTA in *Loligo vulgaris* (Paulij et al., 1992). EDTA rips out and complex metal ions from the treated medium and so inactivates metalloproteases.

Conclusion

The results presented above provide an overview of the lifetime of the HO in *S. officinalis*. The first evidences for cell proliferation are recognizable within the epithelium at embryonic stage 22-23, while first secretory vesicles can be observed at stage 23 and secretion of chorion-digesting enzymes is evident at stage 27 (Fig. 10). Degradation of the HO is completed two days after hatching, whereby an autophagic process has been recognized for the first time in cephalopods to explain HO cell degradation. Based upon NOS detection results, NOS immunopositivity was not found in the HO cells after hatching, suggesting a possible NO role in cell death signaling. Given that the presence of Fe and Cu was confirmed in the HO and connective tissue (but not in the normal mantle tissue) of *S. officinalis* hatchlings, they may likewise be related to enzymatic activity during cell decay of the HO. These results will contribute to the planning of upcoming molecular biological investigations of key cell death proteins to provide a better understanding of the complex processes of cytoplasmic degradation and developmental cell death in cephalopods.

Acknowledgements

The authors would like to particularly thank Dr. Teresa Mattiello for her support and cooperation during the stay at the Stazione Zoologica Anton Dohrn, Naples, Italy. Her experience and knowledge allowed the appropriate collection of the *Sepia officinalis* embryos used in this research project. This study was kindly funded by the Austrian Science Fund FWF (Project No. P 21135-B17).

Table legends

Table 1: EDX-evaluation of metal contents (iron and copper) in the integument around the hatching gland according to the reference in Fig. 7A (embryonic stage 29, Area 1-5) and in the egg integument (embryonic stage 24). The high error levels are caused by the low concentration of iron and copper in relation to the detection limits of this technique.

Figure legends

Fig. 1 Egg composition of *Sepia officinalis*. **(A)** The egg is enclosed in a chorion membrane and several vitelline layers (stage 23, egg capsule removed). **(B)** A multi-layered egg capsule composed of numerous layers (outermost on top) serves as outer protection (stage 23), whereby a clear distinction between capsule and vitelline layers cannot be established. **(C)** The outermost capsule layers contain the highest amount of incorporated ink droplets and other, exogenous inclusions, presumably bacteria (arrowheads) (stage 23). The insert points to the internal, variably orientated, filamentous structure, which is emphasized with stronger contrast. **(D)** The left-hand layers are highly compressed whereas the inner layers (bracket) are intermediated by lower density areas (stage 30). **ch**, chorion; **id**, ink droplet; **vi**, vitelline layer. **Scale bars**: 200 µm (A), 100 µm (B), 1 µm (C), 10 µm (D).

Fig. 2 Embryonic stages 23 (A-C) and 24 (D-I): **(A)** At stage 23 the lateral bands of the Hoyle organ are clearly pronounced in relation to the normal mantle epithelium (ma), while only a short part of the dorsal band has developed so far. Ciliary tufts are visible below the posterior mantle pole and along the anterior mantle edge (arrows). **(B)** The development of the Hoyle organ can be recognized by the elevated epithelium surface. Initial accumulations of secretory granules already occur in the apical region of the gland cells. **(C)** The synthesizing organelles display a high activity in assembling secretory material. Tubules are aligned along the vertical cell axes. The arrow shows the migration direction of the granules (towards the apical cell pole). **(D)** At stage 24 the three bands of the Hoyle organ are clearly visible externally. Ciliary tufts cover the whole mantle evenly. **(E)** Shows a part near the distal end of the dorsal band at stage 24, where a very initial differentiation of the Hoyle organ cells can be observed. The cell height has not yet increased but within the epithelium several cell divisions can be observed by means of the beginning chromatin condensation (arrows). **(F)** A constricted nucleus (arrow) in telophase with a centriole at the nuclear pole (arrowhead). The aborning Hoyle organ cells are accompanied by a degradation of other epithelium cells, which display a conspicuous degraditive chromatin condensation, apparently associated with cell death (stars).

(G) Cross section of a proximal region of the dorsal band. The recessed middle part displays the tips of the secretory cells, accompanied laterally by continuous ciliated epithelial cells **(H)** Distally in the secretory cells, accumulations of spherical secretory granules are evident. Basally in the cell the granules have low density but condense increasingly during their migration towards the cell tips while becoming more electron dense and smaller in size (finally 1 – 1.5 µm). **(I)** The movement of the granules is apparently realized by longitudinal microtubules acting as sliding elements. **cc**, ciliated cells; **ch**, condensed chromatin; **fi**, fin; **go**, Golgi bodies; **HO**, Hoyle organ; **ma**, mantle; **mi**, mitochondrion; **mt**, microtubules; **mv**, microvilli; **rER**, rough endoplasmic reticulum; **sg**, secretory granules; **za** zonula adherens. **Scale bars**: 200 µm (A, D), 50 µm (B), 1 µm (C, I), 2 µm (E, H), 5 µm (F), 50 µm (G).

Fig. 3 Embryonic stages 25-26 (A-C) and 27 (D-F): **(A)** Posterior view of the Hoyle organ (SEM) and an associated virtual micro CT cross section (insert). **(B)** The granules have a uniform density but electron transparent areas indicate the beginning bipartity of the granules. Microvilli cover the cell surface **(C)** Above the nucleus the synthesis is still highly active within the secretory cells, indicated by the bulk of endoplasmic reticulum and the assembling secretory granules. **(D)** At stage 27 the dispersion of the ciliated cells, lining the dorsal band of the Hoyle organ, change to a feather-like pattern. **(E)** The cross section of this region illustrates the presence of several rows of ciliated cells (Arrows). **(F)** First indications of a secretory process are obvious at stage 27. **mv**, microvilli; **rER**, rough endoplasmic reticulum; **sg**, secretory granules; **sm**, secreted material. **Scale bars**: 200 µm (A), 1 µm (B), 2 µm (C, F), 50 µm (D), 20 µm (E).

Fig. 4 Embryonic stages 28 (A-C), 29 (D-F) and 30 (G-K): **(A)** Cross section of the Hoyle organ showing the mature gland cells and the laterally bordering ciliated cells (stage 28). The insert shows a related virtual micro CT section. **(B)** Apical pole of a secretory cell, tightly packed with granules and covered with microvilli and glycocalix on the surface. **(C)** Synthesis area of a gland cell showing endoplasmic reticulum, Golgi bodies and forming secretory granules. **(D)** SEM illustration of a stage 29 embryo. The erosion of the epithelial cells is clearly visible laterally from the dorsal band (arrow heads). Some areas completely lack epithelial cells (arrow) and expose the basal membrane. **(E)** Cross section (stage 29) showing a distinct reduction of the gland in relation to stage 28, effected by continuous secretion and stagnating synthesis. Moreover, the epithelial cells tend increasingly to be empty. **(F)** Detail of the surface view illustrating the ciliated cells around the Hoyle organ which form a feather-

like pattern. The arrows indicate the secretory cell areas. **(G)** SEM illustration of a stage 30 embryo. The areas of eroded epithelial cells are labelled by arrow heads. **(H)** The apical areas of these epithelial cells are completely dissolved. The arrows indicate the secretory cell areas. **(I)** An intact epithelium area near the posterior pole with the final appearance of the ciliated gland border before depletion of the organ and its accompanying structures. The arrows indicate the secretory cell areas. **(J)** Cross section of the Hoyle organ (stage 30). The volume of the secretory cells is significantly decreased. **(K)** Although the synthesis seems to be finished, the endoplasmic reticulum still appears intact. **cc**, ciliated cells; **ci**, cilia; **ct**, ciliary tufts; **db**, dorsal band; **ec**, epithelial cells; **gc**, glycocalix; **go**, Golgi bodies; **HO**, Hoyle organ, **mv**, microvilli; **nu**, nucleus; **rER**, rough endoplasmic reticulum; **sc**, secretory cells; **sg**, secretory granules. **Scale bars**: 20 µm (A, E, J), 1 µm (B, C, K), 500 µm (D, G), 50 µm (F, H, I). Image 4A reprinted from Cyran et al. (2013) with permission from Elsevier.

Fig. 5 Degradation of the Hoyle organ, one day after hatching. **(A)** Light microscopic image of the dorsal mantle epithelium. The remaining Hoyle organ (label) is considerably reduced after one day. **(B)** The secretory cells are characterized by autolysosomes containing membrane stacks, mitochondria, ribosomes and parts of granules. The single-membraned autolysosomes illustrate the stage after the cytoplasm-incorporating autophagosom fuses with a lysosome and is subsequently digested. **(C)** During autophagic degradation, Golgi bodies are reactivated and bud off numerous vesicles. **al**, autolysosome; **ct**, connective tissue; **ec**, epithelial cells; **go**, Golgi bodies; **gv**, Golgi vesicles. **Scale bars**: 50 µm (A), 1 µm (B), 500 nm (C).

Fig. 6 Degradation of the Hoyle organ in a two-day old juvenile. **(A, B)** Overview of the regressing gland. The connective tissue is still slightly elevated. **(C)** Detail of the degrading secretory cells showing a late phase of digesting autolysosomes. The previously massively increased Golgi body abundance, visible one day after hatching, no longer exists. **al**, autolysosome; **ct**, connective tissue; **ec**, epithelial cells; **HO**, Hoyle organ. **Scale bars**: 50 µm (A), 20 µm (B), 1 µm (C).

Fig. 7 Vibratome cross section (100 µm thick) of the HO with the surrounding epithelium and connective tissue in a hatched specimen. Positive labelling of NOS (overlaid with a light microscopic image) is highlighted in green, showing a high presence within some epithelium

cells and an even dispersion in the connective tissue. By contrast, the cells of the HO are not stained. **ct**, connective tissue; **ec**, epithelial cells; **HO**, Hoyle organ. **Scale bar**: 100 µm.

Fig. 8 Ciliated mantle epithelium cells. **(A)** SEM image of a group of ciliary tufts dorsally on the mantle (stage 22). **(B)** The ciliated cells are characterized by a small cell volume but a considerable dense cytoplasm, dense microvilli and a conspicuous glycocalix (stage 28). **(C)** Later in development (late stage 30), the formerly dense cytoplasm of this ciliary tuft cell loosens. Indeed, the close association of the ciliary roots with mitochondria becomes visible. **cc**, ciliated epithelium cell; **ce**, centriol; **ci**, cilia; **cr**, ciliary root; **ct**, ciliary tuft; **gc**, glycocalix; **go**, Golgi bodies; **mi**, mitochondria; **mv**, microvilli. **Scale bars**: 10 µm (A), 2 µm (B), 500 nm (C). Image 8C reprinted from Cyran et al. (2013) with permission from Elsevier.

Fig. 9 Distribution of copper and iron in the Hoyle organ and adjacent tissues (embryonic stage 29), evaluated by energy-dispersive X-ray spectroscopy (EDX): **(A)** Backscatter image indicating five measuring areas on a two µm thick resin section. Point 1 is the negative control beyond the tissue without copper or iron. Point 2 is an almost empty epithelium cell, also lacking both metals. Points 3 and 4 (HO) as well as 5 (connective tissue) contain small amounts of iron and copper (table 1). **(B)** EDX-spectrum of point 3. **(C)** TEM image of granules of the Hoyle organ combined with an EFTEM copper distribution map in yellow. **(D)** EELS spectrum of a relating Hoyle organ granule. **ct**, connective tissue; **ec**, epithelial cells; **HO**, Hoyle organ; **sg**, secretory granules**. Scale bars**: 50 µm (A), 500 nm (C).

Fig. 10 Development phases of the Hoyle organ: **(A)** Illustrates the overall chronology of the gland development, synthesis, secretion and degradation; details described in the text.

References

Abele, D., T. Brey, & E. Philipp, 2009. Bivalve models of aging and the determination of molluscan lifespans. Experimental Gerontology 44: 307-315.

Arbeitman, M. N., E. E. M. Furlong, F. Imam, E. Johnson, B. H. Null, B. S. Baker, M. A. Krasnow, M. P. Scott, R. W. Davis, & K. P. White, 2002. Gene expression during the life cycle of *Drosophila melanogaster*. Science 297: 2270-2275.

Arnold, J. M. & C. T. Singley, 1989. Ultrastructural changes in the cells of the Hoyle organ during hatching of the squid *Loligo pealei*. Journal of Cephalopod Biology 1: 1-14.

Arnold, J. M. & L. D. Williams-Arnold, 1980. Development of the ciliature pattern on the embryo of the squid *Loligo pealei*: A scanning electron microscope study. Biological Bulletin 159: 102-116.

Ashford, T. P. & K. R. Porter, 1962. Cytoplasmic components in hepatic cell lysosomes. Journal of Cell Biology 12: 198-202.

Basit, F., S. Cristofanon, & S. Fulda, 2013. Obatoclax (GX15-070) triggers necroptosis by promoting the assembly of the necrosome on autophagosomal membranes. Cell Death and Differentiation 20: 1161-1173.

Berry, D. L. & E. H. Baehrecke, 2007. Growth arrest and autophagy are required for salivary gland cell degradation in *Drosophila*. Cell 131: 1137-1148.

Boletzky, S., 1982. Developmental aspects of the Mantle Complex in Coleoid Cephalopods. Malacologia 23: 165-175.

Boletzky, S. v., 1966. Zum Schlüpfen von *Octopus vulgaris* Lam. Verhandlungen der Naturforschenden Gesellschaft in Basel 77: 164-170.

Boletzky, S. v., 1973. Association of mitochondria with ciliary rootlets in squid embryos. Cytobiologie 8: 164-167.

Boletzky, S. v., 1979. Ciliary locomotion in squid hatching. Experientia 35: 1051-1053.

Boletzky, S. v., 1986. Encapsulation of cephalopod embryos: A search for functional correlations. American Malacological Bulletin 4: 217-227.

Boletzky, S. v., 1991. The terminal spine of sepiolid hatchlings: its development and functional morphology (Mollusca: Cephalopoda). Bulletin of Marine Science 49: 107-112.

Boletzky, S. v., 1998. Cephalopod eggs and egg masses. Oceanography and Marine Biology: An Annual Review 36: 341-370.

Boletzky, S. v., 2003. Biology of Early Life Stages in Cephalopod Molluscs. Advances in Marine Biology 44: 143-203.

Boletzky, S. v., 2012. Hatch-as hatch-can: tricks of the trade in coleoid hatchlings (Mollusca: Cephalopoda). Neues Jahrbuch für Geologie und Paläontologie - Abhandlungen 266: 67-76.

Boletzky, S. v., A. Andouche, & L. Bonnaud-Ponticelli, 2016. A developmental table of embryogenesis in *Sepia officinalis*. Vie et Milieu - Life & Environment 66: 11-23.

Bonapace, L., B. C. Bornhauser, M. Schmitz, G. Cario, U. Ziegler, F. K. Niggli, B. W. Schafer, M. Schrappe, M. Stanulla, & J. P. Bourquin, 2010. Induction of autophagy-dependent necroptosis is required for childhood acute lymphoblastic leukemia cells to overcome glucocorticoid resistance. Journal of Clinical Investigation 120: 1310-1323.

Boucaud-Camou, E., M. Yim, & A. Tresgot, 1985. Feeding and Digestion of Young *Sepia officinalis* L. (Mollusca: Cephalopoda) during Post-Hatching Development. Vie Milieu 35: 263-266.

Bustamante, P., J. L. Teyssie, S. W. Fowler, O. Cotret, B. Danis, P. Miramand, & M. Warnau, 2002. Biokinetics of zinc and cadmium accumulation and depuration at different stages in the life cycle of the cuttlefish *Sepia officinalis*. Marine Ecology Progress Series 231: 167-177.

Castellano, I., E. Ercolesi, & A. Palumbo, 2014. Nitric oxide affects ERK signaling through down-regulation of MAP kinase phosphatase levels during larval development of the ascidian *Ciona intestinalis*. PLoS One 9: e102907.

Clark, S. L., 1957. Cellular Differentiation in the Kidneys of Newborn Mice Studied with the Electron Microscope. Journal of Biophysical and Biochemical Cytology 3: 349-362.

Clarke, P. G. H., 1990. Developmental Cell-Death - Morphological Diversity and Multiple Mechanisms. Anatomy and Embryology 181: 195-213.

Comes, S., A. Locascio, F. Silvestre, M. d'Ischia, G. L. Russo, E. Tosti, M. Branno, & A. Palumbo, 2007. Regulatory roles of nitric oxide during larval development and metamorphosis in *Ciona intestinalis*. Developmental Biology 306: 772-784.

Cyran, N., W. Klepal, Y. Staedler, J. Schoenenberger, & J. von Byern, 2015. Alterations in the mantle epithelium during transition from hatching gland to adhesive organ of *Idiosepius pygmaeus* (Mollusca, Cephalopoda). Mechanisms of Development 135: 43-57.

Cyran, N., W. Klepal, & J. von Byern, 2011. Ultrastructural characterization of the adhesive organ of *Idiosepius biserialis* and *Idiosepius pygmaeus* (Mollusca, Cephalopoda). Journal of the Marine Biological Association of the United Kingdom 91: 1499-1510.

Cyran, N., Y. Staedler, J. Schoenenberger, W. Klepal, & J. von Byern, 2013. Hatching glands in cephalopods - A comparative study. Zoologischer Anzeiger 253: 66-82.

D'Aniello, A., G. D'Onofrio, M. Pischetola, & J. M. Denuce, 1989. Effect of pH, salinity and Ca2+, Mg2+, K+ and SO4 2+ ions on hatching and viability of *Loligo vulgaris* embryo. Comparative Biochemistry and Physiology - Part A 94: 477-481.

Denuce, J. M. & A. Formisano, 1982. Circumstantial evidence for an active contribution of Hoyle gland to enzymatic hatching of cephalopod embryos. Archives Internationales de Physiologie de Biochimie et de Biophysique 90: 185-186.

Di Cristo, C., G. Fiore, V. Scheinker, G. Enikolopov, M. d'Ischia, A. Palumbo, & A. Di Cosmo, 2007. Nitric oxide synthase expression in the central nervous system of *Sepia officinalis*: an in situ hybridization study. European Journal of Neuroscience 26: 1599-1610.

Dunn, W. A., 1990a. Studies on the Mechanisms of Autophagy - Formation of the Autophagic Vacuole. Journal of Cell Biology 110: 1923-1933.

Dunn, W. A., 1990b. Studies on the Mechanisms of Autophagy - Maturation of the Autophagic Vacuole. Journal of Cell Biology 110: 1935-1945.

Eide, D. J., 1998. The molecular biology of metal ion transport in *Saccharomyces cerevisiae*. Annual Review of Nutrition 18: 441-469.

Eskelinen, E. L., 2008. To be or not to be? Examples of incorrect identification of autophagic compartments in conventional transmission electron microscopy of mammalian cells. Autophagy 4: 257-260.

Eskelinen, E. L., F. Reggiori, M. Baba, A. L. Kovacs, & P. O. Seglen, 2011. Seeing is believing: The impact of electron microscopy on autophagy research. Autophagy 7: 935-956.

Faussek, V., 1901. Untersuchungen über die Entwicklung der Cephalopoden. Mitteilungen aus der Zoologischen Station zu Neapel 14: 83-237.

Fiore, G., A. Poli, A. Di Cosmo, M. d'Ischia, & A. Palumbo, 2004. Dopamine in the ink defence system of *Sepia officinalis*: Biosynthesis, vescicular compartmentation in mature ink gland cells, nitric oxide (NO)/cGMP-induced depletion and fate in secreted ink. Biochemical Journal 378: 785-791.

Fioroni, P., 1963. Zur embryonalen und postembryonalen Entwicklung der Epidermis bei zehnarmigen Tintenfischen. Verhandlungen der Naturforschenden Gesellschaft in Basel 74: 149-160.

Fioroni, P., 1978. Morphogenese der Tiere: Cephalopoda. VEB Gustav Fischer Verlag, Jena.

Fioroni, P., 1990. Our recent Knowledge of the Development of the cuttlefish (*Sepia officinalis*). Zoologischer Anzeiger 224: 1-25.

Folkis, V. V., Stupina A.S., Martinenko O.A., Toth S., & Timchenko A.I., 1984. Aging of neurons in the mollusc *Lymnaea stagnalis*. Structure, function and sensitivity to transmitters. Mechanisms of Ageing and Development 25: 91-102.

Galluzzi, L., J. M. Vicencio, O. Kepp, E. Tasdomir, M. C. Maiuri, & G. Kroemer, 2008. To die or not to die: That is the autophagic question. Current Molecular Medicine 8: 78-91.

Galluzzi, L., I. Vitale, J. M. Abrams, E. S. Alnemri, E. H. Baehrecke, M. V. Blagosklonny, T. M. Dawson, V. L. Dawson, W. S. El-Deiry, S. Fulda, E. Gottlieb, D. R. Green, M. O. Hengartner, O. Kepp, R. A. Knight, S. Kumar, S. A. Lipton, X. Lu, F. Madeo, W. Malorni, P. Mehlen, G. Nunez, M. E. Peter, M. Piacentini, D. C. Rubinsztein, Y. Shi, H. U. Simon, P. Vandenabeele, E. White, J. Yuan, B. Zhivotovsky, G. Melino, & G. Kroemer, 2012. Molecular definitions of cell death subroutines: recommendations of the Nomenclature Committee on Cell Death 2012. Cell Death and Differentiation 19: 107-120.

Gledhill, M., E. P. Achterberg, K. Li, K. N. Mohamed, & M. J. Rijkenberg, 2015. Influence of ocean acidification on the complexation of iron and copper by organic ligands in estuarine waterscopper by organic ligands in estuarine waters. Marine Chemistry 177: 421-433.

Gomi, F., M. Yamamoto, & T. Nakazawa, 1986. Swelling of Egg During Development of the Cuttlefish, *Sepiella japonica*. Zoological Science 3: 641-645.

Green, T. J., D. Raftos, P. Speck, & C. Montagnani, 2015. Antiviral immunity in marine molluscs. Journal of General Virology 96: 2471-2482.

Guimaraes, C. A. & R. Linden, 2004. Programmed cell deaths - Apoptosis and alternative deathstyles. European Journal of Biochemistry 271: 1638-1650.

Jecklin, L., 1934. Beitrag zur Kenntnis der Laichgallerten und der Biologie der Embryonen decapoder Cephalopoden.: 595-673.

Johansen, T. & T. Lamark, 2011. Selective autophagy mediated by autophagic adapter proteins. Autophagy 7: 279-296.

Kerr, J. F., A. H. Wyllie, & A. R. Currie, 1972. Apoptosis: a basic biological phenomenon with wide-ranging implications in tissue kinetics. British Journal of Cancer 26: 239-257.

Kiss, T., 2010. Apoptosis and its functional significance in molluscs. Apoptosis 15: 313-321.

Klepal, W., D. Gruber, & B. Pflugpfelder, 2008. Natural cyclic degeneration by a sequence of programmed cell death modes in *Semibalanus balanoides* (Linnaeus, 1767) (Crustacea, Cirripedia, Thoracica). Zoomorphology 127: 49-58.

Klionsky, D. J., F. C. Abdalla, H. Abeliovich, R. T. Abraham, A. Acevedo-Arozena, K. Adeli, L. Agholme, M. Agnello, P. Agostinis, J. A. Aguirre-Ghiso, H. J. Ahn, O. Ait-Mohamed, S. Ait-Si-Ali, T. Akematsu, S. Akira, H. M. Al-Younes, M. A. Al-Zeer, M. L. Albert, R. L. Albin, J. Alegre-Abarrategui, M. F. Aleo, M. Alirezaei, A. Almasan, M. Almonte-Becerril, A. Amano, R. Amaravadi, S. Amarnath, A. O. Amer, N. Andrieu-Abadie, V. Anantharam, D. K. Ann, S. Anoopkumar-Dukie, H. Aoki, N. Apostolova, G. Arancia, J. P. Aris, K. Asanuma, N. Y. O. Asare, H. Ashida, V. Askanas, D. S. Askew, P. Auberger, M. Baba, S. K. Backues, E. H. Baehrecke, B. A. Bahr, X. Y. Bai, Y. Bailly, R. Baiocchi, G. Baldini, W. Balduini, A. Ballabio, B. A. Bamber, E. T. W. Bampton, G. Banhegyi, C. R. Bartholomew, D. C. Bassham, R. C. Bast, H. Batoko, B. H. Bay, I. Beau, D. M. Bechet, T. J. Begley, C. Behl, C. Behrends, S. Bekri, B. Bellaire, L. J. Bendall, L. Benetti, L. Berliocchi, H. Bernardi, F. Bernassola, S. Besteiro, I. Bhatia-Kissova, X. N. Bi, M. Biard-Piechaczyk, J. S. Blum, L. H. Boise, P. Bonaldo, D. L. Boone, B. C. Bornhauser, K. R. Bortoluci, I. Bossis, F. Bost, J. P. Bourquin, P. Boya, M. Boyer-Guittaut, P. V. Bozhkov, N. R. Brady, C. Brancolini, A. Brech, J. E. Brenman, A. Brennand, E. H. Bresnick, P. Brest, D. Bridges, M. L. Bristol, P. S. Brookes, E. J. Brown, J. H. Brumell, N. Brunetti-Pierri, U. T. Brunk, D. E. Bulman, S. J. Bultman, G. Bultynck, L. F. Burbulla, W. Bursch, J. P. Butchar, W. Buzgariu, S. P. Bydlowski, K. Cadwell, M. Cahova, D. S. Cai, J. Y. Cai, Q. Cai, B. Calabretta, J. Calvo-Garrido, N. Camougrand, M. Campanella, J. Campos-Salinas, E. Candi, L. Z. Cao, A. B. Caplan, S. R. Carding, S. M. Cardoso, J. S. Carew, C. R. Carlin, V. Carmignac, L. A. M. Carneiro, S. Carra, R. A. Caruso, G. Casari, C. Casas, R. Castino, E. Cebollero, F. Cecconi, J. Celli, H. Chaachouay, H. J. Chae, C. Y. Chai, D. C. Chan, E. Y. Chan, R. C. C. Chang, C. M. Che, C. C. Chen, G. C. Chen, G. Q. Chen, M. Chen, Q. Chen, S. S. L. Chen, W. L. Chen, X. Chen, X. M. Chen, X. Q. Chen, Y. G. Chen, Y. Y. Chen, Y. Q. Chen, Y. J. Chen, Z. X. Chen, A. Cheng, C. H. K. Cheng, Y. Cheng, H. Cheong, J. H. Cheong, S. Cherry, R. Chess-Williams, Z. H. Cheung, E. Chevet, H. L. Chiang, R. Chiarelli, T. Chiba, L. S. Chin, S. H. Chiou, F. V. Chisari, C. H. Cho, D. H. Cho, A. M. K. Choi, D. Choi, K. S. Choi, M. E. Choi, S. Chouaib, D. Choubey, V. Choubey, C. T. Chu, T. H. Chuang, S. H. Chueh, T. Chun, Y. J. Chwae, M. L. Chye, R. Ciarcia, M. R. Ciriolo, M. J. Clague, R. S. B. Clark, P. G. H. Clarke, R. Clarke, P. Codogno, H. A. Coller, M. I. Colombo, S. Comincini, M. Condello, F. Condorelli, M. R. Cookson, G. H. C. I. Coppens, R. Corbalan, P. Cossart, P. Costelli, S.

Costes, A. Coto-Montes, E. Couve, F. P. Coxon, J. M. Cregg, J. L. Crespo, M. J. Cronje, A. M. Cuervo, J. J. Cullen, M. J. Czaja, M. D'Amelio, A. Darfeuille-Michaud, L. M. Davids, F. E. Davies, M. De Felici, J. F. de Groot, C. A. M. de Haan, L. De Martino, A. De Milito, V. De Tata, J. Debnath, A. Degterev, B. Dehay, L. M. D. Delbridge, F. Demarchi, Y. Z. Deng, J. Dengjel, P. Dent, D. Denton, V. Deretic, S. D. Desai, R. J. Devenish, M. Di Gioacchino, G. Di Paolo, C. Di Pietro, G. Diaz-Araya, I. Diaz-Laviada, M. T. Diaz-Meco, J. Diaz-Nido, I. Dikic, S. P. Dinesh-Kumar, W. X. Ding, C. W. Distelhorst, A. Diwan, M. Djavaheri-Mergny, S. Dokudovskaya, Z. Dong, F. C. Dorsey, & V. Dosenko, 2012. Guidelines for the use and interpretation of assays for monitoring autophagy. Autophagy 8: 445-544.

Klionsky, D. J., E. H. Baehrecke, J. H. Brumell, C. T. Chu, P. Codogno, A. M. Cuervo, J. Debnath, V. Deretic, Z. Elazar, E. L. Eskelinen, S. Finkbeiner, J. Fueyo-Margareto, D. Gewirtz, M. Jaattela, G. Kroemer, B. Levine, T. J. Melia, N. Mizushima, D. C. Rubinsztein, A. Simonsen, A. Thorburn, M. Thumm, & S. A. Tooze, 2011. A comprehensive glossary of autophagy-related molecules and processes (2nd edition). Autophagy 7: 1273-1294.

Kroemer, G. & B. Levine, 2008. Autophagic cell death: the story of a misnomer. Nature Reviews Molecular Cell Biology 9: 1004-1010.

Lacoue-Labarthe, T., E. Réveillac, F. Oberhänsli, J. L. Teyssié, R. Jeffree, & J. P. Gattuso, 2011. Effects of ocean acidification on trace element accumulation in the early-life stages of squid *Loligo vulgaris*. Aquatic Toxicology 105: 207-217.

Leise, E. M., S. C. Kempf, N. R. Durham, & D. J. Gifondorwa, 2004. Induction of metamorphosis in the marine gastropod *Ilyanassa obsoleta*: 5HT, NO and programmed cell death. Acta Biologica Hungarica 55: 293-300.

Leist, M. & M. Jaattela, 2001. Four deaths and a funeral: From caspases to alternative mechanisms. Nature Reviews Molecular Cell Biology 2: 589-598.

Lemaire, J., 1972. Table du dévelopment embryonnaire de *Sepia officinalis* L. (Mollusque, Céphalopode). Bulletin de la Société Zoologique de France 95: 773-782.

Levine, B. & D. J. Klionsky, 2004. Development by self-digestion: Molecular mechanisms and biological functions of autophagy. Developmental Cell 6: 463-477.

Levine, B. & J. Y. Yuan, 2005. Autophagy in cell death: an innocent convict? Journal of Clinical Investigation 115: 2679-2688.

Liou, W., H. J. Geuze, M. J. H. Geelen, & J. W. Slot, 1997. The autophagic and endocytic pathways converge at the nascent autophagic vacuoles. Journal of Cell Biology 136: 61-70.

Maiuri, M. C., E. Zalckvar, A. Kimchi, & G. Kroemer, 2007. Self-eating and self-killing: crosstalk between autophagy and apoptosis. Nature Reviews Molecular Cell Biology 8: 741-752.

Mates, J. M., C. Perez-Gomez, & I. N. De Castro, 1999. Antioxidant enzymes and human diseases. Clinical Biochemistry 32: 595-603.

Matsuno, A. & M. Ouji, 1988. Ultrastructural studies on development of the tail gland of a cuttlefish, *Sepiella japonica*. Development, Growth & Differentiation 30: 673-680.

Mattiello, T., M. Costantini, B. Di Matteo, S. Livigni, A. Andouche, L. Bonnaud, & A. Palumbo, 2012. The dynamic nitric oxide pattern in developing cuttlefish *Sepia officinalis*. Developmental Dynamics 241: 390-402.

Mattiello, T., M. d'Ischia, & A. Palumbo, 2013. Nitrix oxide in chromatic body patterning elements of *Sepia officinalis*. Journal of Experimental Marine Biology and Ecology 447: 128-131.

Mattiello, T., G. Fiore, E. R. Brown, M. d'Ischia, & A. Palumbo, 2010. Nitric Oxide Mediates the Glutamate-dependent Pathway for Neurotransmission in *Sepia officinalis* Chromatophore Organs. Journal of Biological Chemistry 285: 24154-24163.

Mcphee, C. K., M. A. Logan, M. R. Freeman, & E. H. Baehrecke, 2010. Activation of autophagy during cell death requires the engulfment receptor Draper. Nature 465: 1093-1096.

Migliaccio, O., I. Castellano, G. Romano, & A. Palumbo, 2014. Stress response to cadmium and manganese in *Paracentrotus lividus* developing embryos is mediated by nitric oxide. Aquatic Toxicology 156: 125-134.

Miramand, P. & D. Bentley, 1992. Concentration and distribution of heavy metals in tissues of two cephalopods, *Eledone cirrhosa* and *Sepia officinalis* from the French coast of the English channel. Marine Biology 114: 407-414.

Miramand, P., P. Bustamante, D. Bentley, & N. Koueta, 2006. Variation of heavy metal concentrations (Ag, Cd, Co, Cu, Fe, Pb, V, and Zn) during the life cycle of the common cuttlefish *Sepia officinalis*. Science of the Total Environment 361: 132-143.

Moore, M. N., 2008. Autophagy as a second level protective process in conferring resistance to environmentally-induced oxidative stress. Autophagy 4: 254-256.

Moore, M. N., A. Viarengo, P. Donkin, & A. J. S. Hawkins, 2007. Autophagic and lysosomal reactions to stress in the hepatopancreas of blue mussels. Aquatic Toxicology 84: 80-91.

Moreau, P., K. Moreau, A. Segarra, D. Tourbiez, M. A. Travers, D. C. Rubinsztein, & T. Renault, 2015. Autophagy plays an important role in protecting Pacific oysters from OsHV-1 and *Vibrio aestuarianus* infections. Autophagy 11: 516-526.

Morel, F. M. M., A. J. Milligan, & M. A. Saito, 2003. Marine bioinorganic chemistry: The role of trace metals in the oceanic cycles of major nutrients. In Elderfield, H. (eds), Treatise on Geochemistry. Elsevier Science 113-143.

Nakakoshi, M., H. Nishioka, & E. Katayama, 2011. New versatile staining reagents for biological transmission electron microscopy that substitute for uranyl acetate. Journal of Electron Microscopy 60: 401-407.

Nixon, M. & K. Mangold, 1998. The early life of *Sepia officinalis*, and the contrast with that to *Octopus vulgaris*. Journal of Zoology, London 245: 407-421.

Novikoff, A. B. & E. Essner, 1962. Cytolysomes and mitochondrial degeneration. Journal of Cell Biology 15: 140-146.

O'Brian, C. E., 2017. Behavioral development in embryonic and early juvenile cuttlefish (*Sepia officinalis*). Developmental Psychobiology 59: 145-160.

Ogawa, N. & Y. Ohi, 1968. On the chorion and the hatching enzyme of the medaka, *Oryzias latipes*. Zoological Magazine 77: 151-156.

Orelli, M. v., 1959. Über das Schlüpfen von *Octopus vulgaris*, *Sepia officinalis* und *Loligo vulgaris*. Revue Suisse de Zoologie 66: 330-343.

Palumbo, A., 2005. Nitric oxide in marine invertebrates: A comparative perspective. Comparative Biochemistry and Physiology Series A Molecular & Integrative Physiology 142: 241-248.

Palumbo, A., A. Poli, A. DiCosmo, & M. dIschia, 2000. N-methyl-D-aspartate receptor stimulation activates tyrosinase and promotes melanin synthesis in the Ink gland of the cuttlefish *Sepia officinalis* through the nitric oxide/cGMP signal transduction pathway - A novel possible role for glutamate as physiologic activator of melanogenesis. Journal of Biological Chemistry 275: 16885-16890.

Paulij, W. P., H. C. C. M. Verhoof, & J. M. Denuce, 1992. Partial purification and characterization of Loligo vulgaris hatching enzyme obtained from hatching medium. Comparative Biochemistry and Physiology Series B 101: 617-622.

Paulij, W. P., W. Zurburg, J. M. Denuce, & E. J. Vanhannen, 1990. The effect of copper on the embryonic development and hatching of *Sepia-Officinalis*. Archives of Environmental Contamination and Toxicology 19: 797-801.

Pörtner, H. O. & S. Zielinski, 1998. Environmental constraints and the physiology of performance in squids. African Journal of Marine Science 20: 207-217.

Reynolds, E. S., 1963. The use of lead citrate at high pH as an electron-opaque stain in electron microscopy. Journal of Cell Biology 17: 208-212.

Scott, R. C., G. Juhasz, & T. P. Neufeld, 2007. Direct induction of autophagy by Atg1 inhibits cell growth and induces apoptotic cell death. Current Biology 17: 1-11.

Shigeno, S., H. Kidokoro, T. Goto, K. Tsuchiya, & S. Segawa, 2001. Early ontogeny of the japanese common squid *Todarodes pacificus* (Cephalopoda, Ommastrephidae) with special reference to its Characteristic Morphology and Ecological Significance. Zoological Science 18: 1011-1026.

Sohal, R. S. & W. C. Orr, 1992. Relationship Between Antioxidants, Prooxidants, and the Aging Process. Annals of the New York Academy of Sciences 663: 74-84.

Stockdale, A., E. Tipping, E. Lofts, & R. J. G. Mortimer, 2016. Effect of Ocean Acidification on Organic and Inorganic Speciation of Trace Metals. Environmental Science & Technology 50: 1906-1913.

Thumm, M., R. Egner, B. Koch, M. Schlumpberger, M. Straub, M. Veenhuis, & D. H. Wolf, 1994. Isolation of Autophagocytosis Mutants of *Saccharomyces cerevisiae*. FEBS Letters 349: 275-280.

Tsujimoto, Y. & S. Shimizu, 2005. Another way to die: autophagic programmed cell death. Cell Death and Differentiation 12: 1528-1534.

Tsukada, M. & Y. Ohsumi, 1993. Isolation and Characterization of Autophagy-Defective Mutants of Saccharomyces-Cerevisiae. FEBS Letters 333: 169-174.

Vidal, E. A., R. Villanueva, J. P. Andrade, I. G. Gleadall, J. Iglesias, N. Koueta, C. Rosas, S. Segawa, B. Grasse, R. M. Franco-Santos, C. B. Albertin, C. Caamal-Monsreal, M. E. Chimal, E. Edsinger-Gonzales, P. Gallardo, P. C. Le, C. Pascual, K. Roumbedakis, & J. Wood, 2014. Cephalopod culture: current status of main biological models and research priorities. Adv.Mar.Biol. 67: 1-98.

Villanueva, R. & P. Bustamante, 2006. Composition in essential and non-essential elements of early stages of cephalopods and dietary effects on the element profiles of *Octopus vulgaris* paralarvae. Aquaculture 261: 225-240.

von Byern, J., A. Kerbl, M. T. Nödl, G. Bello, Y. Staedler, J. Schoenenberger, & N. Cyran, 2016. Spine Formation as a Hatching Tool in *Euprymna scolopes* (Mollusca, Cephalopoda, Sepiolidae). Malacologia 59: 231-238.

Wintrebert, P., 1928. L´Eclosion par digestion de la coque chez les poissons, les amphibiens et les céphalopodes dibranchiaux décapodes. Comptes rendus de l'Association des Anatomistes Nancy 1928: 496-503.

Wolf, G. & W. Decleir, 1980. A study of copper and copper proteins in the eggs of *Sepia officinalis* L. Annales de la Société royale zoologique de Belgique 110: 115-122.

Wollesen, T., R. Loesel, & A. Wanninger, 2009. Pygmy squid and giant brains: mapping the complex cephalopod CNS by phalloidin staining of vibratome sections and whole-mount preparatations. Journal of Neuroscience Methods 179: 63-67.

Wyllie, A. H., J. F. Kerr, & A. R. Currie, 1980. Cell death: the significance of apoptosis. International Review of Cytology 68: 251-306.

Yamagami, K., 1973. Some enzymological properties of a hatching enzyme (chorionase) isolated from the fresh-water teleost, *Oryzias latipes*. Comparative Biochemistry and Physiology Series B Biochemistry & Molecular Biology 46: 603-616.

Yasumasu, S., I. Iuchi, & K. Yamagami, 1988. Medaka Hatching Enzyme Consists of 2 Kinds of Proteases Which Act Cooperatively. Zoological Science 5: 191-195.

Yasumasu, S., I. Iuchi, & K. Yamagami, 1989a. Isolation and some properties of low choriolytic enzyme (LCE), a component of the hatching enzyme of the teleost, *Oryzias latipes*. Journal of Biochemistry 105: 212-218.

Yasumasu, S., I. Iuchi, & K. Yamagami, 1989b. Purification and partial characterization of high choriolytic enzyme (HCE), a component of the hatching enzyme of the teleost *Oryzias latipes*. Journal of Biochemistry 105: 204-211.

Yousefi, S., R. Perozzo, I. Schmid, A. Ziemiecki, T. Schaffner, L. Scapozza, T. Brunner, & H. U. Simon, 2006. Calpain-mediated cleavage of Atg5 switches autophagy to apoptosis. Nature Cell Biology 8: 1124-1132.

Yu, L., F. Y. Wan, S. Dutta, S. Welsh, Z. H. Liu, E. Freundt, E. H. Baehrecke, & M. Lenardo, 2006. Autophagic programmed cell death by selective catalase degradation. Proceedings of the National Academy of Sciences of the United States of America 103: 4952-4957.

Yung Ko Ching, M., 1930. Contribution á l´etude cytologique de l´ovogenese, du developpment et de quelques organes chez les cephalopodes. Annales de L´Institut Oceanographique 7: 300-364.

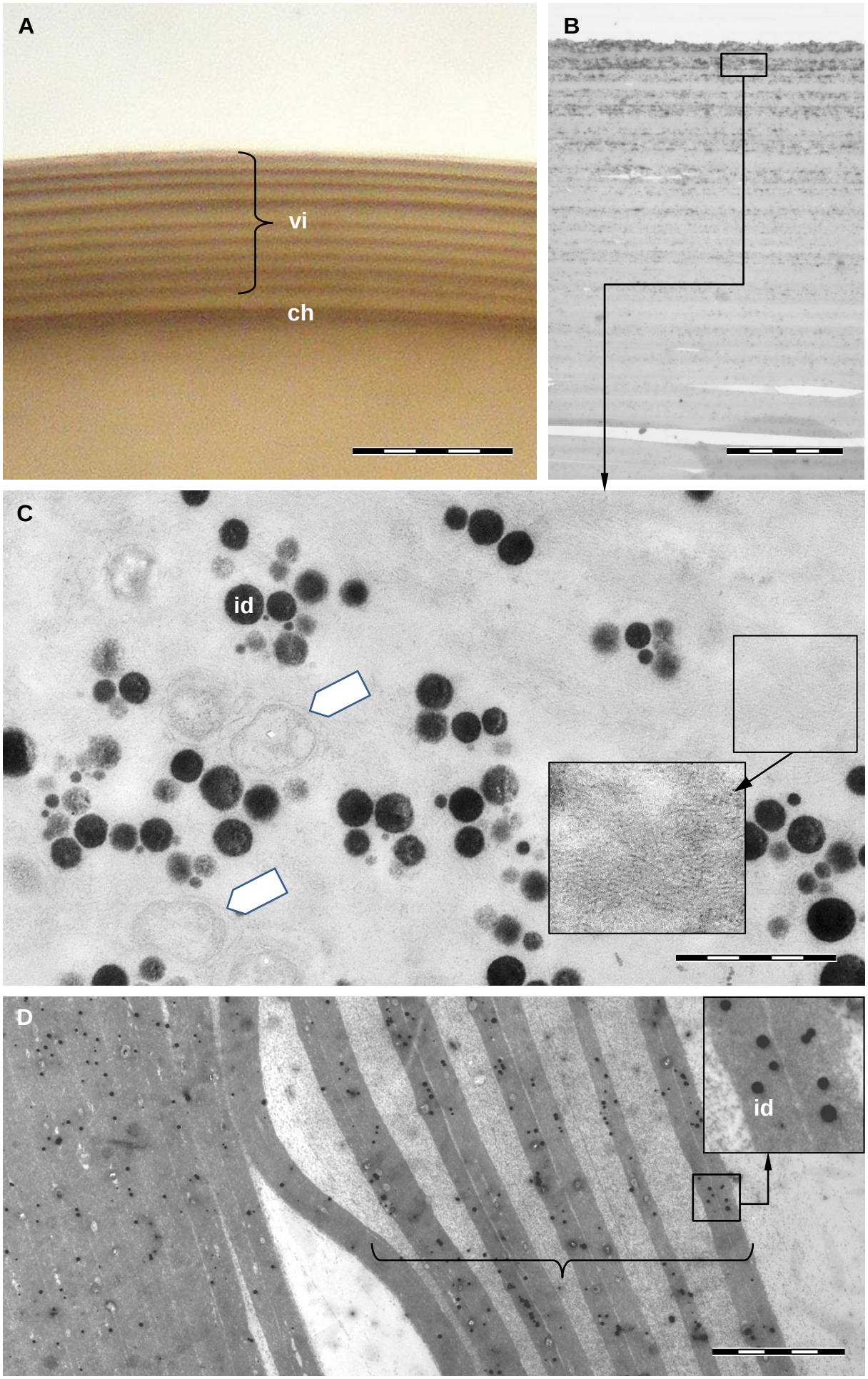

Fig. 1

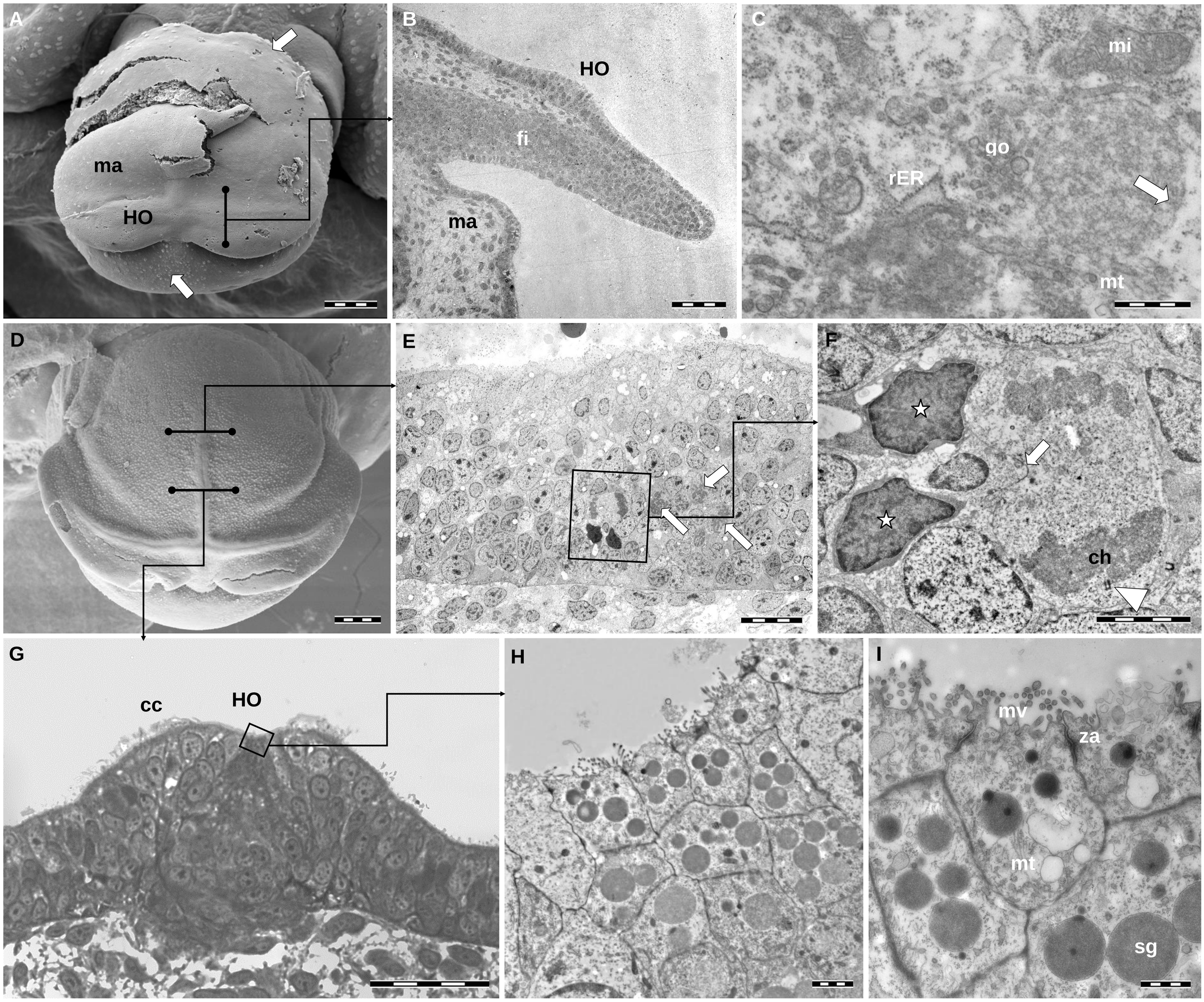

Fig. 2

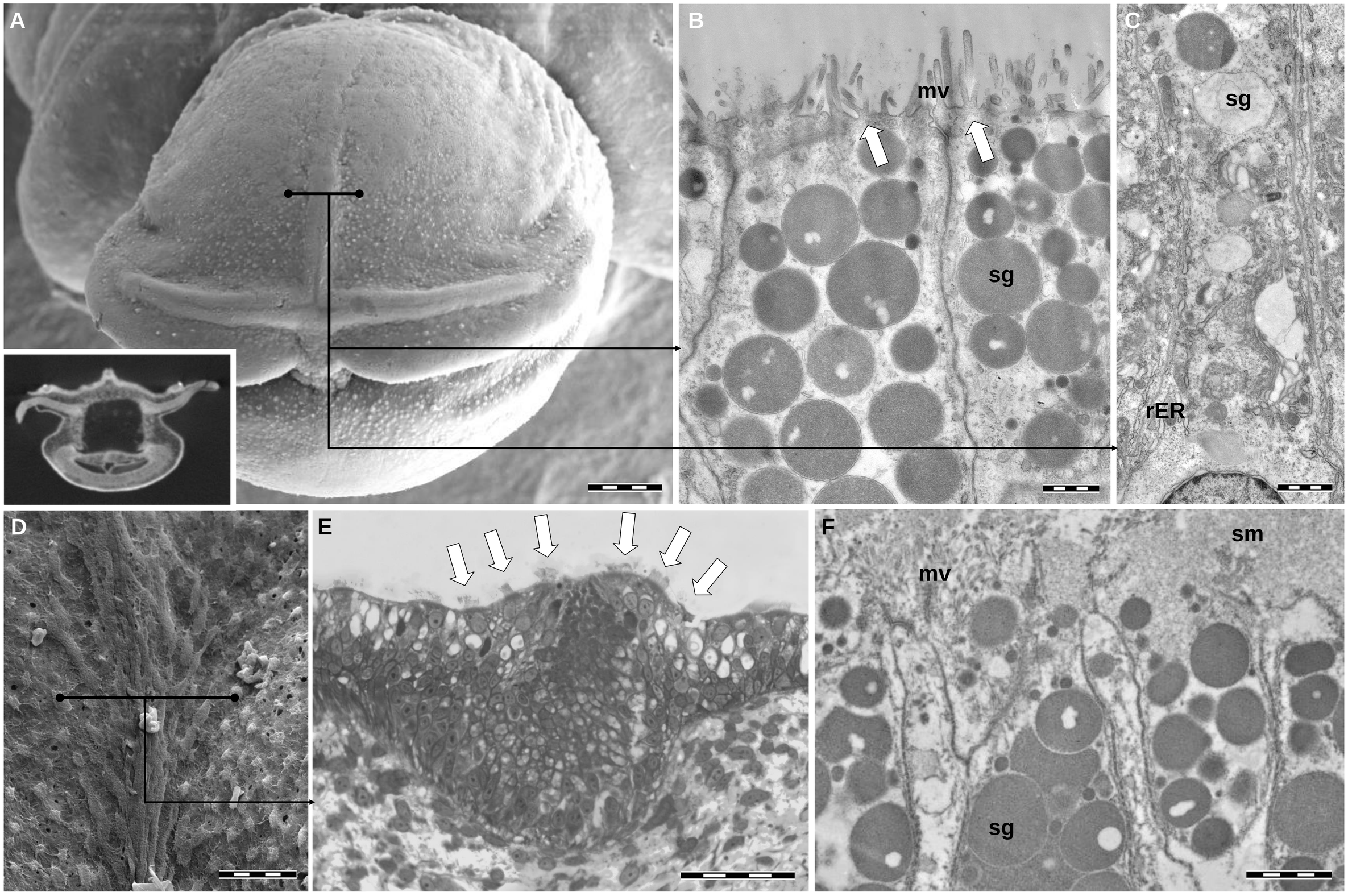

Fig. 3

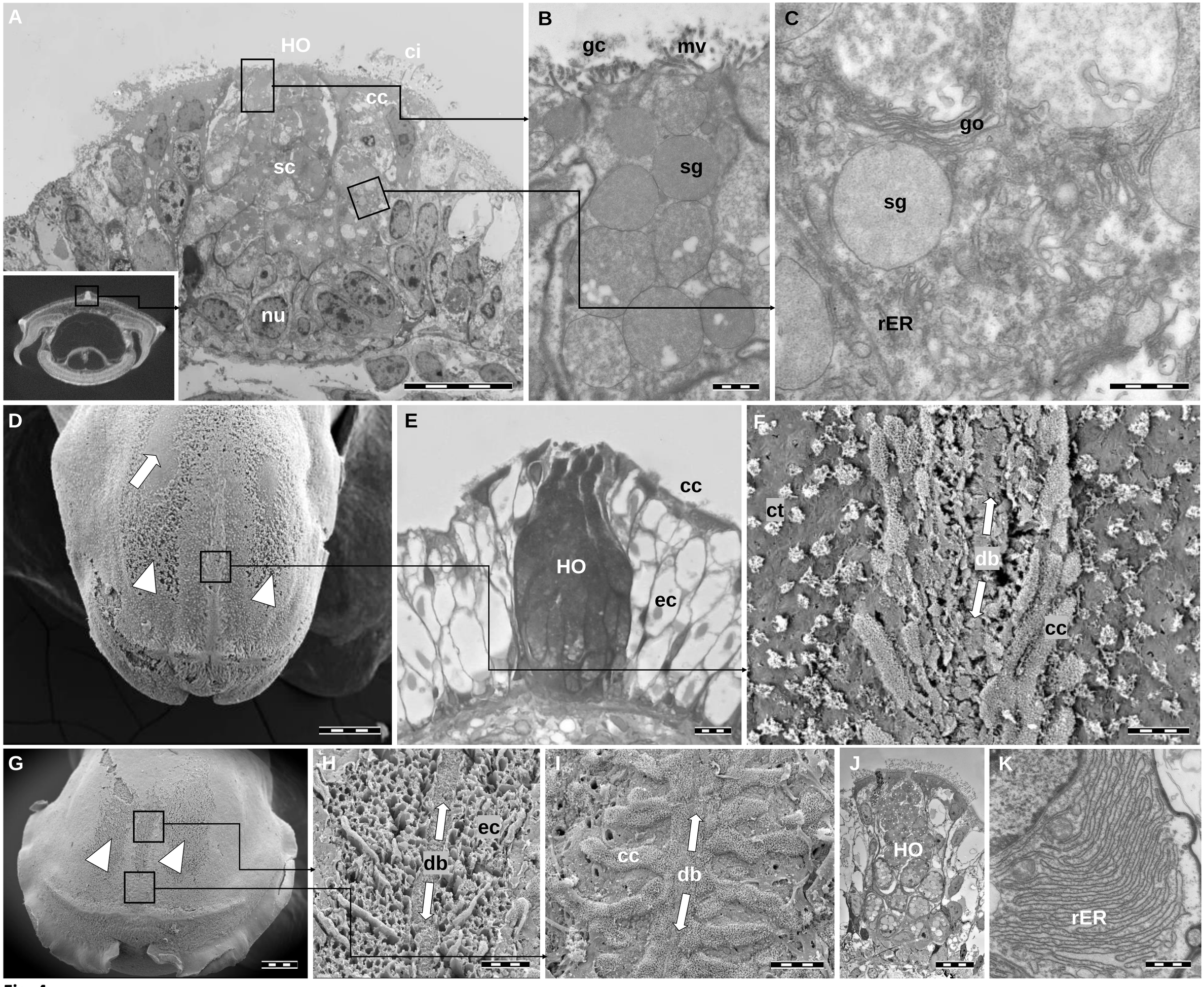
A
HO
ci
cc
sc
nu
B
gc
mv
sg
C
go
sg
rER
D
E
cc
HO
ec
F
ct
db
cc
G
H
ec
db
I
cc
db
J
HO
K
rER

Fig. 4

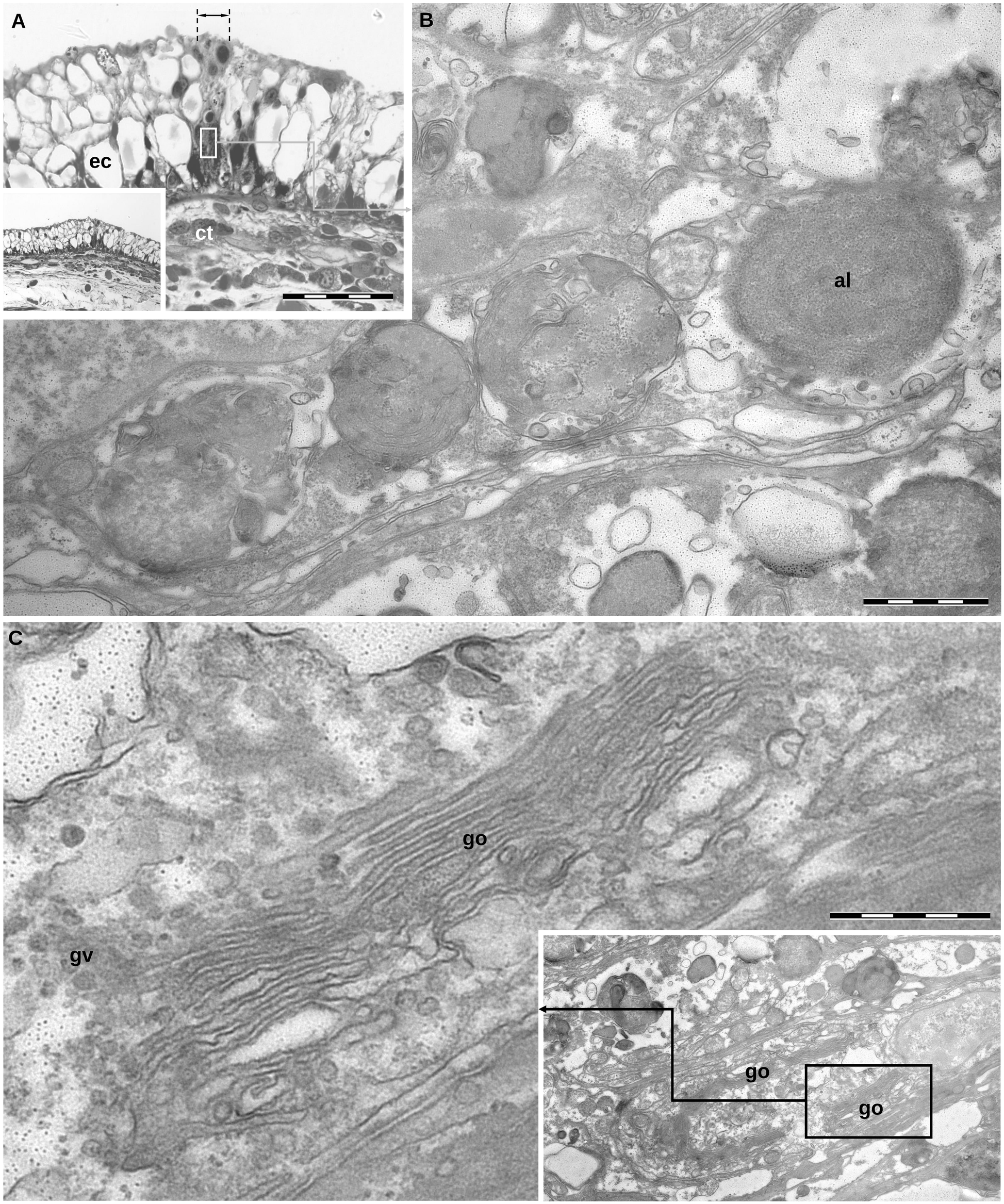

Fig. 5

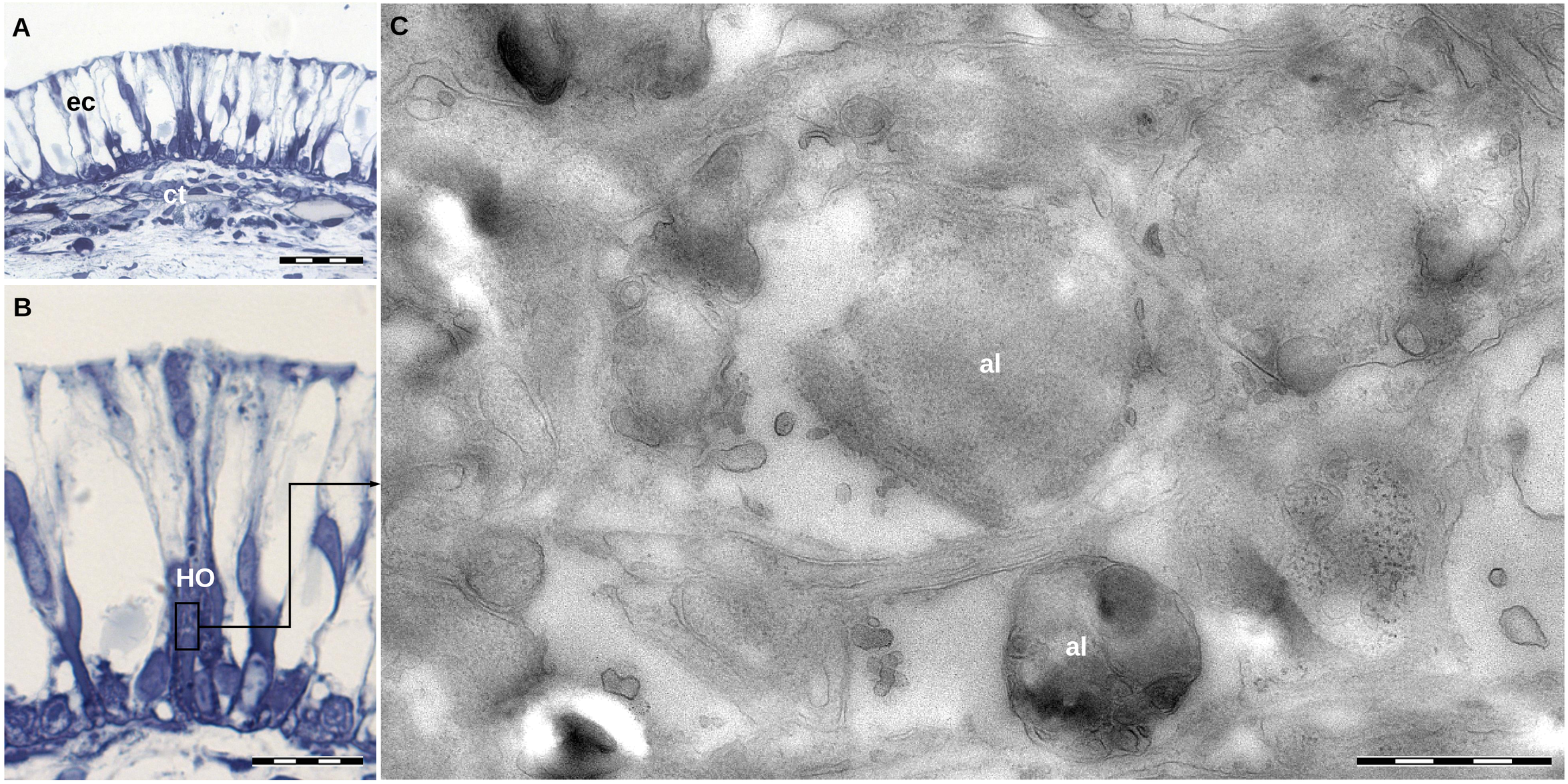

Fig. 6

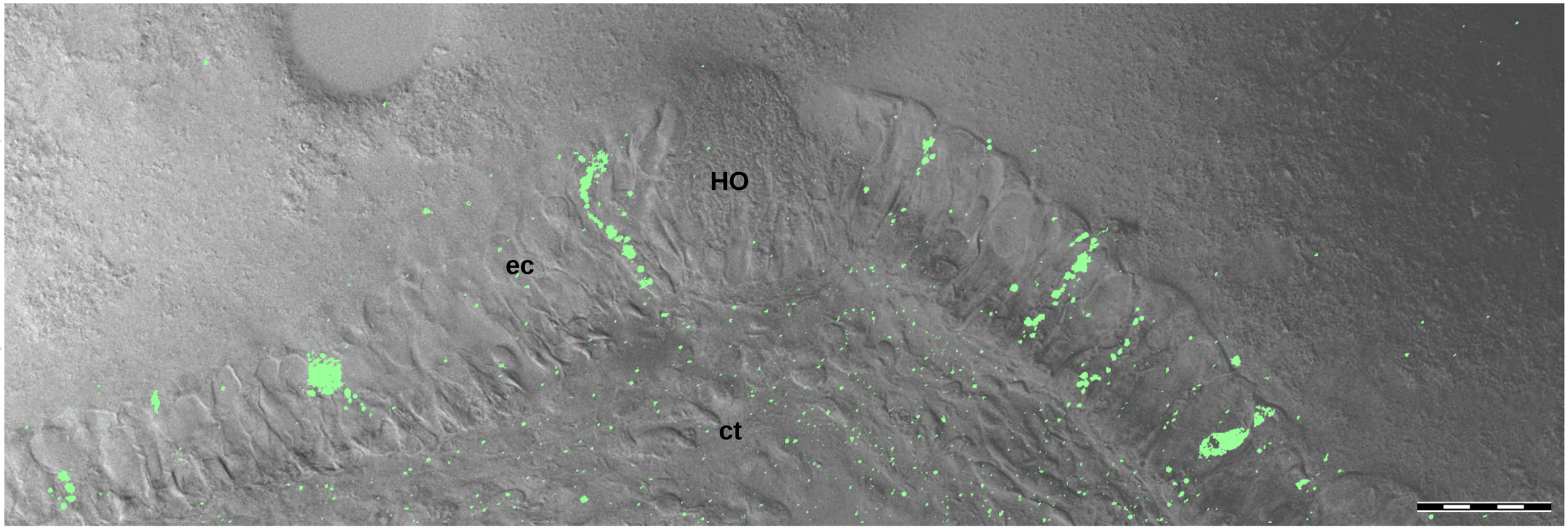

Fig. 7

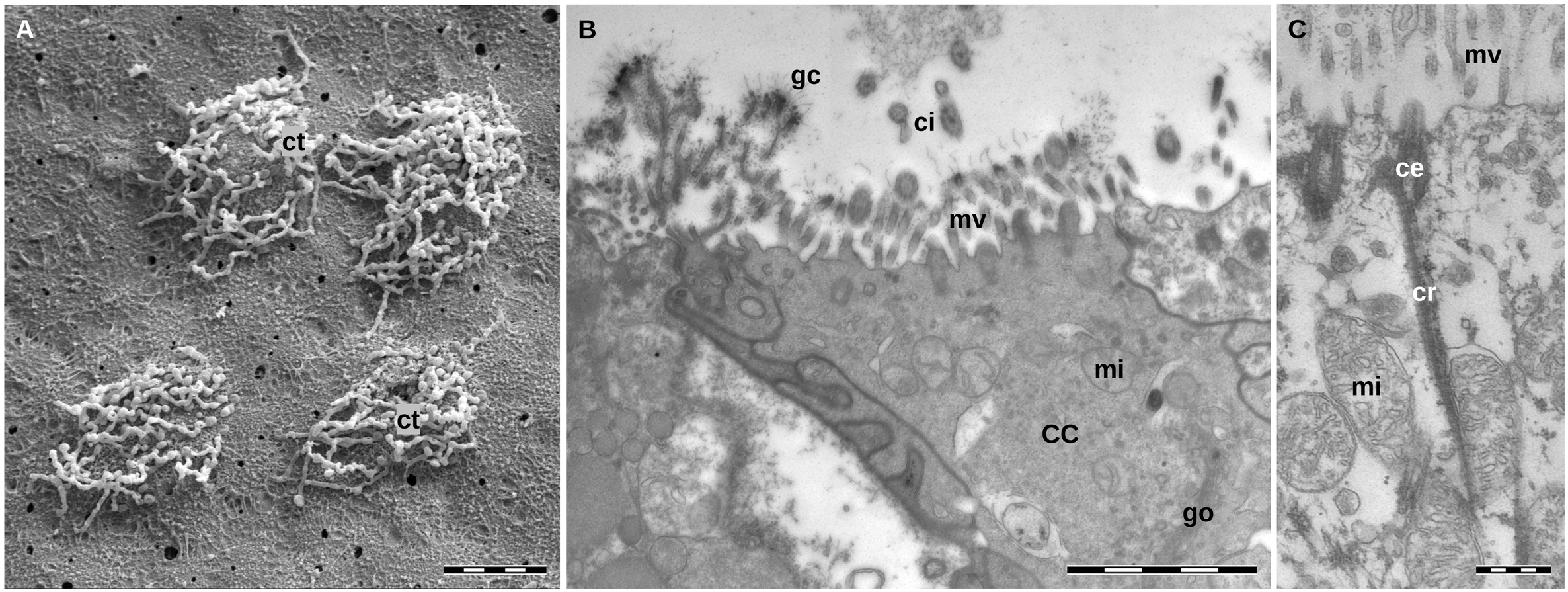

Fig. 8

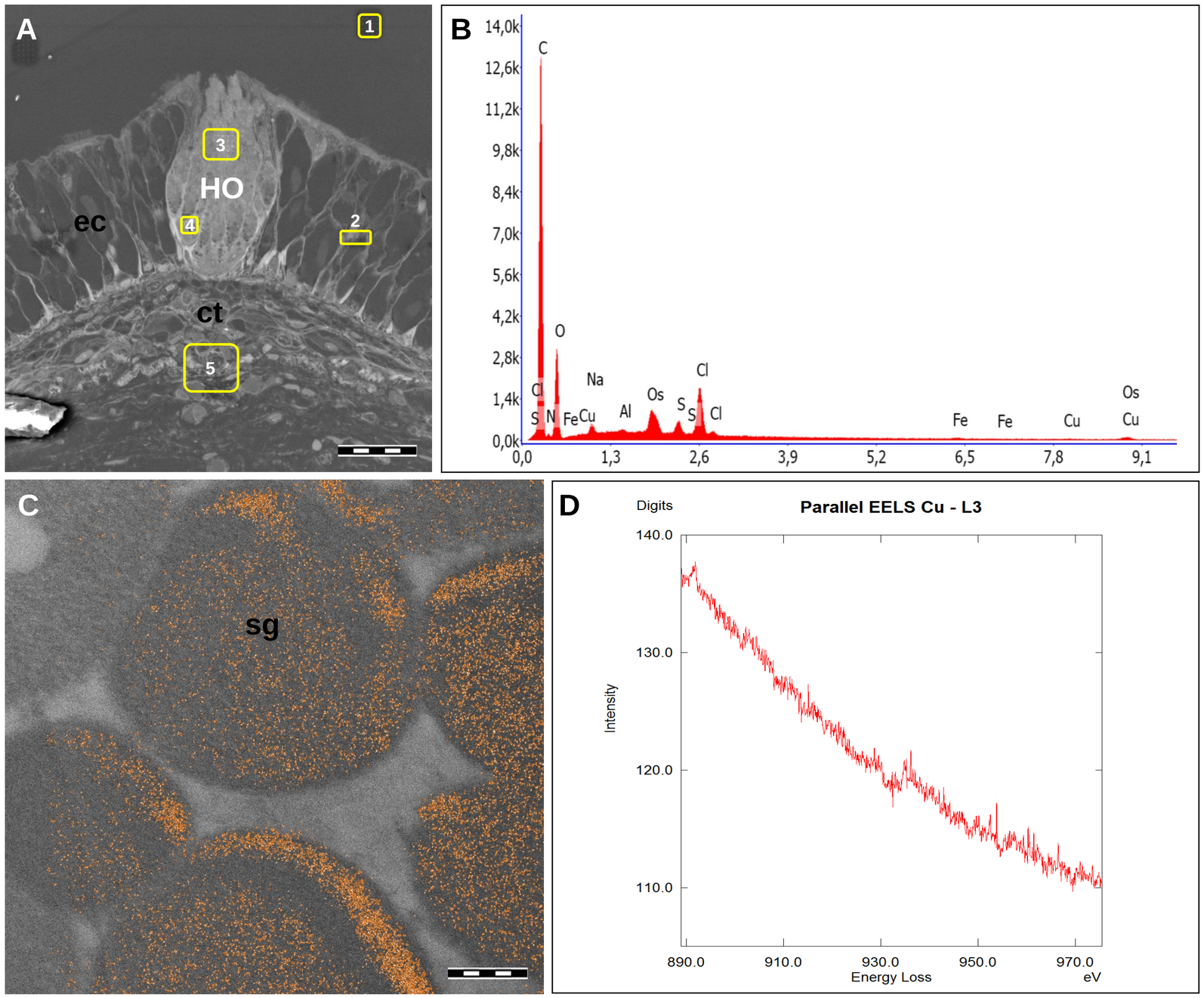
A
1
3
HO
ec
4
2
ct
5
B
14,0k
12,6k
11,2k
9,8k
8,4k
7,0k
5,6k
4,2k
2,8k
1,4k
0,0k
C
O
Na
Cl
Os
S
Cl
Cl
S
N
Fe
Cu
Al
S
Cl
Fe
Fe
Cu
Os
Cu
0,0
1,3
2,6
3,9
5,2
6,5
7,8
9,1
C
sg
D
Digits
Parallel EELS Cu - L3
140.0
130.0
120.0
110.0
Intensity
890.0
910.0
930.0
950.0
970.0
Energy Loss
eV

Fig. 9

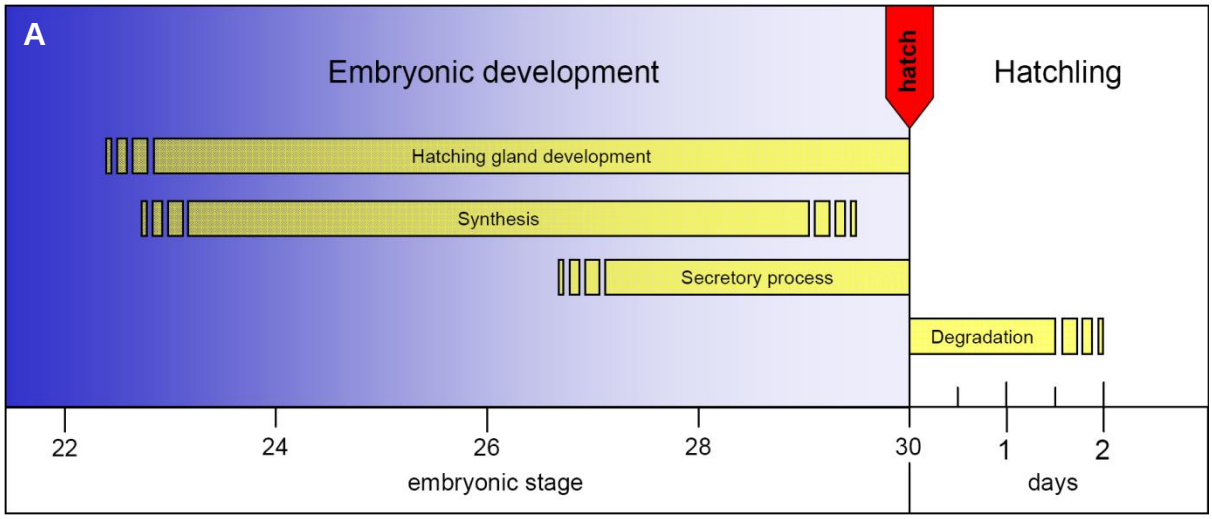
A
Embryonic development
hatch
Hatchling
Hatching gland development
Synthesis
Secretory process
Degradation
22
24
26
28
30
1
2
embryonic stage
days

Fig. 10

V. Discussion

Within this PhD project, financially supported by the Austrian Science Fund FWF (Project No. P 21135-B17), several aspects of the HO (Hoyle organ) of nine species belonging to three major recent cephalopod groups (Octopoda, Sepiida, Teuthida) have been elucidated. The studies include comparative morphology, organ differentiation and degradation, side effects of the choriolytic gland (e.g. lysis of epithelial cells) and likewise the concurrent differentiation of the ciliary patches associated with hatching and perivitelline flow.

Hoyle Organ – morphology

All six observed decapod species possess a clearly visible anchor-shaped HO, composed of numerous uniform secretory cells. In cross section, the number of secretory cells side by side vary between 6 (*I. pygmaeus*) and 20 (*S. lessoniana*) cells. The gland is elevated relative to the epithelial surface level. This increased height is caused by a thickening of the connective tissue underlying the HO. In *Sepia officinalis*, *Loligo gahi* and *Sepioteuthis lessoniana* moreover the secretory cells are twice as high as the epithelium, making the elevation more obvious. The benefit of an elevated HO seems to be a better exposure of the gland to the chorion membrane, which helps to apply the choriolytic enzymes.

Within the observed Octopoda, only *Tremoctopus gracilis* has scattered uniform secretory cells of the HO. The cells are not elevated, which is comprehensible in view of the closely-fitting chorion. *Octopus vulgaris* and *Argonauta hians* lack any HO-associated secretory cells. A choriolytic hatching support may be less important in Octopoda. Instead, Kölliker bundles (Brocco et al., 1974; Fioroni, 1962b; Stelzner et al., 1997), stiff spine-like hatching devices on mantle surface and head perforate the chorion membrane mechanically (Orelli, 1959; Boletzky, 1986). Moreover, the three studied octopod species *Tremoctopus gracilis*, *Octopus vulgaris* and *Argonauta hians*, belonging to the finless (incirrate) Octopoda,

lack an additional egg capsule, probably due to the active protection of the fertilized eggs by the female (Boletzky, 1986).

Hoyle Organ – secretory cells

The height of the secretory cells varies according to the species-typical epithelium from 10 µm in *Tremoctopus gracilis* up to 100 µm in *Sepioteuthis lessoniana* and the consistently spherical secretory granules have diameters between 1.5 and 3 µm. On the other hand, no relevant differences in terms of synthesis activity, such as rER/Golgi-ratio, could be observed. In most of the decapod species (*Loligo gahi*, *Architeuthis* sp., *Sepia officinalis* and *Sepioteuthis lessoniana*) granules of varying electron density could be observed in the choriolytic cells. This gradient were already described for *Loligo pealei* and *Sepiella japonica* (Matsuno & Ouji, 1988; Arnold & Singley, 1989), termed as bipartity (Arnold & Singley, 1989). It was supposed that they either represent two chemical phases that mix after release or represent a fixation artifact. As the bipartity occurs frequently in this study and constantly in some species while never in others, the artifact hypothesis is rather unlikely. Furthermore, the bipartite granules appear only in later stages of the HO to an increasing degree and predominantly near the cell tips, where the granules are smaller and more electron dense. Accordingly, this condensation process of the granules during their migration towards the cell surface seems more plausible as cause for the formation of the density gradient and even of hollow areas.

Hoyle Organ –associated cells

While the HO of the sepiid *Euprymna scolopes* is not clearly delimited from the mantle epithelium and even interspersed by small epithelial cells, the other observed decapod species have an explicit lateral limitation formed mostly by specific cells that isolate the secretory cells from the regular mantle epithelium: In *Idiosepius pygmaeus* a slender epithelial

cell type bordering the secretory cells. Compared to regular epithelial cells these cells have elongated microvilli (0.5 µm resp. 1 µm length), a denser cytoplasm and longitudinal filaments. A cell type with almost equal features has been described as possible supporting cell for secretion in the adhesive organ of the adult Idiosepiidae (Cyran et al., 2011). In *Sepia officinalis*, ciliated cells are aligned parallel to the secretory cells. Those cells resemble the cells forming the ciliary tufts, numerously scattered on the whole mantle during late embryonic development and responsible for the perivitelline flow in decapods (Boletzky, 1979; Arnold & Williams-Arnold, 1980), but their cilia are shorter (5 µm resp. 10 µm). In earlier HO stages (until embryonic stage 26), the ciliated cells are strictly parallel aligned beside the secretory cells but form increasingly lateral branches with an initially low but increasing angle up to 90 degrees before hatching. Similar alterations in the pattern of the HO-aligning ciliary cells have been observed in *Loligo pealei* (Arnold & Williams-Arnold, 1980). In the investigated teuthids *Loligo, Sepioteuthis* and *Architeuthis*, the lateral HO limitation is not characterized by a specific cell type but by a morphological distortion of the adjoining epithelium, consisting of regular microvilli covered cells and the obligatory ciliary tufts: The growing secretory cells push the epithelial cells distally and aside instead of replacing them (as e.g. in *Sepia officinalis*). This leads to an epithelial fold that partly (in *Loligo gahi*) or completely (in *Sepioteuthis* and *Architeuthis*) covers the tips of the secretory cells.

The HO – aligning ciliary cells were observed to generate a flow towards the mantle edge in *Loligo pealei* (Arnold & Williams-Arnold, 1980) that may also help maintaining a slight pressure of the HO against the chorion and a pinpoint secretion. In cross section the ciliary cells appear brush-like. It is therefore conceivable that those ciliary cells in *Sepia officinalis* and *Loligo paelei*, respective the microvilli-covered cells in *Idiosepius pygmaeus* improve the dispersion of the choriolytic secretion when sliding with their posterior mantle pole along the chorion.

An additional cell type similar to the alpha cells, supposedly with adhesive function, that are located in low numbers on the crossing point of the HO of *Loligo pealei* (Arnold & Singley, 1989) were not found in the observed species. The closely related *Loligo gahi* did not show such an attachment behavior in our study. Rather the embryos applied the enzymes to several sites by continuously changing their position during the last day before hatching. The embryos were never observed to remain in the same position but steadily slide with their posterior mantle tip along the chorion.

HO – dimensions

Compared to the Octopoda, the prominent, distinctly-anchor shaped HO in the Decapoda, contains scores of choriolytic cells. This high number of cells complies with the expected high requirements of choriolytic enzymes arising from the large perivitelline space and the thick egg capsule in Sepiida respective the joint egg jelly in Teuthida (Boletzky, 1998). It has been indicated that the gland dimensions diverge depending on the amount of required enzymes. For comparison within the Decapoda, the 'gland dimension' is estimated by the number of choriolytic cells laterally side by side as well as by size and filling level of the cells.

Within the Sepiida, the HO of *Idiosepius* embryos has the smallest dimension in relation to the body size. That seems plausible in view of a smaller perivitelline space (1.2 x body length) than e.g. in *Sepia* (1.5 x body length) and the observed almost strictly localized application of enzymes. The egg integument is moreover strongly reduced in its thickness until hatching and the embryos are able to use their arms to push against the opposite egg pole during hatching. The larger HO dimension in *Sepia* correlates with the larger perivitelline space that may dilute and weaken the enzyme effect. The early appearance of the HO already at embryonic stage 23 (25 for the other observed species) and the early beginning of secretion at stage 27 (29 for the other observed species) indicate the necessity of a high enzyme

amount. In *Euprymna*, the interpretation is less obvious. Although the perivitelline space is only slightly bigger than the embryo, the dimension of the HO is comparatively large. It should be noted that the HO of *Euprymna* differs from the other cephalopods by showing no clear lateral limitation. Moreover the animals use their terminal spine to facilitate hatching.

For Teuthida with their large perivitelline space (1.5 – 2 x body length) and the spacious egg cluster jelly (Boletzky, 1998), a comparatively high amount of enzymes is expected. This is true for *Loligo gahi* and *Sepioteuthis lessoniana*. Besides, it could be observed that the *Loligo gahi* embryos actively disperse the enzymes with its wiping tail along the egg integument while changing their position about once per hour. This unsteady behavior may be important to finally ensure hatching on a position that is not blocked by a neighboring egg but it may also increase the enzyme requirement. While Sepiida with their single eggs can hatch at any position and therefore rather keep one position to puncture the chorion as observed for *Idiosepius*, for the Teuthida this additional investment of scattering the enzymes on different areas seems to be essential to survive. In relation to the other Teuthida, the HO of *Architeuthis* sp. is inconspicuous. It has a lower number of secretory cells with only small aggregations of secretory vesicles, and the gland is only slightly elevated. As this sample has been stored in formalin for 20 years, an extraction of cell contents cannot be excluded and fresh samples of this enigmatic species are currently not available.

HO - degradation

The degradative alterations of the HO are obvious immediately after hatching in *Idiosepius pygmaeus*, *Euprymna scolopes*, *Sepia officinalis* and *Loligo gahi*. In these four species the gland is already distinctly reduced by releasing the majority of the cell content, but it was never observed to be empty. This indicates surplus enzyme production to ensure hatching also under difficult conditions (Boletzky, 2012).

In *I. pygmaeus* and *E. scolopes* the first evidence for degradation is swelling and breakdown of endoplasmic reticulum in pieces, agglutination of organelle remnants with secretory vesicles and empty spaces in the cytoplasm. Concurrently the cells continue shrinking. In *I. pygmaeus*, clumped cytoplasmic compartments (without membrane encapsulation) have been observed to be ingested by neighbouring epithelial cells and within one day the gland completely disappeared. In *E. scolopes* the degradation is prolonged, as the 'clumping-stage' could be noted only two days post-hatching. Later degradative stages could not be traced by lack of appropriate samples. Due to fixation problems in the hatchlings of *L. gahi*, the interpretation of the cell degradation is difficult. Indications of membranous break down, clumping and empty spaces in the cytoplasm suggest similar characteristics as described for *I. pygmaeus* and *E. scolopes*. The observed alterations of the HO in these three species can be assigned to a necrotic cell death or necroptosis, a triggered form of cell death with an intact nucleus and a necrotic appearance of the cytoplasm (Guimaraes & Linden, 2004; Leist & Jaattela, 2001).

In *Sepia officinalis*, the observed degradative changes differ considerably from the three other investigated species: Several hours after hatching, the lower third of the so far mainly laterally shrunk secretory cells is characterized by autophagic vacuoles. The vacuoles have a single membrane, a characteristic of autolysosomes or degradative autophagic vacuoles (Liou et al., 1997; Dunn, 1990a, 1990b). The nucleus appears active and large Golgi cisterns arise, as expected for autophagic cell death (Clarke, 1990; Klepal et al., 2008; Berry & Baehrecke, 2007). In almost two days old hatchlings, the content of the autophagic vacuoles is degraded beyond recognition and the Golgi bodies have disappeared. The nucleus shows distinct indications of disintegration by some floccular precipitations.

Earlier studies on the degrading HO in *Sepiella japonica* (Matsuno & Ouji, 1988) revealed indications of clumping and large cytoplasm free areas in the basal region of the cells similar to the current observations in *I. pygmaeus* and *E. scolopes*. In *Loligo pealei*

(Arnold & Singley, 1989), the degradation of the HO is described as ‘empty membranous vesicles interspersed with amorphous floccular material’ near the apical surface, while basally in the cells numerous small membraneous pieces, presumably broken ER-cisterns, are obvious. The changes basally in the cells and the floccular material are reminiscent of the necrotic features in *I. pygmaeus* and *E. scolopes*, whereas the vacuolized cytoplasm recalls the vacuolized appearance described for autophagy. It cannot be excluded that those vacuoles are empty secretory vesicles and not autophagic vacuoles.

Both the necroptosis and the autophagic cell death are typical strategies for depletion of cell clusters or whole organs (Bursch, 2001; Kitanaka & Kuchino, 1999; Trump et al., 1997), while apoptotic cell death has been observerd in connection with degradation of solitary cells (Kerr et al., 1972; Wyllie et al., 1980). Accordingly, beside the HO in cephalopods, likewise the hatching glands in amphibians, composed of several scattered cell clusters, show indications of autophagic cell death like lysosomes with incorporated cytoplasmic components (membrane stacks, mitochondria and other organelle residues) and an intact nucleus (Yoshizaki & Katagiri, 1975; Yoshizaki, 1973). On the other hand, the solitary hatching gland cells in teleosts show typical apoptotic nuclear alterations such as chromatin condensation, multivesicular bodies and spherical cytoplasm-remnants ingested by adjacent epithelial cells (Rojo et al., 1997; Schoots et al., 1983; Yamamoto et al., 1979).

Programmed cell death is a highly complex process involving scores of genes and triggering molecules and has numerous interdependencies (Chautan et al., 1999; Oppenheim et al., 2001). Neither follow even clear classified cell death processes comparable genetic pathways in all cases, nor do the observed alterations always correspond to one type of cell death only. Moreover, under changing environmental or physiological conditions cell death pathways can diverge from typical characteristics, leading to intermediate and overlapping types (Bursch, 2001; Klepal et al., 2008). There are currently no clear indications, why the

HO of cephalopod follow different cell death strategies and whether the observed characteristics are species specific or an environmental and physiological adaption.

In *Sepia officinalis* an increasing damage of the epithelial cells around the HO could be observed from stage 29 onwards. So far, we assume a physical abrasion effect by rubbing with the mantle along the chorion before hatching in connection with the almost empty epithelial cells. Latter is a common phenomenon in cephalopod paralarvae (Fioroni, 1963; Orelli, 1959; Boletzky, 1982). At least loss of individual or groups of epithelial cells after hatching has already been observed in *Loligo pealei* (Arnold & Williams-Arnold, 1980). A purely fixation induced artifact is unlikely, as the effect is observable exclusively from stage 29 onwards. A fixation enhanced effect in connection with the increasingly structurally weakened epithelial cells can however not be excluded.

***Idiosepius pygmaeus* Hoyle organ / Adhesive organ**

The cellular alterations within the mantle epithelium in *I. pygmaeus* have been traced from embryonic stage 25 until 12 days old paralarvae. The aim was to elucidate whether the earlier described embryonic gland (von Byern et al., 2006) belongs to the HO or represents an early stage of the adhesive organ (AO). It could be confirmed, that the cells of the embryonic gland increase in size and amount of content until embryonic stage 29 and subsequently are reduced and disappear completely about one day after hatching. Therefore the previously observed gland can clearly be referred to as HO. With the exception of the microvilli-bordered secretory cells, unique for *I. pygmaeus*, the gland correlates with the typical features of the HO in other Sepiids, such as the anchor-shape, the cell arrangement and in particular the pre-hatching secretion process.

Both, columnar and granular cells, explicitly defining the AO, were found only later in the paralarvae: First appearance of columnar cells has been proved for seven days old hatchlings in the same area as the HO. The cells develop in small groups directly adjacent to

each other. Ten days after hatching, the columnar cells are already separated from each other by epithelial cells, as they are usually found in adults (Cyran et al., 2011). Also, first granular cells appear at this stage. However, the first attachment behavior was described for a 12 days old juvenile under artificial conditions at 32°C (von Byern et al., 2006). Ultimately, a direct transition from HO to AO can be excluded.

***Sepia officinalis* – Nitric oxide, metalloproteases**

HO-development and several other developmental processes are triggered by activation or inhibition of nitric oxide (NO). As the HO grows, levels of both the NO and the NO-synthase (NOS) increase in correlation until shortly before hatching (Mattiello et al., 2012). The lack of NOS in the HO of hatchlings (this study) may likewise correlate with a lack of NO (not measured) but does not prove its complete absence. Nevertheless, assuming a concurrent decline of NO, a possible explanation may be the role of NO in inhibiting cell death signals (CDS) in molluscs (Leise et al., 2004). In this case, the lapse of NO would terminate the CDS-inhibition and allow elimination of the cells.

The metals Cu and Fe could be meassured within the HO and the connective tissue of *S. officinalis* at embryonic stage 29, while the epithelial cells are free of these metals. In teleost hatching enymes, Mg and Zn are described to improve the choryolytic effectiveness (Yasumasu et al., 1989b) which may also be achieved by Cu and Fe in *Sepia officinalis*. Uptake of trace metals may also be of ecological relevance in future in view of ocean acidification, leading to changes in solubility of Cu and Fe (Gledhill et al., 2015) and bioaccumulation of metals in *Sepia officinalis* (Lacoue-Labarthe et al., 2011).

Conclusion

It could be shown that gland dimensions, secretory amount and pre-hatching behavior predominantly correlate with the size of the perivitelline space and the thickness of the egg

shell. Participation of metal ions in strengthening the enzyme effectiveness appears to be a common concept for choriolytic glands and should subsequently be examined also for other cephalopod species. The results relating to cell death strategies during HO-degradation give a first insight into the variability of these processes in cephalopods. This study will provide a fundament for upcoming molecular biological and immune-histochemical investigations on participating genes and mediator molecules.

References

Arbeitman, M. N., E. E. M. Furlong, F. Imam, E. Johnson, B. H. Null, B. S. Baker, M. A. Krasnow, M. P. Scott, R. W. Davis & K. P. White, 2002. Gene expression during the life cycle of *Drosophila melanogaster*, Science 297: 2270-2275.

Arkhipkin, A., V. V. Laptikhovsky & D. Middleton, 2000. Adaptations for cold water spawning in loliginid squid: *Loligo gahi* in Falkland waters, Journal of Molluscan Studies 66: 551-564.

Arndt, E.& K. Hurka, 1992. Beschreibung der Larven der mitteleuropäischen Pterostichus-Arten (Col., Carabidae, Pterostichini), Entomologische Nachrichten und Berichte 36: 103-110.

Arnold, J. M.& C. T. Singley, 1989. Ultrastructural changes in the cells of the Hoyle organ during hatching of the squid *Loligo pealei*. 1-14.

Arnold, J. M.& L. D. Williams-Arnold, 1980. Development of the ciliature pattern on the embryo of the squid *Loligo pealei*: A scanning electron microscope study. 102-116.

Berry, D. L.& E. H. Baehrecke, 2007. Growth arrest and autophagy are required for salivary gland cell degradation in *Drosophila*, Cell 131: 1137-1148.

Boletzky, S., 1982. Developmental aspects of the Mantle Complex in Coleoid Cephalopods, Malacologia 23: 165-175.

Boletzky, S. v., 1979. Ciliary locomotion in squid hatching. 1051-1053.

Boletzky, S. v., 1986. Encapsulation of cephalopod embryos: A search for functional correlations. 217-227.

Boletzky, S. v., 1991. The terminal spine of sepiolid hatchlings: its development and functional morphology (Mollusca: Cephalopoda). 107-112.

Boletzky, S. v., 1998. Cephalopod eggs and egg masses, Oceanography and Marine Biology: An Annual Review 36: 341-370.

Boletzky, S. v., 2003. Biology of Early Life Stages in Cephalopod Molluscs. 143-203.

Boletzky, S. v., 2012. Hatch-as hatch-can: tricks of the trade in coleoid hatchlings (Mollusca: Cephalopoda). 67-76.

Brocco, S. L., R. M. O´Clair & R. A. Cloney, 1974. Cephalopod Integument: The Ultrastructure of Kölliker´s organs and their relationship to Setae. 293-308.

Bursch, W., 2001. The autophagosomal-lysosomal compartment in programmed cell death, Cell Death and Differentiation 8: 569-581.

Chang, Y.& P. Y. Chen, 2016. Hierarchical structure and mechanical properties of snake (*Naja atra*) and turtle (*Ocadia sinensis*) eggshells, Acta Biomaterialia 31: 33-49.

Chautan, M., G. Chazal, F. Cecconi, P. Gruss & P. Golstein, 1999. Interdigital cell death can occur through a necrotic and caspase-independent pathway, Current Biology 9: 967-970.

Clarke, P. G. H., 1990. Developmental Cell-Death - Morphological Diversity and Multiple Mechanisms, Anatomy and Embryology 181: 195-213.

Cyran, N., W. Klepal, Y. Staedler, J. Schoenenberger & J. von Byern, 2015. Alterations in the mantle epithelium during transition from hatching gland to adhesive organ of *Idiosepius pygmaeus* (Mollusca, Cephalopoda). 43-57.

Cyran, N., W. Klepal & J. von Byern, 2011. Ultrastructural characterization of the adhesive organ of *Idiosepius biserialis* and *Idiosepius pygmaeus* (Mollusca, Cephalopoda). 1499-1510.

Cyran, N., Y. Staedler, J. Schoenenberger, W. Klepal & J. von Byern, 2013. Hatching glands in cephalopods - A comparative study, Zoologischer Anzeiger 253: 66-82.

Dunn, W. A., 1990a. Studies on the Mechanisms of Autophagy - Formation of the Autophagic Vacuole, Journal of Cell Biology 110: 1923-1933.

Dunn, W. A., 1990b. Studies on the Mechanisms of Autophagy - Maturation of the Autophagic Vacuole, Journal of Cell Biology 110: 1935-1945.

Fan, T. J.& C. Katagiri, 2001. Properties of the hatching enzyme from *Xenopus laevis*, European Journal of Biochemistry 268: 4892-4898.

Fioroni, P., 1962a. Die embryonale Entwicklung der Hautdrüsen und des Trichterorganes von *Octopus vulgaris* Lam., Acta Anatomica 50: 264-295.

Fioroni, P., 1962b. Die embryonale Entwicklung der Kölliker´schen Organe von *Octopus vulgaris* Lam., Revue Suisse de Zoologie 69: 497-511.

Fioroni, P., 1963. Zur embryonalen und postembryonalen Entwicklung der Epidermis bei zehnarmigen Tintenfischen. 149-160.

Garcia, R. A., 2007. An "egg-tooth"-like structure in titanosaurian sauropod embryos, Journal of Vestibular Research 27: 247-252.

Gledhill, M., E. P. Achterberg, K. Li, K. N. Mohamed & M. J. Rijkenberg, 2015. Influence of ocean acidification on the complexation of iron and copper by organic ligands in estuarine waterscopper by organic ligands in estuarine waters, Marine Chemistry 177: 421-433.

Guimaraes, C. A.& R. Linden, 2004. Programmed cell deaths - Apoptosis and alternative deathstyles, European Journal of Biochemistry 271: 1638-1650.

Hibbard, H., 1937. The hatching of the squid. 385.

Hoshi, M.& T. Numakunai, 1981. Hatching enzyme of the solitary ascidian, *Halocynthia roretzi*, Acta embryologiae et morphologiae experimentalis 2: 163-169.

Hoyle, W. E., 1889. VI. On a tract of modifies epithelium in the embryo of *Sepia*. 58-60.

Ishida, J., 1936. An enzyme dissolving the fertilization membrane of sea-urchin eggs, Annotationes Zoologicae Japonenses 15: 453-459.

Jecklin, L., 1934. Beitrag zur Kenntnis der Laichgallerten und der Biologie der Embryonen decapoder Cephalopoden. Mathematisch-Naturwissenschaftlichen Abteilung der Philosophischen Fakultät der Universität Basel, 595-673.

Kafatos, F. C.& C. M. Williams, 1964. Enzymatic mechanism for the escape of certain moths from their cocoons, Science 146: 538-540.

Kerr, J. F., A. H. Wyllie & A. R. Currie, 1972. Apoptosis: a basic biological phenomenon with wide-ranging implications in tissue kinetics, British Journal of Cancer 26: 239-257.

Kitamura, Y.& C. Katagiri, 1998. Characterization of the hatching enzyme from embryos of an anuran amphibian, *Rana pirica*. 153-164.

Kitanaka, C.& Y. Kuchino, 1999. Caspase-independent programmed cell death with necrotic morphology, Cell Death and Differentiation 6: 508-515.

Klepal, W., D. Gruber & B. Pflugpfelder, 2008. Natural cyclic degeneration by a sequence of programmed cell death modes in *Semibalanus balanoides* (Linnaeus, 1767) (Crustacea, Cirripedia, Thoracica), Zoomorphology 127: 49-58.

Lacoue-Labarthe, T., E. Réveillac, F. Oberhänsli, J. L. Teyssié, R. Jeffree & J. P. Gattuso, 2011. Effects of ocean acidification on trace element accumulation in the early-life stages of squid *Loligo vulgaris*, Aquatic Toxicology 105: 207-217.

Leise, E. M., S. C. Kempf, N. R. Durham & D. J. Gifondorwa, 2004. Induction of metamorphosis in the marine gastropod *Ilyanassa obsoleta*: 5HT, NO and programmed cell death, Acta Biologica Hungarica 55: 293-300.

Leist, M.& M. Jaattela, 2001. Four deaths and a funeral: From caspases to alternative mechanisms. 589-598.

Liou, W., H. J. Geuze, M. J. H. Geelen & J. W. Slot, 1997. The autophagic and endocytic pathways converge at the nascent autophagic vacuoles, Journal of Cell Biology 136: 61-70.

Matsuno, A.& M. Ouji, 1988. Ultrastructural studies on development of the tail gland of a cuttlefish, *Sepiella japonica*. 673-680.

Mattiello, T., M. Costantini, B. Di Matteo, S. Livigni, A. Andouche, L. Bonnaud & A. Palumbo, 2012. The dynamic nitric oxide pattern in developing cuttlefish *Sepia officinalis*, Developmental Dynamics 241: 390-402.

Mcphee, C. K., M. A. Logan, M. R. Freeman & E. H. Baehrecke, 2010. Activation of autophagy during cell death requires the engulfment receptor Draper, Nature 465: 1093-1096.

Nabhitabhata, J., 1994. Rearing of Thai pygmy cuttlefish, *Idiosepius thailandicus* Chot., Okut. & Chait.,I.: some biological aspects. 19 pp. (in Thai).

Naef, A., 1928. Die Cephalopoden. Friedländer & Sohn, Berlin: 1-357.

Nuttall, G. H. F., 1917. The biology of *Pediculus humanus*, Parasitology 10: 80-185.

Oppenheim, R. W., R. A. Flavell, S. Vinsant, D. Prevette, C. Y. Kuan & P. Rakic, 2001. Programmed cell death of developing mammalian neurons after genetic deletion of caspases, Journal of Neuroscience 21: 4752-4760.

Orelli, M. v., 1959. Über das Schlüpfen von *Octopus vulgaris*, *Sepia officinalis* und *Loligo vulgaris*. 330-343.

Paulij, W. P., H. C. C. M. Verhoof & J. M. Denuce, 1992. Partial purification and characterization of Loligo vulgaris hatching enzyme obtained from hatching medium, Comparative Biochemistry and Physiology Series B 101: 617-622.

Perona, R. M.& P. M. Wassarman, 1986. Mouse blastocysts hatch *in vitro* by using a trypsin-like proteinase associated with cells of mural trophectoderm, Developmental Biology 114: 42-52.

Rojo, M. C., M. J. Blanquez & M. E. Gonzalez, 1997. Ultrastructural evidence for apoptosis of pavement cells, chloride cells, and hatching gland cells in the developing branchial area of the trout Salmo trutta. 637-651.

Sasaki, M., 1921. On an adhering habit of a pygmy cuttlefish, *Idiosepius pygmaeus* Steenstrup. 209-213.

Sawada, H., K. Yamazaki & M. Hoshi, 1990. Trypsin-like hatching protease from mouse embryos: Evidence for the presence in culture medium and its enzymatic properties, Journal of Experimental Biology 254: 83-87.

Schoots, A. F. M., P. A. C. M. Evertse & J. M. Denuce, 1983. Ultrastructural changes in hatching-gland cells of pike embryos (*Esox lucius* L.) and evidence for their degeneration by apoptosis. 573-589.

Sikes, E. K., 1930. Larvae of Ceratophyllus wickhami and other Species of Fleas, Parasitology 22: 242-259.

Sikes, E. K.& V. B. Wigglesworth, 1931. The Hatching of Insects from the Egg, and the Appearance of Air in the Tracheal System, Journal of Cell Science 74: 165-192.

Stelzner, S., G. Sundermann & P. Fioroni, 1997. Structure and function of the duct of Kölliker in paralarvae of *Loligo vulgaris* Lam. (Cephalopoda), Vie Milieu 47: 161-164.

Suwanmala, J., J. von Byern & J. Nabhitabhata, 2006. Observation of *Idiosepius pygmaeus* (Cephalopoda, Idiosepiidae) at Klong Bangrong, Phuket Island, Thailand. 49-51.

Trump, B. F., I. K. Berezesky, S. H. Chang & P. C. Phelps, 1997. The pathways of cell death: Oncosis, apoptosis, and necrosis, Toxicologic Pathology 25: 82-88.

von Byern, J., A. Kerbl, M. T. Nödl, G. Bello, Y. Staedler, J. Schoenenberger & N. Cyran, 2016. Spine Formation as a Hatching Tool in *Euprymna scolopes* (Mollusca, Cephalopoda, Sepiolidae), Malacologia 59: 231-238.

von Byern, J.& W. Klepal, 2007. Occurrence of *Idiosepius pygmaeus* (Cephalopoda, Idiosepiidae) in Indonesian waters, Annalen des Naturhistorischen Museums in Wien 108 B: 137-144.

von Byern, J., L. Rudoll, N. Cyran & W. Klepal, 2008. Histochemical characterization of the adhesive organ of three *Idiosepius* spp. species, Biotechnic & Histochemistry 83: 29-46.

von Byern, J., S. Shigeno, W. Klepal & T. Kasugai, 2006. Postembryonic development of the adhesive organ in *Idiosepius* under artificial conditions. In Moltschaniwskyj, N. A., G. T. Pecl, J. Semmens & G. D. Jackson (eds), Hobart, Tasmania: 54.

von Querner, F. R., 1927. Die Köllikerschen Büschel jugendlicher Octopoden, nebst einigen Bemerkungen zur Histologie der Haut dieser Formen, Zeitschrift für Zellforschung und mikroskopische Anatomie 4: 237-265.

Weismann, A., 1863. Die Entwickelung von *Musca vomitoria* im Ei, Zeitschrift für wissenschaftliche Zoologie 13: 107-220.

Wetherbee, D. K., 1959. Egg Teeth and Hatched Shells of Various Bird Species, Bird-Banding 30: 119-121.

Wheeler, W. M., 1899. The Embryology of *Blatta germanica* and *Doryphora decemlineata*, Journal of Morphology 16: 291-374.

Willemse, M.& J. M. Denuce, 1973. Hatching gland in the teleosts, *Brachydanio rerio*, *Danio malabaricus*, *Moenkhausia oligolepis* and *Barbus schuberti*. 169-177.

Wyllie, A. H., J. F. Kerr & A. R. Currie, 1980. Cell death: the significance of apoptosis, International Review of Cytology 68: 251-306.

Yamagami, K., 1972. Isolation of a choriolytic enzyme (Hatching enzyme) of the teleost, *Oryzias atipes*, Developmental Biology 29: 343-348.

Yamamoto, M., I. Iuchi & K. Yamagami, 1979. Ultrastructural changes of the teleostean hatching gland cell during natural and electrically induced precocious secretion. 162-174.

Yasumasu, S., I. Iuchi & K. Yamagami, 1989a. Isolation and some properties of low choriolytic enzyme (LCE), a component of the hatching enzyme of the teleost, *Oryzias latipes*, Journal of Biochemistry 105: 212-218.

Yasumasu, S., I. Iuchi & K. Yamagami, 1989b. Purification and partial characterization of high choriolytic enzyme (HCE), a component of the hatching enzyme of the teleost *Oryzias latipes*, Journal of Biochemistry 105: 204-211.

Yasumasu, S., M. Uzawa, A. Iwasawa & N. Yoshizaki, 2010. Hatching mechanism of the chinese soft-shelled turtle *Pelodiscus sinensis*, Comparative Biochemistry and Physiology Series B Biochemistry & Molecular Biology 155: 435-441.

Yoshizaki, N., 1973. Ultrastructure of the hatching gland cells in the South African clawed toad, *Xenopus laevis*, Journal of the Faculty of Science Ser. 6, Zoology 18: 469-480.

Yoshizaki, N.& C. Katagiri, 1975. Cellular basis for the production and secretion of the hatching enzyme by frog embroys. 203-212.

V. Abstract

Animals release from their eggs by means of mechanical tools (egg teeth, hatching spine), body expansion or by chemical support of choriolytic enzymes synthesized in a hatching gland. Most observed cephalopods possess an appropriate gland on their posterior mantle pole, referred to as Hoyle organ (HO). It differs structurally between the octopods (line-shaped) and cuttlefishes and squids (anchor-shaped). The HO develops during late embryonic stages, synthesizes enzymes to weaken the egg shell and degrades after hatching within a few days. The degeneration process of the HO is far from being resolved but the rapid cellular degradation indicates a programmed cell death strategy. This study comprises nine coleoid species of the order Sepiida, Sepiolida, Teuthida and Octopoda. Main objectives are 1.) a comparison of the HO morphology in correlation with the respective egg encapsulation design and the hatching and pre-hatching behavior; 2.) to characterize and specify the HO development, maturation and degradative cell alterations after hatching. While all investigated decapodiform species have an anchor-shaped HO, only in one octopodiform species a hatching gland could be observed, whereas the other two lack this structure. The HO degradation is accomplished within 2 days by a type of necrotic cell death or autophagic cell death. The results mainly confirm a correlation between egg encapsulation and dimension of the gland. Contribution of triggered cell death mechanisms appear to be obvious for the observed species. However, a clear definition of cell death mode is difficult at this stage, since those processes are quite complex, dynamic and show overlapping characteristics. Future characterization of specific mediator proteins and gene expression pattern will help to point out the diversity of cell death strategies in cephalopods and fully understand the process of HO degradation.

V. Zusammenfassung

Der Schlüpfvorgang aus dem Ei kann entweder durch Ausdehnung des Körpers und Kollaps der Eischalen erfolgen oder die Tiere verwenden mechanische Vorrichtungen (Eizähne oder spezielle Dornen) bzw. choriolytische Enzyme aus speziellen Schlüpfdrüsen. Bei den meisten untersuchten Cephalopoden ist eine derartige Drüse, das Hoyle Organ (HO), am hinteren Ende des Mantels zu finden. Das Organ ist als waagrechte Linie bei Oktopoden und als ankerförmige Struktur bei Dekapoden erkennbar. Es wird während der späten Embryonalentwicklung angelegt, synthetisiert Enzyme zum Auflösen der Eihüllen und wird nach dem Schlüpfen innerhalb weniger Tage abgebaut. Die intrazellulären Vorgänge während dieses Abbauprozesses sind bei Cephalopoden nur wenig untersucht, das unmittelbare Einsetzen nach dem Schlüpfen jedenfalls spricht für einen programmierten Zelltod. Diese Studie umfasst neun Arten der Ordnungen Sepiida, Sepiolida, Teuthida and Octopoda. Ziele dieser Studie sind vergleichende morphologische Untersuchungen des HO in Korrelation mit der Dicke der jeweiligen Eihülle und dem Schlüpfverhalten, die Charakterisierung der Stadien der Drüsenentwicklung und -reifung sowie die zellulären Vorgänge während des Organabbaus. Bei allen untersuchten Dekapoden konnte die Existenz eines ankerförmigen HO bestätigt werden, aber nur eine der untersuchten Oktopodenarten besitzt eine linienförmige Drüse, während bei den beiden anderen Arten keine entsprechenden Zellen nachgewiesen werden konnten. Der Abbau des HO erfolgt mittels programmiertem Zelltod (nekrotisch oder autophagisch) und ist innerhalb von ein bis zwei Tagen abgeschlossen. Die Ergebnisse bestätigen weitgehend eine Korrelation zwischen Eigröße, Schalendicke und Dimension des HO. Die rasche Rückbildung der Drüse erfolgt offensichtlich mit Hilfe von genetisch gesteuerten Zelltod-Mechanismen, obwohl eine klare Zuordnung wegen der überlappenden morphologischen Merkmale nicht immer möglich ist. Künftige molekularbiologische Analysen hinsichtlich spezifischer Zelltod-Mediator-Proteine und Genexpressionsmuster sind erforderlich, um das Verständnis für die Komplexität und Variabilität von Zelltod-Mechanismen bei Cephalopoden zu vertiefen.

VIII. Acknowledgement

I am deeply grateful to Prof. Dr. Waltraud Klepal for her engaged supervision, productive discussions and encouragement during this PhD project. I would like to particularly thank Dr. Janek von Byern for giving me the opportunity to be part of this FWF-supported project (Project No. P 21135-B17). His experience in manifold fields of research guaranteed substantial discussion on numerous details of this study and his networking abilities with the scientific communities facilitated constructive cooperations with renowned scientists in the field of cephalopod research. I am very thankful to Daniela Gruber, Marieluise Weidinger, Vanessa Zheden and of course all other colleagues of the core facility CIUS for fruitful discussions and a stimulating working climate.

I am grateful to Jitima Suwanmala MSc. and Dr. Charuay Sukhsangchan from the Kasetsart University Bangkok, Thailand, for their assistance in collecting and cultivating *Idiosepius pygmaeus* and *Argonauta hians*. I want to thank Dr. Anna Palumbo and Dr. Teresa Mattiello from the Stazione Zoologica Anton Dohrn, Naples, Italy, for providing embryonic stages of *Sepia officinalis*, for their guidance and for the permission to use their labs. Samples of *Euprymna scolopes* were kindly provided by Dr. Marie Therese Nödl and Dr. Heinz Gert de Couet from the University of Hawaii, Manoa, USA. I want to thank Dr. Paul Brickle and Dr. Alexander Arkhipkin from the Falkland Islands Fisheries Department, UK, for their supervision of rearing *Loligo gahi* embryos and hatchlings. I am thankful to Dr. Pedro Domingues from the Instituto Espanol de Oceanografía in Spain for providing embryos of *Octopus vulgaris*. Hatchlings of *Sepioteuthis lessoniana* and *Tremoctopus gracilis* were kindly given by Dr. Richard Young of the University of Hawaii, Manoa, USA. Finally I want to thank the staff of the Johann Wolfgang Goethe-Universität, Frankfurt am Main, Germany, for providing embryonic stages of *Architeuthis* sp. from their collection.

VIII. Curriculum Vitae

Research Focus
Cell biology, embryonic development and epithelial glands in molluscs, cell death processes

Education

1998	High-school graduation certificate (Vienna)
1998-2008	Diploma study Zoology, University of Vienna, Austria (Diploma thesis: "Ultrastructural characterization of the adhesive organ of *Idiosepius* (Mollusca, Cephalopoda)")
since 9. 2008	PhD study Zoology, University of Vienna, Austria (PhD thesis: "Comparative studies of the Hoyle organ in cephalopods")

Awards

2004	Travel Grant for Cape Town, South Africa from the University of Vienna
2005	Short time grant (KWA) for Thailand from the University of Vienna
2006	Poster Award for: "Structure and composition of the adhesive organ of *Idiosepius* (Cephalopoda, Mollusca)", Hobart, Tasmania
2009	Short time grant (KWA) for Elba, Italy from the University of Vienna
2012	Scholarship honour of the ‚Theodor Körner Fond' in the amount of 3000,- Euro for „Klebstoffanalyse bei heimischen Schnecken"

Project collaborations

2008-2010	
2004-2008	FWF project: "Research on the adhesive organ of *Idiosepius thailandicus*", University of Vienna, Austria
2006	„3D-reconstructions for comparative studies in cephalopods", University of Vienna, Austria
2007-2008	„Investigations of potential diet-related risks of Bt-Mais in a long term feeding experiment with laboratory mouse", University of Veterinary Medicine, Vienna
2008-2011	Project collaboration in the FWF project: "Characterization of hatching glands in two cephalopod species", University of Vienna, Austria
2012-2015	Project collaboration in the FWF project: "Catcher in the cave - Fishing strategy of a Jamaican fungus gnat *Neoditomyia farri*", University of Vienna, Austria

Scientific publications

Peer reviewed articles

Cyran N., Palumbo A., Klepal W., Vidal E., Städler, Y., Schönenberger, J., & von Byern, J. (2016): The short life of the Hoyle organ of *Sepia officinalis* - Formation, differentiation and degradation by programmed cell death. Hydrobiologia, 10.1007/s10750-017-3291-3

von Byern, J., **Cyran, N.**, Klepal, W., Nödl, M. T. & Klinger, L. (2016): Characterization of the adhesive dermal secretion of *Euprymna scolopes* Berry, 1913 (Cephalopoda). Zoology 120, 73-82

von Byern, J., Dorrer, V., Merritt, D. J., Chandler, P., Stringer, I., Marchetti-Deschmann, M., McNaughton, A., **Cyran, N.**, Thiel, K., Noeske, M. & Grunwald, I. (2016): Characterization of the fishing lines in titiwai (=*Arachnocampa luminosa* Skuse, 1890) from New Zealand and Australia. PLoS ONE. 11 (12): e0162687

von Byern, J., Kerbl, A., Nödl, M-T., Bello, G., Städler, Y., Schönenberger, J. & **Cyran, N.** (2016): Spine Formation as a Hatching Tool in *Euprymna scolopes* (Mollusca, Cephalopoda, Sepiolidae). Malacologia. 59, 2, S. 231-238

von Byern, J., Dicke, U., Heiss, E., Grunwald, I., Gorb, S., Staedler, Y. & **Cyran, N.** (2015): Morphological characterization of the glandular system in the salamander *Plethodon shermani* (Caudata, Plethodontidae). Zoology. 118, 5, 334-347

Cyran N., Klepal W., Städler Y., Schönenberger J. & von Byern J. (2015): Alterations in the mantle epithelium during transition from hatching gland to adhesive organ of *Idiosepius pygmaeus* (Mollusca, Cephalopoda). Mechanisms of Development, 135, 43–57.

Cyran, N., Städler, Y., Schönenberger, J., Klepal, W. & Von Byern, J. (2013): Hatching glands in cephalopods – a comparative study. Zoologischer Anzeiger. 253, 1, 66-82.

Von Byern, J., Wani, R., Schwaha, T., Grunwald, I. & **Cyran**, N. (2012): Old and sticky-adhesive mechanisms in the living fossil *Nautilus pompilius* (Mollusca, Cephalopoda). Zoology. 115, 1, 1-11.

Cyran, N., Klepal, W. & Von Byern, J. (2011): Ultrastructural characterization of the adhesive organ of *Idiosepius biserialis* and *Idiosepius pygmaeus* (Mollusca: Cephalopoda). Journal of the Marine Biological Association of the United Kingdom. 91, 7, 1499-1510.

Von Byern, J., Scott, R., Griffiths, C., Micossi, A., Grunwald, I. & **Cyran**, N. (2011): Characterization of the Adhesive Areas in *Sepia tuberculata* (Mollusca, Cephalopoda). Journal of Morphology. 272, 10, S. 1245-1258 14 S.

Nürnberger, S., **Cyran**, N., Albrecht, C., Redl, H. R., Vecsei, V. & Marlovits, S. (2011): The influence of scaffold architecture on chondrocyte distribution and behavior in matrix-associated chondrocyte transplantation grafts. Biomaterials. 32, 4, 1032-1040.

Von Byern, J., Rudoll, L., **Cyran**, N. & Klepal, W. (2008): Histochemical characterization of the adhesive organ of three *Idiosepius* spp. Biotechnic and Histochemistry: a journal for microtechnic and histochemistry. 83, 1, S. 29-46 18 S.

Book Chapter

Cyran N., Klinger L., Scott R., Griffiths C., Schwaha T., Zheden V., Ploszczanski L. & von Byern J. (2010): "Characterization of the Adhesive Systems in Cephalopods" in Adhesive Systems From Nature to Technical and Medical Application; Springer Wien New York: Springer, Editors: Janek von Byern und Ingo Grunwald, 53-86 (Book Chapter).

Power, A. M., Zheden, V., Von Byern, J. & **Cyran, N.** (2010): "Arthropoda – Pedunculata" in Adhesive Systems From Nature to Technical and Medical Application; Springer Wien New York: Springer, Editors: Janek von Byern und Ingo Grunwald, 53-86 (Book Chapter).

Research trips

08. 2004 – 09. 2004
Capture, cultivation and preparation of *Euprymna scolopes* (Cephalopoda), Cape Town, South Africa

03. 2006 – 04. 2006
Capture, cultivation and preparation of *Idiosepius pygmaeus and Idiosepius biserialis* (Cephalopoda), Marine Station Phuket, Thailand.

11. 2008 – 12. 2008
Cultivation and preparation of *Loligo gahi*, Fisheries department, Stanley, Falkland Islands,UK

03. 2009 – 03. 2009
Cultivation and preparation of *Sepia officinalis*, Stazione Zoologica Anton Dohrn, Napoli, Italy

10. 2009 – 10. 2009
Capture and preparation of *Octopus vulgaris* und *Sepia officinalis*; HYDRA Institute for Marine Sciences, Elba, Italy